KV-9 Report 6-81-15

Bolted connections with flush endplates and haunched beams

Tests and limit state design methods

Ir. P. Zoetemeijer

June 1981

Stevinweg 4, Delft - Tel. 015-782329

CONTENTS

Contents Page

Contents

SUMMARY

Tests are described on semi-rigid beam-to-column connections with flush-end-plates and haunched beams.
The results are checked with limit state design methods for stiffened and unstiffened column-flanges.
It appears that these methods can also be used for the design of the flush-end-plates, provided that the beam-web or beam-flange do not fail.
The methods to check the latter failure mechanisms are developed.
Formulae to determine the limit state design load of the haunch are also given.
The dimensions of the welds appear to depend on the failure-mechanism which determines the limit state moment and on the desired rotational capacity.

0. INTRODUCTION

The aims of the tests reported herein were:

- to check a new design method for the tension side of flush-end plates in connections with haunched beams.
- to check new ideas of stiffening which are desirable from an eco-economic point of view.
- to show undergraduates the influence of various kinds of stiffeners on the behaviour of beam-to-column connections.

0.1 New design-method

In the first place this research has to confirm the adequacy of a limit state design method for the tension side of beam-to-column connections with stiffened column-flanges or flush-end plates.
This design method was initially developed by Doornbos [1] , for stiffened column-flanges.
It was then extended to flush-end plates and modified by Zoetemeijer as described in [2] .

Another purpose of the tests was to determine the contribution of bolts added in the first boltline and the force distribution when more boltrows without stiffeners are applied whereas the column flange thickness is small.

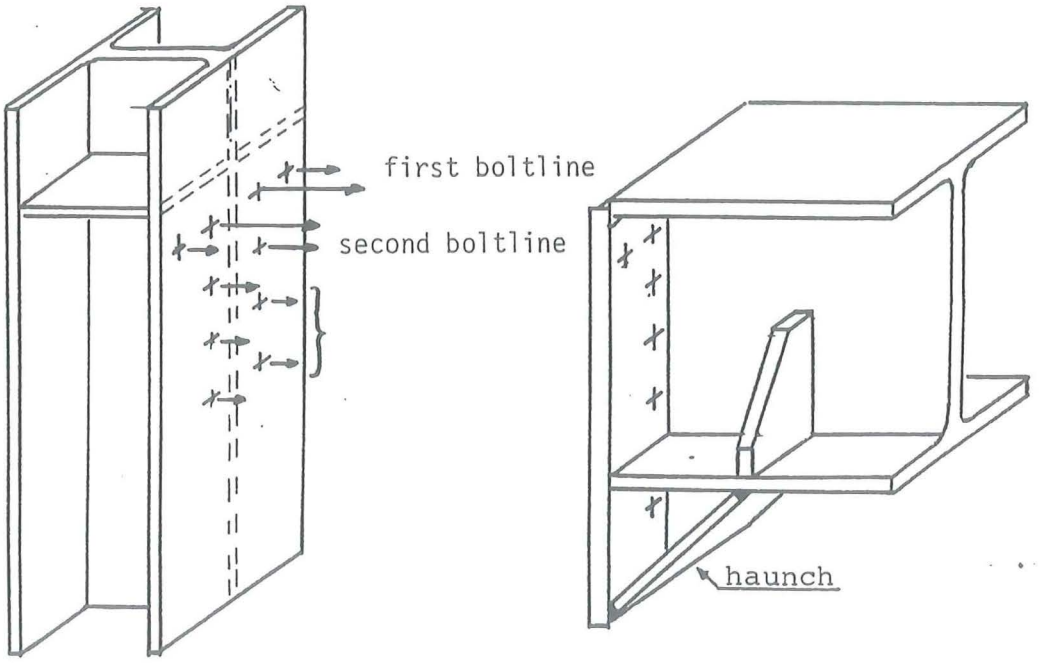

Fig. 1: Purpose of the tests: - to confirm the design method of the corner bolts
- to develop a design method which takes into account the contribution of the other bolts.
- to check the behaviour of the haunched beam.

It was doubted that the contribution of the boltrows without stiffeners is rectilinear with the distance to the point of rotation

0.2. New ideas of stiffening

Another point of research was the strengthening of the column-web on the compression-side of the connection.
The use of diaphragms to avoid buckling of the column-web is not advisable from an economic point of view |3| .
However avoiding the use of stiffeners is not always possible. An economic solution seemed to be the welding of a plate flat on the column-web as shown in fig. 2 |4| which is called "web doubler".

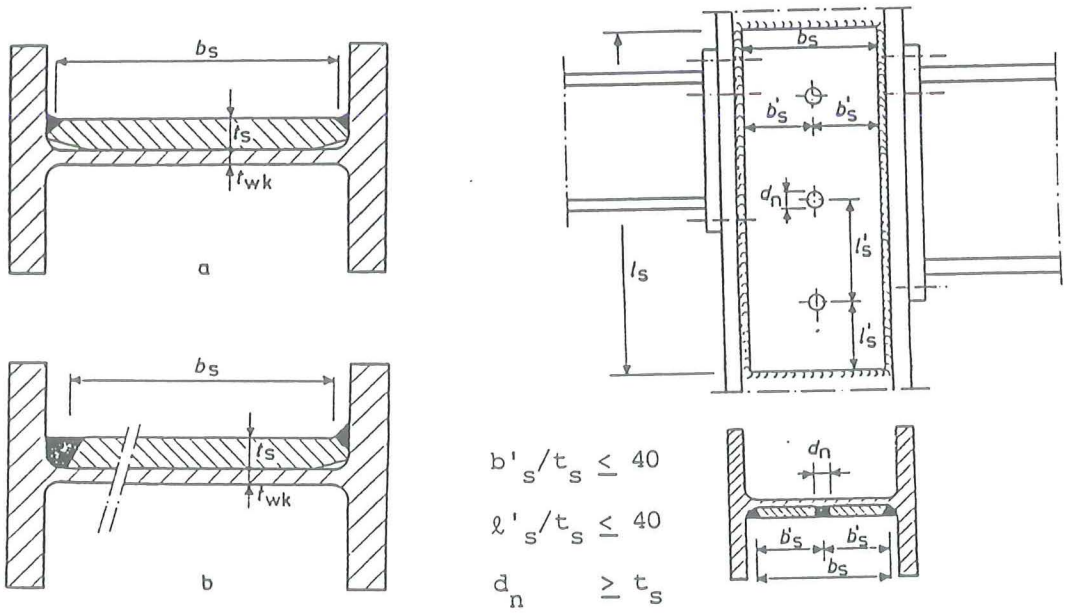

Fig. 2. : Methods of stiffening of column-webs

The methods proposed for welding, either filling the space between plate and flange over the fillet or grinding the plate to cover the fillet, are rather expensive as has appeared in practice. That is why another method of welding as shown in figure 3 was tried.

The plates as shown in figure 2 are mainly designed to transfer the shear force in an unbalanced connection. The behaviour of the plate as shown in figure 3 is only checked on the compression force in a balanced connection.

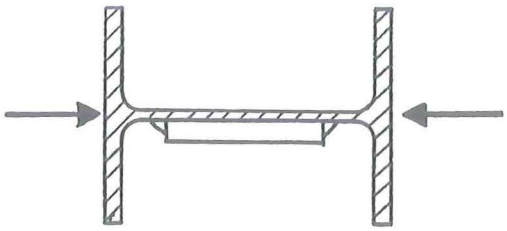

Fig. 3.: A more economic way of welding of the stiffener.

In order to facilitate the use of mechanical equipment for tightening the bolts, a question was risen: Can the haunch-flange be avoided if the haunch-web is given a larger thickness?
This question is also studied in this report.

0.3. Research with undergraduates

It is the policy of the Department of Civil Engineering of the Delft University of Technology that undergraduates majoring in Structural Engineering have to carry out some research in the laboratory.
The intention of this policy is that the undergraduates get knowledge about the possibilities in the laboratories and some background to be able to assess the implications of technical reports.
The undergraduates carry out this research in their third year of education when they have studied the basic theories in the fields of structures.
The tests carried out, had to give sufficient contents in the applications of the basic theories.

The section "Steelstructures" uses this possibility for research mainly to check new design methods and to find out answers on questions asked by engineers working in the field of practice.

It is evident, that serving all the aims mentioned caused rather complicated types of testspecimens.

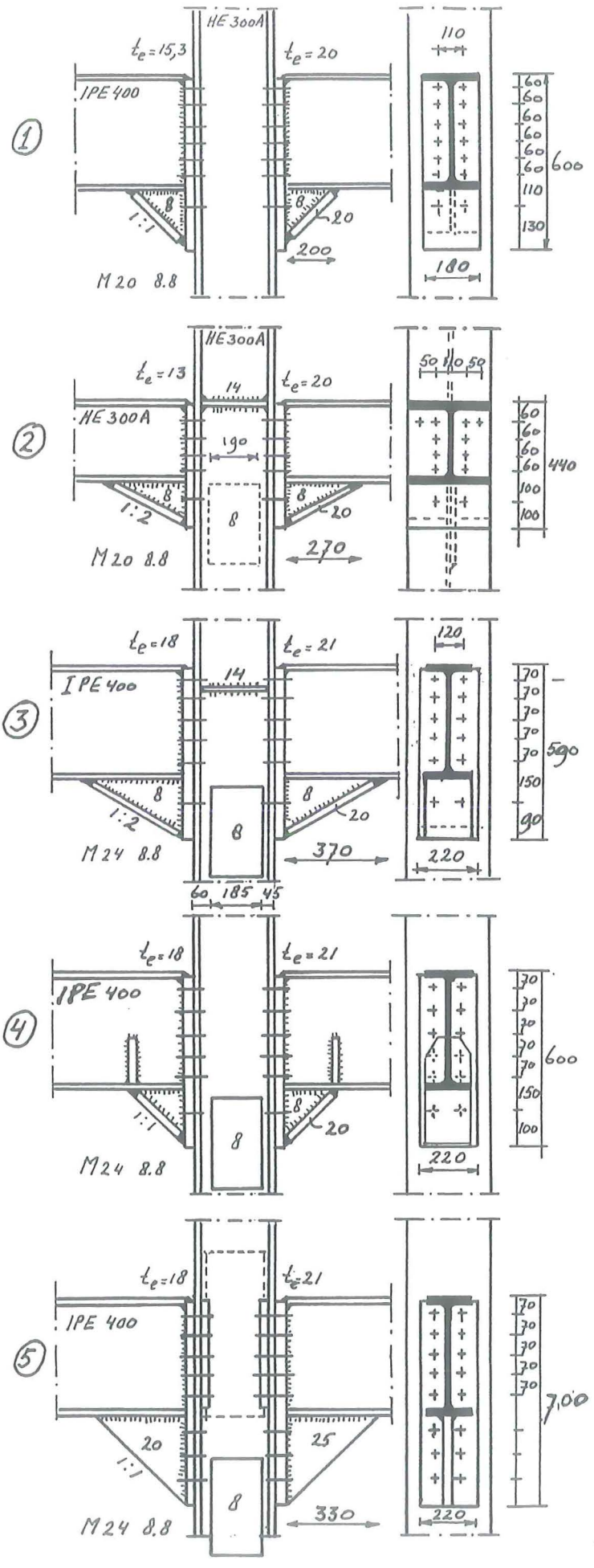

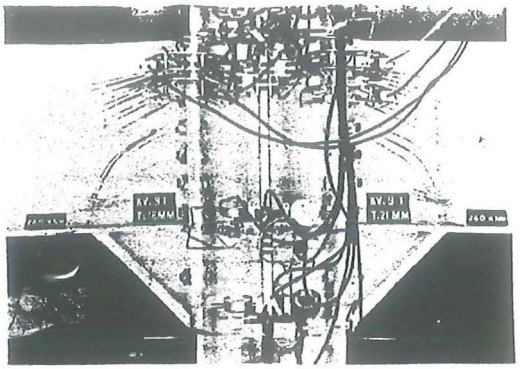

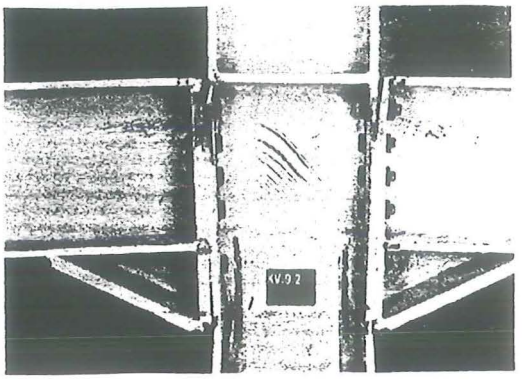

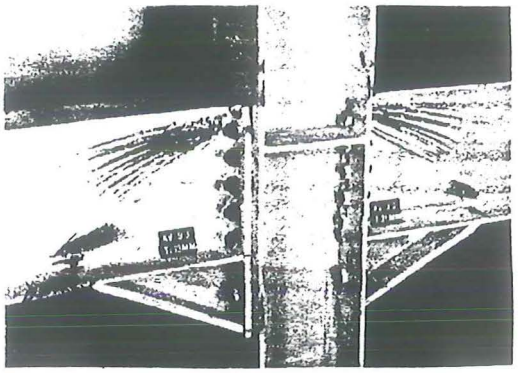

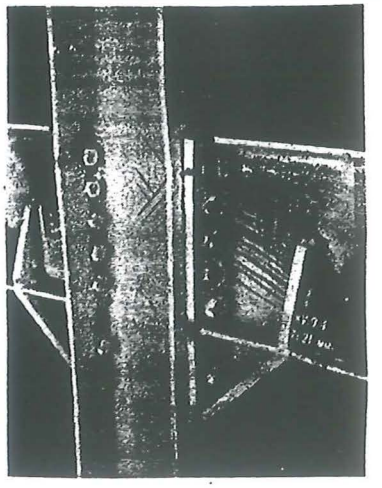

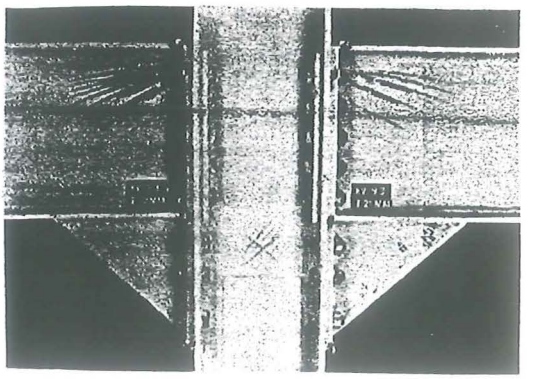

Fig.4.: Testspecimens

1. DESCRIPTION OF THE TESTSPECIMENS

1.0. General

A review of the testspecimens with the dimensions is given in figure 4.

The dimensions of all the fillet welds were made 4 mm with the exception of the inner fillet weld between the end-plate and the beam-flange at the tension side as shown in figure 5.

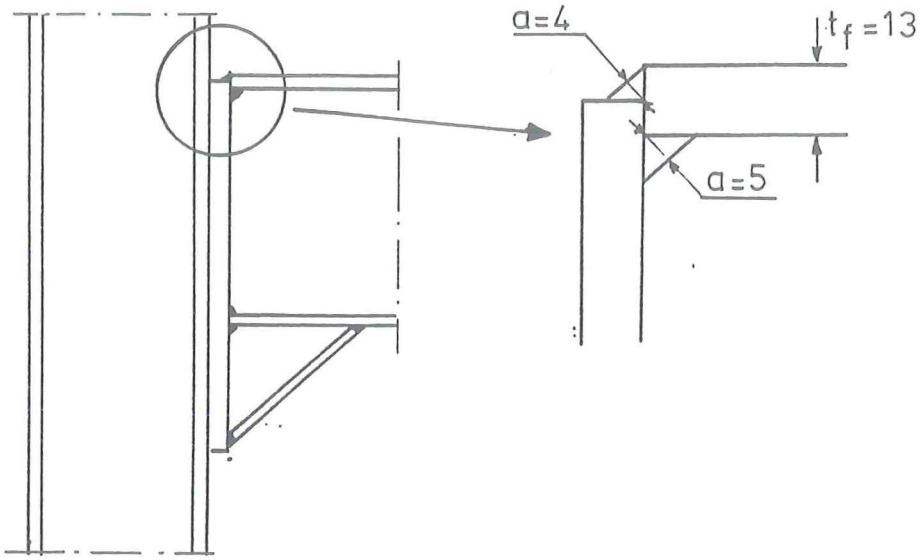

Fig. 5.: Fillet weld between end-plate and beam-flange at the tension side of the connections

The reason will be explained in chapter 4.2.3.2. with the methods of computation.

The horizontal distances between the bolts are based on the expectation that the deformation of the column-flange due to bending remains small when the distance between the bolt-head and the toe of the fillet is smaller than 1.25 times the flange thickness.
This expectation was risen by the results of tests with flush-end plates where the distance between the fillet weld and the bolt-head was smaller than 1.25 times the end-plate thickness [2] .
In that case the actual load of a bolt below the corner bolt was proportional to the load in the corner bolt and the distance to the point of reaction at the compression side as shown in figure 6.

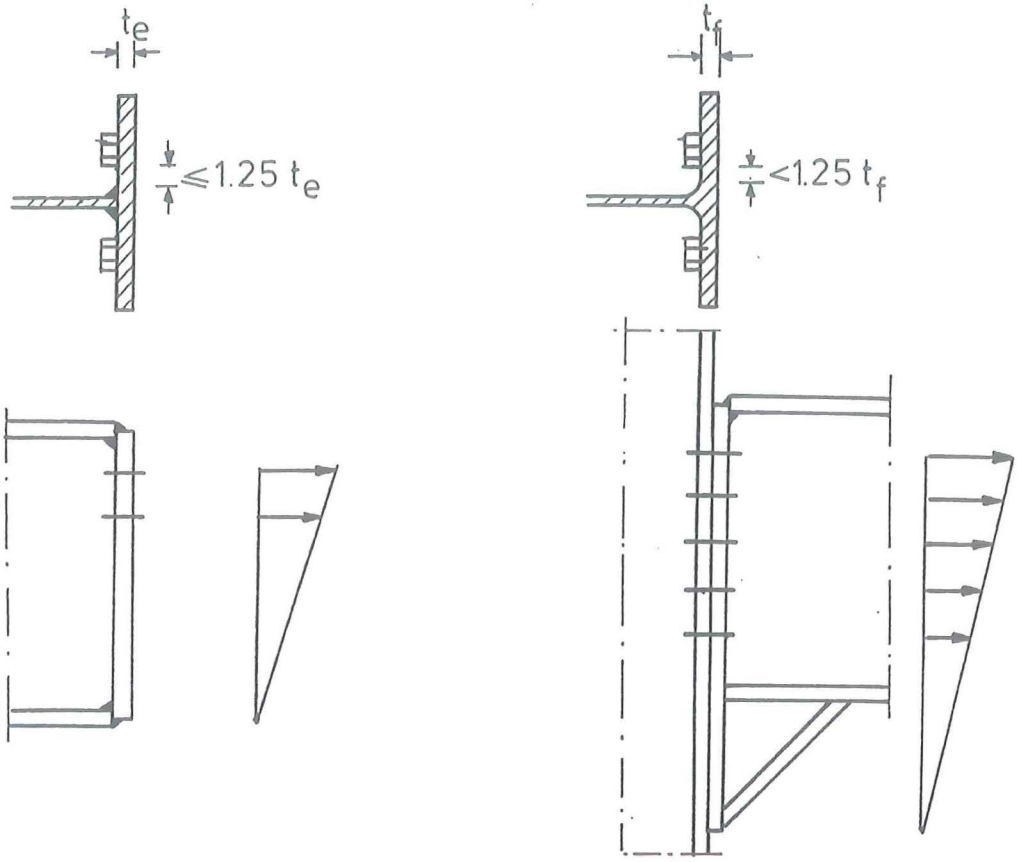

Observed force distribution in end-plate connections [2]

Expected force distribution in these tests

Fig. 6.: Considerations which determined the horizontal bolt distance

The horizontal distance between the bolts is chosen to confirm the expectation that this behaviour will also occur with column-flanges.

In tests 1 through 4 the haunch-flanges used were 20 mm thick to ensure that no failure of this part of the connection would occur.
In chapter 4.2.8 with the methods of computation, it will be shown that this thickness is sufficient.

1.1. Testspecimen 1

This testspecimen was meant as a reference to check the effects of the various stiffening methods.
The end-plate thickness 15.3 mm was based on the wish to reach yielding of the bolt simultaneously with yielding of end plate and column-flange. Owing to the higher bolt strength than expected, this purpose was not fulfilled.
The end-plate thickness 20 mm was based on the wish to transfer the bolt-force more by shear than by bending of the end-plate.

During testing, parts of the connection were strengthened as indicated in the discussion.

1.2. Testspecimen 2

Instead of using an IPE 400 section, a beam section of HE 300A was used to check the contribution of a bolt added in the uppermost boltline parallel to the beam-flange and the stiffener.
The end-plate thickness 13 mm was chosen equal to the column-flange thickness. The end-plate thickness 20 mm was based on the idea that the contribution of the second bolt would become larger with an increase of the end-plate thickness.
This idea may only be true if the column-flange has sufficient strength.
The column-web was strengthened with a web doubler plate welded on one side of the web with fillet welds a = 4 mm.
The slope of the haunch-flange was taken as 1:2 in order to decrease the vertical component of the force transferred by the flange to avoid buckling of the beam-web.
Buckling of the column-web was meant to be avoided by the web doubler plate.

1.3. Testspecimen 3

After having carried out test 2, the strengthening of the column-web with one plate appeared to be inadequate.
That was why in test 3 through 5 the plates were attached on both sides of the column-web with fillet welds a = 4 mm.
In order to check the influence of the distance, s, between the toe of the fillet-weld and the fillet of the section (figure 7), two different values were chosen.
The smaller distance was chosen on the side with the thicker end-plate.

The stiffener on the tension side was welded with butt-welds between the flanges because there was no room for the bolt-heads.
As far as the slope of the haunch-flange is concerned the same considerations are valid as mentioned with test 2.

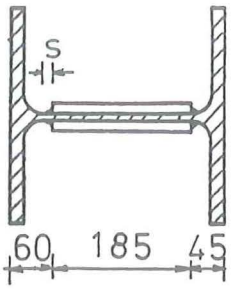

Fig. 7.: Web doubler plates on the compression-side of test 3 through 5.

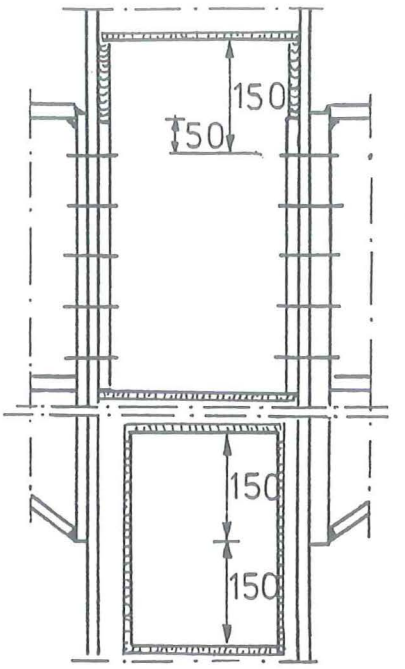

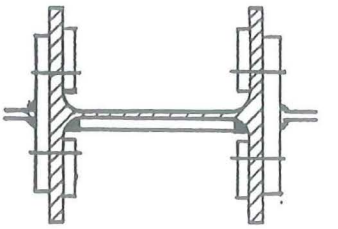

Fig. 8.: Strengthening-plates on the tension-side of test 5.

1.4. Testspecimen 4

The purpose of this specimen was to confirm the phenomena observed in test 1 but with a different bolt dimension and bolt configuration. Since test 1 failed prematurely on the compression-side of column and beam, stiffening was applied at these places to cause failure of the tension-side of the connection.

1.5. Testspecimen 5

This testspecimen was used to show the adequacy of a haunch without a flange.

To be able to research the behaviour of the haunches the column was strengthened on the tension-side.

This was done by applying backing plates (16 mm) along the column-flanges to avoid yielding at the vertical boltlines.

Due to the use of these backing plates it was expected that the force distribution would be more linearly proportional than in the previous tests.

In order to avoid failure by yielding of the column-web on the tension-side, this part of the connection was strengthened with a plate of 8 mm thickness. This plate was welded over the fillets on one side of the web as shown in figure 8.

2. MATERIAL PROPERTIES

2.1. Dimensions

The actual and nominal dimensions of the European rolled sections used in these tests are given in figure 9.

2.2. Mechanical properties

The mechanical properties were determined for all the plate-material and the material of the European rolled sections.
The results are summarized in table 1.

2.3. Load deformation curves of the bolts in appendix 1

The load-deformation characteristics, necessary for determining the bolt loads from the measured bolt elongations, were obtained before the tests were carried out.
For this purpose two bolts were calibrated with the grip of the bolt equal to that of the corresponding bolts used in the test specimens.
The loads of the bolts were increased step by step until fracture occurred.
At each increment the elongation of the bolt was measured.

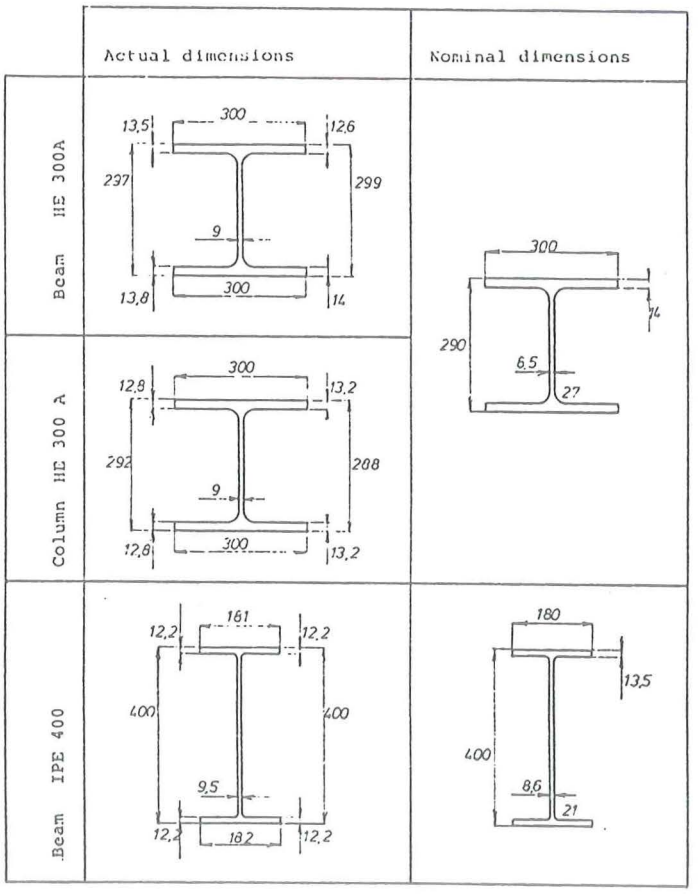

Fig. 9.: Dimensions of the European rolled sections used.

Mechanical properties of the material				
Beam section	Column section	Location test-specimen	σ_y N/mm^2	σ_u N/mm^2
IPE 400		flange long.	256	394
		flange trans.	231	393
		web long.	287	441
		web trans.	293	432
HE 300A		flange long.	266	428
		flange trans.	303	425
		web long.	294	461
		web trans.	296	448
	HE 300A	flange long.	257	387
		flange trans.	267	405
		web long.	293	389
		web trans.	302	413

Yield stress of Plate material.	
thickness in mm	σ_y N/mm^2
13	270
15,3	270
18	266
20	266
21	310

Table 1. Material properties.

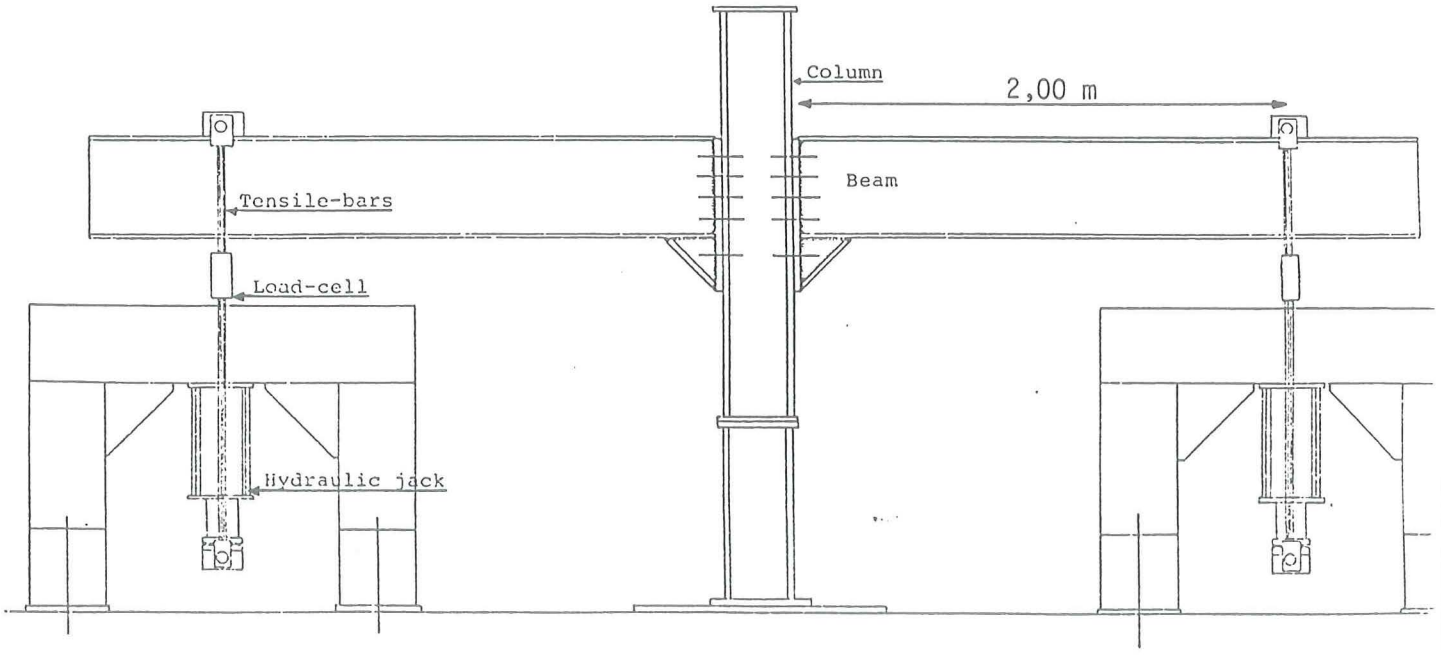

Fig. 10.: Test set-up.

3. TEST SET-UP AND PROCEDURE

The test arrangement is shown schematically in figure 10.
The loads, were applied by means of two hydraulic jacks on both sides of the column, each with a capacity of 200 kN.
The loads were measured with load cells, in series with the hydraulic jacks.

The load cells had a capacity of 100 kN each. The deflections of the various parts of the testspecimen were measured with linear displacement transducers and gauges as shown in the photograph of figure 4, at locations indicated in figure 11.

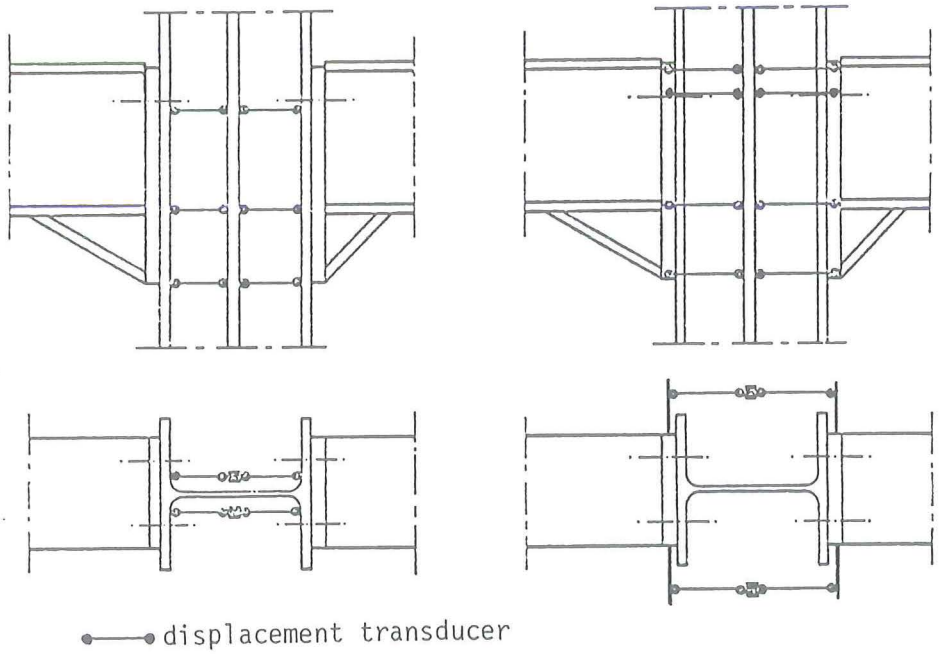

Fig. 11.: Locations of displacement transducers.

Because attention was particularly drawn to the local behaviour of the various components of the connection, overall behaviour was neglected.
It was initially thought that the moment-rotation characteristic of the connection could be derived from the local measurements.
This appeared to be not the case because yielding also occurred in the haunched part of the beam, while deflections were measured only between the centre line of the column and the end plates.

The bolt elongations were measured with extensometers (see fig. 36). The elongation of the bolt caused the leaf springs in the extensometers to bend. The changing of the electrical resistance of the strain gauges due to this bending served as a measure of bolt elongation.
The high strength bolts were tightened arbitrarily with hand wrenches. The initial elongation due to the tightening was measured and taken into account in computing the bolt loads.

Prior to testing, the testspecimens were white-washed to provide a visual display of the yielding patterns.

In each test the load was applied in specific increments and the data were recorded directly if no yielding occurred.
Otherwise, measurements were recorded only after the deflections had stabilized when yielding occurred.
It was tried to increase the loads simultaneously on both sides of the column.

4. COMPUTATION METHODS

4.0 General

During testing many failure mechanisms were observed.
These failure mechanisms were analyzed by following the path of the forces starting from the centre line of the column to the cross section of the beam where the haunch starts.
The failure mechanism which gives the lower limit state design strength determines the limit state design moment of the connection.

Starting from the centre line of the column, the possible failure mechanisms on the tension side are:

1°. failure of the column-web due to tension
2°. failure of the column-flange due to bending in combination with failure of the bolt
3°. failure of the end-plate due to bending in combination with failure of the bolt
4°. failure of the beam-web due to tension
5°. failure of the beam-web due to shear
6°. failure of the beam in the section where the haunch starts.

The possible failure mechanisms on the compression-side are:

7°. failure of the column-web due to buckling or yielding
8°. failure of the haunch-flange due to yielding
    a. at the column-side
    b. at the beam-side
9°. failure of the beam-web due to compression
10°. failure of the beam-flange due to buckling.

The locations of these failure-mechanisms are indicated in figure 12.

The computation methods will be explained in the same sequence as the failure modes are mentioned.
The computations are given in appendix 2,(page 83). The results are summarized in table 2 and 3 at pages 21 and 23.
Table 2 gives the limit state loads mainly determined by the dimensions of the column and the end-plate.
Table 3 gives the limit state loads determined by the failure mechanisms which occur in the haunched part of the beam.

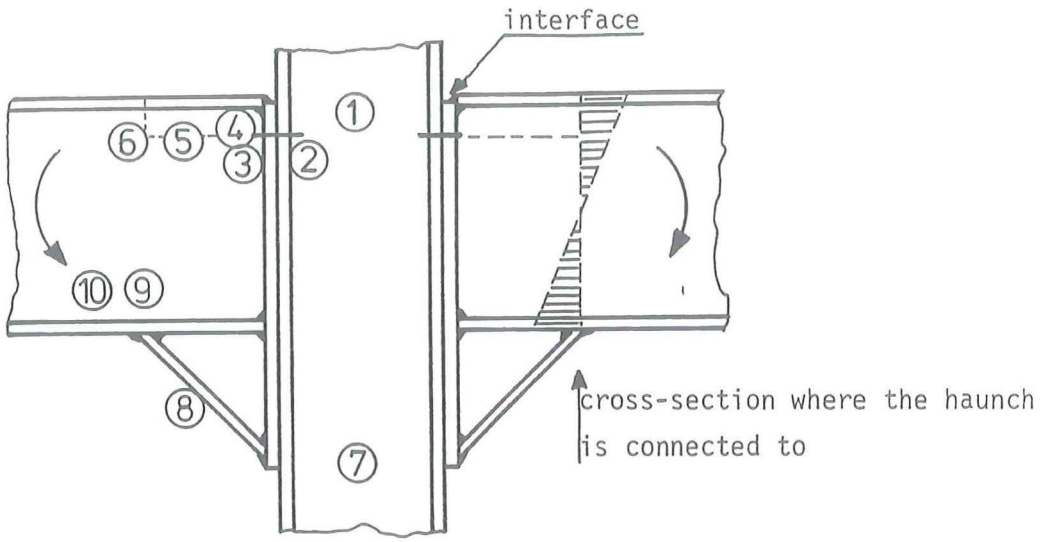

Figure 12.: Locations of the failure mechanisms contemplated

4.1. Conversion of limit state design strength into limit state design moments

4.1.1. Table 2

The lower limit state design strength at a boltline, determined by one of the first four failure modes, is indicated with an asterisk in table 2 and is used for the computation of the limit state design bending moment.
If the sum of the limit state design loads determined by tension is larger than the limit state design load on the compression-side determined by failure of colum-web or haunch, then the limit state design loads at the boltlines are reduced as indicated in column (10) of table 2.
This reduction is only executed for test 1.
It is performed by starting with the lower bolt; taking into account that the point of rotation depends on the strength of the compression side.
If this strength is exceeded, the deflection on the compression-side will increase rapidly.
This causes a rise of the rotation centre and a decrease of the deformation of the lower bolt firstly.

number and endplate thickness	notation	column-web	column-flange	end-plate	beam-web	column - web	moment	shear design loads	moment design loads	lever - arm	limit state design moment	limit state moment
		kN	kN	kN	kN	kN	kNm	kN	kN	m	kNm	kNm
(1)	(2)	(3)	(4)	(5)	(6)	(7)	(8)	(9)	(10)	(11)	(12)	(13)
1 - 15,3	F_1	394	226*	300	223			226	226	0,53	120	
	F_2	160	92	62*	163			62	62	0,47	29	
	F_3	160	92	84*	163			84	84	0,41	34	
	F_4	160	92	84*	163			84	84	0,35	29	
	F_5	160	92	84*	163			84	84	0,29	24	
	F_6	160	92	84*	163			84	58	0,23	13	
	F_c					598	677	624	598		249	287
1 - 20	F_1	394	214*	>300	270			214	214	0,53	113	
	F_2	160	92*	106	163			92	92	0,47	43	
	F_3	160	92*	140	163			92	92	0,41	38	
	F_4	160	92*	140	163			92	92	0,35	32	
	F_5	160	92*	140	163			92	92	0,29	27	
	F_6	160	92*	140	163			92	16	0,23	4	
	F_c					598	677	674	598		257	293
2 - 13	F_1	286	273+64	286+46	274*			274	274	0,37	101	
	F_2	160	102	48*	159			48	48	0,31	15	
	F_3	160	92	60*	159			60	60	0,25	15	
	F_4	160	92	60*	159			60	60	0,19	11	
	F_c					598	1301	442	442		142	235
2 - 20	F_1	286*	278+64	>286+46	360			286	286	0,37	106	
	F_2	160	102*	114	159			102	102	0,31	32	
	F_3	160	92*	140	159			92	92	0,25	23	
	F_4	160	92*	140	159			92	92	0,19	17	
	F_c					598	1417	572	572		178	235
3 - 18	F_1	366	278	426	275*			275	275	0,52	143	
	F_2	366	278	94*	190			94	94	0,45	42	
	F_3	190	94*	118	190			94	94	0,38	36	
	F_4	190	92*	118	190			92	92	0,31	29	
	F_5	190	92*	118	190			92	92	0,24	22	
	F_c					1020	1040	647	647		272	330
3 - 21	F_1	366	278*	> 426	319			278	278	0,52	145	
	F_2	366	278	150*	190			150	150	0,45	68	
	F_3	190	94*	190	190			94	94	0,38	36	
	F_4	190	92*	190	190			92	92	0,31	29	
	F_5	190	92*	190	190			92	92	0,24	22	
	F_c					1020	1040	696	696		300	382
4 - 18	F_1	431	208*	426	275			208	208	0,52	108	
	F_2	190	92*	94	190			92	92	0,45	41	
	F_3	190	92*	92	190			92	92	0,38	35	
	F_4	190	92*	118	190			92	92	0,31	29	
	F_5	190	92*	118	190			92	92	0,24	22	
	F_c					1020	827	576	576		235	322
4 - 21	F_1	431	208*	> 426	319			208	208	0,52	108	
	F_2	190	92*	150	190			92	92	0,45	41	
	F_3	190	92*	> 150	190			92	92	0,38	35	
	F_4	190	92*	> 150	190			92	92	0,31	29	
	F_5	190	92*	> 150	190			92	92	0,24	22	
	F_c					1020	827	576	576		235	315
5 - 18	F_1	861	302	426	275*			275	275	0,53	146	
	F_2	380	138	94*	190			94	94	0,46	43	
	F_3	380	138	118*	190			118	118	0,39	46	
	F_4	380	138	118*	190			118	118	0,32	38	
	F_5	380	138	118*	190			118	118	0,25	29	
	F_c					1020	723	723	723		302	345
5 - 21	F_1	861	302*	> 426	319			302	302	0,53	160	
	F_2	380	138*	150	190			138	138	0,46	63	
	F_3	380	138*	> 150	190			138	138	0,39	54	
	F_4	380	138*	> 150	190			138	138	0,32	44	
	F_5	380	138*	> 150	190			138	138	0,25	35	
	F_c					1020	854	854	854		356	388

Table 2: Limit state design loads with limit state design moments determined by column and end-plate dimensions.

Test number and end-plate thickness	Shear beam-web		Forces in the cross-section where the haunch is connected to the beam					Result	Lever arm	Limit state design moment		Actual ultimate moment
	Force notation fig. 22 page 34	Force	Force notation fig. 22 page 34	Force	Haunch	Buckling beam Web Reduction yes	Buckling beam Web Reduction no	Limit state design load		at start haunch	at interface	
		kN		kN	kN	kN	kN	kN	m	kNm	kNm	kNm
(1)	(2)	(3)	(4)	(5)	(6)	(7)	(8)	(9)	(10)	(11)	(12)	(13)
1 - 15,3	F_7	53	F_{10}	369	530	442	517	369	0,39	144		
	F_8	91	F_{11}	94				94	0.34	32		
	F_9	319		463				77	0,19	14		
		463	F_{12}	77				540		190	212	287
				540								
1 - 20	F_7	90	F_{10}	419	530	442	517	419	0,39	163		
	F_8	117	F_{11}	107				107	0,34	36		
	F_9	319		526				88	0,19	17		
		526	F_{12}	88				614		216	240	293
				614								
2 - 13	F_7	64	F_{10}	476	699	948	1101	476	0,28	134		
	F_8	73	F_{11}	75				75	0,24	18		
	F_9	414		551				29	0,12	3		
		551	F_{12}	29				580		155	179	235
				580								
2 - 20	F_7	150	F_{10}	583	699	948	1101	583	0,28	163		
	F_8	111	F_{11}	92				92	0,24	22		
	F_9	414		675				36	0,12	4		
		675	F_{12}	36				711		189	220	235
				711								
3 - 18	F_7	75	F_{10}	565	666	757	1008	565	0,39	220		
	F_8	106	F_{11}	207				207	0,34	70		
	F_9	591		772				177	0,19	34		
		772	F_{12}	177				949		324	398	380
				949								
3 - 21	F_7	118	F_{10}	565	666	757	1008	565	0,39	220		
	F_8	143	F_{11}	207				207	0,34	70		
	F_9	591		772				355	0,13	46		
		852	F_{12}	355				1127		336	412	382
				1127								
4 - 18	F_7	75	F_{10}	389	827	n.a	n.a	389	0,39	152		
	F_8	106	F_{11}	112				112	0,34	38		
	F_9	320		501				71	0,19	13		
		501	F_{12}	71				572		203	226	322
				572								
4 - 21	F_7	118	F_{10}	451	827	n.a	n.a	451	0,39	176		
	F_8	143	F_{11}	130				130	0,34	44		
	F_9	320		581				82	0,19	16		
		581	F_{12}	82				663		236	262	315
				663								
5 - 18	F_7	75	F_{10}	422	n.a	n.a	n.a	422	0,39	165		
	F_8	106	F_{11}	121				121	0,34	41		
	F_9	362		543				77	0,19	15		
		543	F_{12}	77				620		221	250	345
				620								
5 - 21	F_7	118	F_{10}	483	n.a	n.a	n.a	483	0,39	188		
	F_8	143	F_{11}	139				139	0,34	47		
	F_9	361		622				88	0,19	17		
		622	F_{12}	88				710		252	285	328
				710								

Remark: All loads are converted into loads in the horizontal direction of the flanges

Table 3: Limit state design loads with limit state design moments determined by haunch and beam dimensions

The lever-arms as stated in column (11) of table 2 are determined by assuming the reaction point being present at 10 mm from the edge of the end-plate for test 1 through 4.
In test 5 the reaction-point is determined by failure of the haunch as it will be explained later.

4.1.2. Table 3 (page 22)

The limit state design loads determined by the failure modes in the haunched part of the beam should be in balance with the forces in the beam-section where the haunch-flange is connected to the beam.
This requirement is used in determining the limit state design bending moment as indicated in table 3.
The limit state design strength determined by shear in the beam-web(column (3)), has been converted into a force distribution in the beam-section where the haunch-flange is connected to. This force distribution is restricted by the limit state design loads determined by yielding of the beam-flange caused by bending stresses (see result of test 3 column (5)).
The meaning of the force symbols is defined in the description of the computation of the limit state design loads (fig. 22 on page 34).

On the compression side, the limit state design load is determined by yielding of the haunch-flange or buckling of the beam-web. The limit state design loads determined by these failure modes are converted into limit state design loads of the beam-flange in the section where the haunch-flange is connected to. This implies that the forces present in the beam-flange and beam-web are supposed to be transferred along the dotted lines as indicated in figure 13.

The resulting limit state design bending moment in the beam-section (column (11 is converted into a bending moment at the interface of end plate and column.

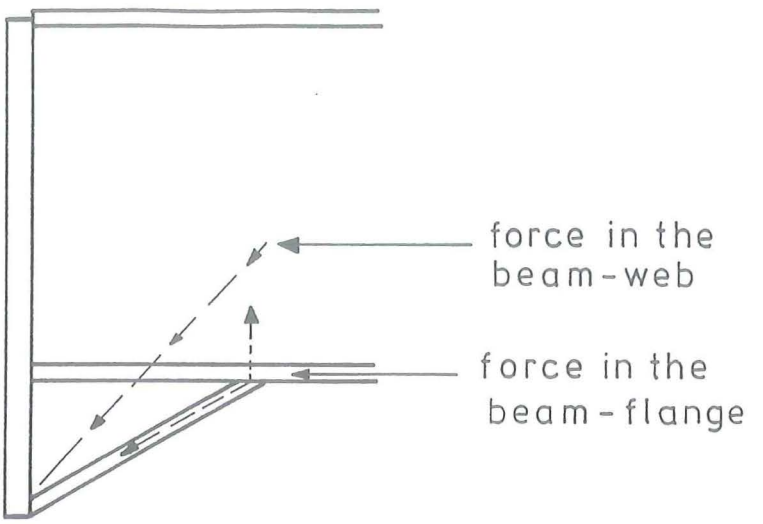

Fig. 13.: Current of forces assumed in the computation of the limit state bending moment determined by failure of the compression side.

4.2. Limit state design loads

4.2.1. Failure of the column-web due to tension

$$\hat{F}_i = t_{w_c} * e_{w_c} * \sigma_{y_{w_c}} \qquad (1)$$

where:
- $\hat{F}_i$ = force transferred by the bolts at boltline i
- i = number of boltline, numbered from the uppermost bolt (1)
- t_{w_c} = thickness of the column web
- $\sigma_{y_{w_c}}$ = actual yield stress of the column-web
- e_{w_c} = effective length of the column-web

The effective length is restricted to the centre distances of the bolts as far as the inner bolts are concerned.

The effective length of the uppermost bolt depends on the situation.

For the unstiffened situation the same formula is used as mentioned in [5]

$$e_{w_c} = \tfrac{1}{2} * a + 2m + 0.625\ n' \qquad (2)$$

in which:

a = centre distance of bolts

m, n' } = same distances as used in the computation of the limit state loads due to bending of the column-flange (see chapter 4.2.2.).

With the stiffened column-flanges, failure of the column-web due to tension may only occur when the column-flange fails due to bending as indicated in figure 14.

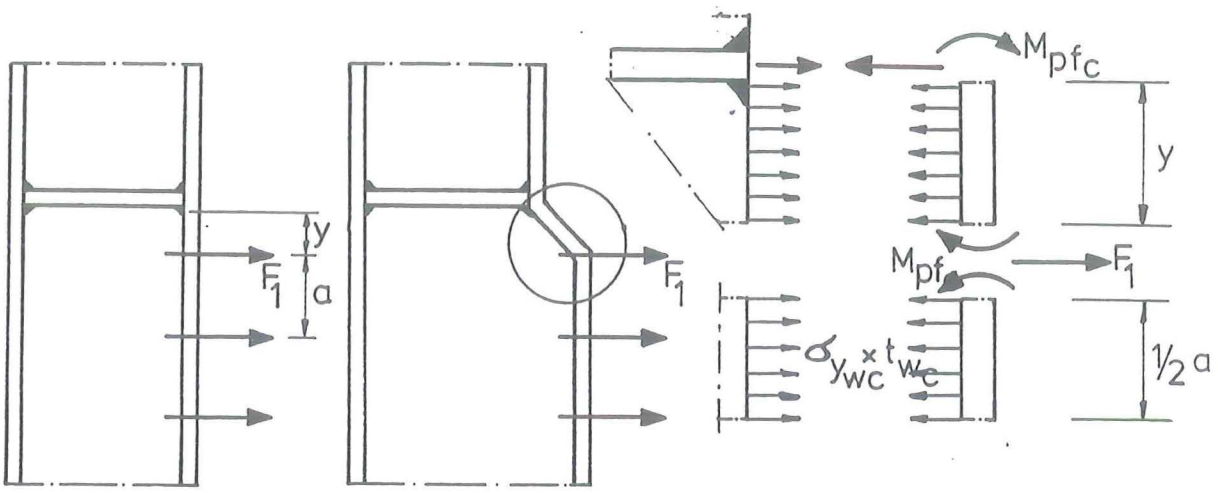

Fig. 14.: Failure of the column-web due to tension in the situation with stiffened flanges.

According to this figure:

$$\hat{F}_1 = \frac{2M_{pf_c}}{y} + (\tfrac{1}{2}y + \tfrac{1}{2}a)\, t_{w_c} * \sigma_{y_{wc}} \qquad (3)$$

where:

M_{pf_c} = plastic moment of the column-flange
y = distance between the boltline and the stiffener.

4.2.2. Failure of the column-flange

Different methods of computation are used:
- for the unstiffened column-flange
- for the stiffened column-flange

4.2.2.1. The unstiffened column-flange

This method was developed in |6| and it is applied in |5|

The design formulae used are:

$$\hat{T} * m - (\hat{B}_t - \hat{T}) * n \leq M_p \qquad (4)$$

$$\hat{T} * m \leq M_p + M_p' \qquad (5)$$

where:

$\hat{B}_t$ = limit state design strength of the bolt

$\hat{T}$ = limit state design strength of the combination of flange and bolt at one side of the column.

M_p = plastic moment that causes a plastic hinge to form at a distance of 0.8 * the root-radius from the column-web.

M_p' = plastic moment that causes a plastic hinge to form at the vertical bolt-line.

m = distance between the plastic hinges formed by M_p and M_p'.

n = distance from the boltline to the location of the prying action being assumed at the outer edge of the end-plate but not greater than 1.25 * m.

n' = distance from the vertical boltline to the edge of the column-flange in the same direction as n.

For convenience, the definitions of the parameters are given in figure 15.

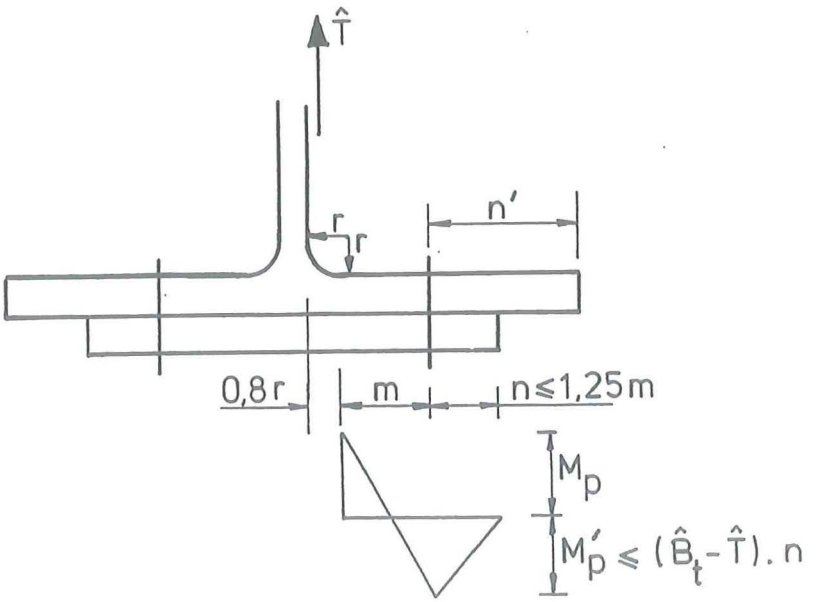

Fig. 15.: Parameters used in formulae (4) and (5).

In the case that $M_p' \geq (\hat{B}_t - T) * n$ formula (4), bolt failure is the determining factor, while in formula (5) failure of the flange due to bending determines the limit state design strength.
The plastic moments M_p and M_p' depend on the effective length of the column-flange.
The formula of the effective length:

$$e_{f_c} = a + 4m + 1.25\ n' \qquad (6)$$

was developed in |6|.
This effective length is restricted by the centre distance of the bolts.

Thus:

$$F_i = 2\hat{T}$$

where $\hat{T}$ is determined separately for each bolt.

4.2.2.2. The stiffened column-flange

For the stiffened column-flange the computation method is used as developed in |1| and modified |2| .
An infinitely long plate bounded by two fixed edges and one free edge, loaded with a concentrated force, was analysed with yield line theory.
The result is a chart as shown in figure 16 with which the ultimate design load of a stiffened column-flange or flush end-plate can be determined.
The various yield line patterns which give the lower upper bound values of the plate are depicted in the chart.
The graphs represent locations of the bolts which give the same limit state design load. This load can be calculated by multiplying the value written at the ends of the graphs with the plastic moment per unit length of the plate
The coordinates of the bolt location are made dimensionless by dividing them by the width of the plate.
Though prying action has some effect on where the yield-lines may form, it is assumed that it does not contribute to the internal energy dissipation.

Thus: $F_i = 2. * \hat{T} = 2\alpha\ m_p \qquad (7)$

where: $m_p = \frac{1}{4} * \sigma_{y f_c} * t_{f_c}^2$

t_{f_c} = thickness of column-flange
$\sigma_{y f_c}$ = actual yield stress of the column-flange
α = factor determined in the chart in figure 16

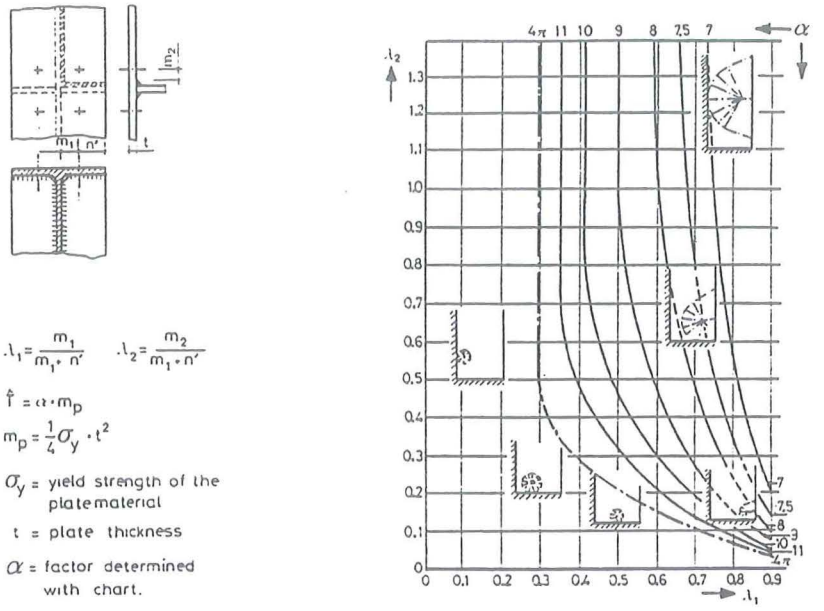

Fig. 16.: Chart for the design strength of the stiffened column-flange.

In order to determine the limit state design strength of a bolt added beside the corner bolt in the boltline adjacent to the stiffener, formulae (4) and (5) of the unstiffened column-flange may be used.

The effective length for this bolt is restricted to the flange width available beyond the failure mechanism caused by the corner bolt.
The width required for the failure mechanism of the corner bolt is supposed to be twice the smaller value of the distances m_1 and m_2 as shown in figure 17.

4.2.2.3. Dimensions of stiffener and welds

The formulae for the stiffened column-flange are only valid if the supporting column-web and stiffener do not yield.
Yielding of the column web is checked with formula (3) as described in 4.2.1.
Yielding of the stiffener and the weld between stiffener and flange may be checked in the same way as described for the connection of beam-flange with end-plate in chapter 4.2.3.2.

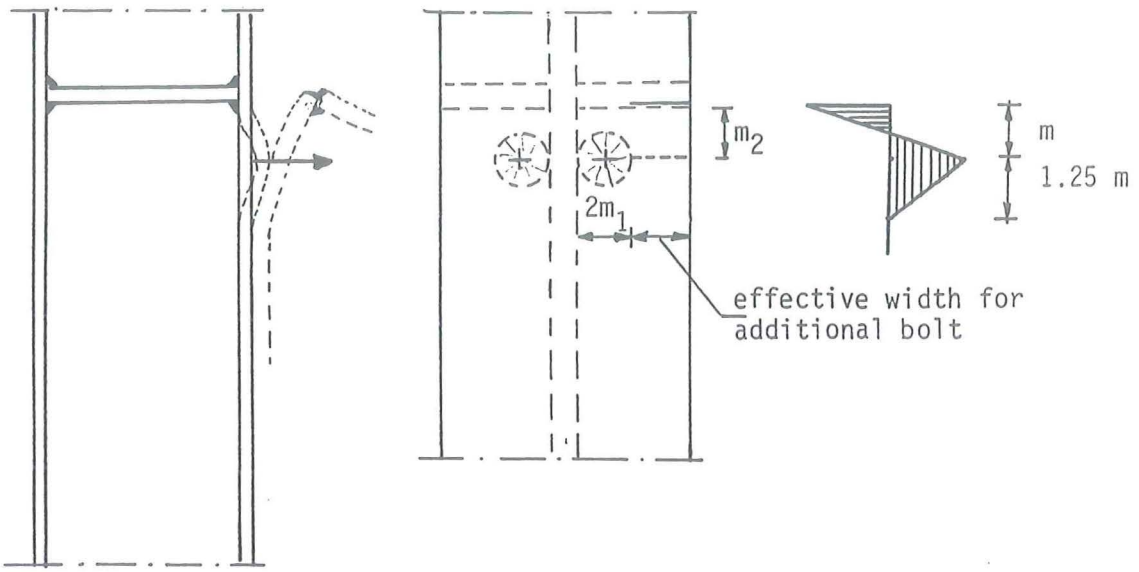

Fig. 17.: Effective length with assumed failure mechanism for an additional bolt adjacent to the stiffener

If the stiffener is located at the same height as the beam-flange, certainty about the strenght will always be reached if the dimensions of the stiffener are chosen equal to those of the beam-flange.
In the case that the stiffener is located between two horizontal boltlines, the stiffener with welds should be dimensioned according to the sum of the limit state loads of the bolts present in the two boltlines.

4.2.3. Failure of the end-plate

4.2.3.1. Comparison with failure of the stiffened column-flange

The methods used for the computation of the limit state design strength of the column-flange are also used for the computation of the end-plate.
However the computation of the end-plate with the additional bolt in the uppermost boltline of test 2 has been changed with respect to the computation of the column-flange. The distance m is taken equal to the centre distance of bolt and flange (see fig. 18).

The bending moment M_p is determined by the plastic moment per unit length of the beam-flange. The effective length for the additional bolt is determined in the same way as described for the column-flange (see chapter 4.2.2.2.). The reason for this way of computation becomes evident after ob-

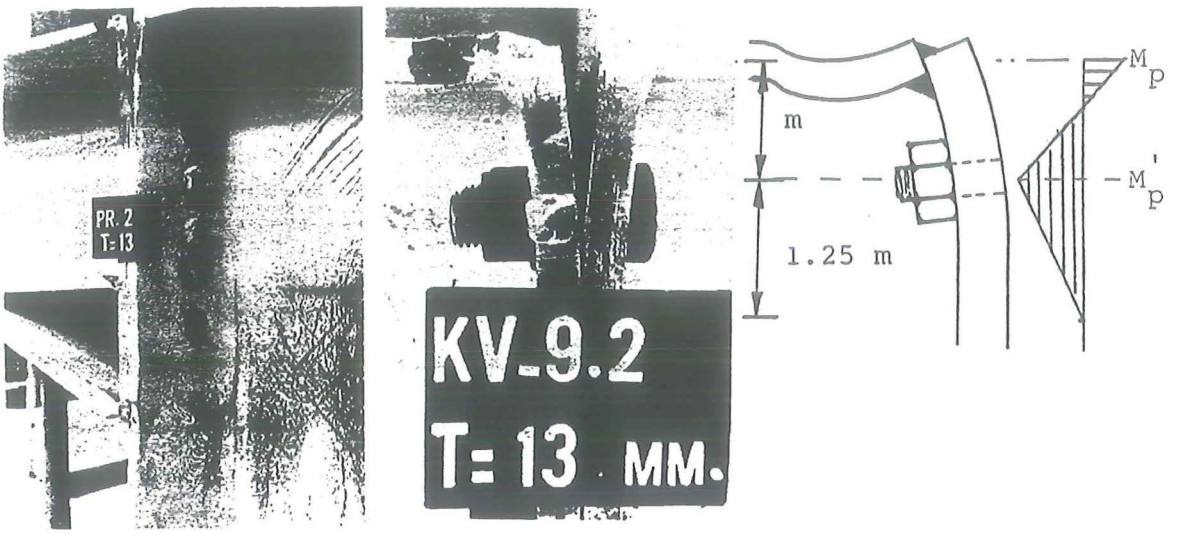

Fig. 18: Bending of the beam-flange caused by the additional bolt.

serving the deformation of the beam-flange as shown in fig. 18.
The beam-flange yields due to the bending caused by the bolt.

4.2.3.2. Welds between end-plate and beam

The dimensions of the welds have to be in accordance with the limit state design strength of the end plate.
The distribution of the limit state design load of the corner bolt is taken as inversely proportional to the distances m_1 and m_2 (see figure 19).
The effective length of the weld is supposed to be twice the distance m_1 or m_2, provided that this length is available.

However, there are situations that the welds should also be dimensioned so, that bending of the beam-flange may occur.

This is the case when a bolt is added to the corner bolt or when failure of the beam-web occurs due to tension (see chapter 4.2.4.)

In this case it may be shown by an iterative process that the fillet weld sizes a_1 and a_2 according to figure 20, are sufficient if they are chosen 0.3 and 0.35 times the flange thickness, provided that the edge of the endplate coincides with the centre of the flange.

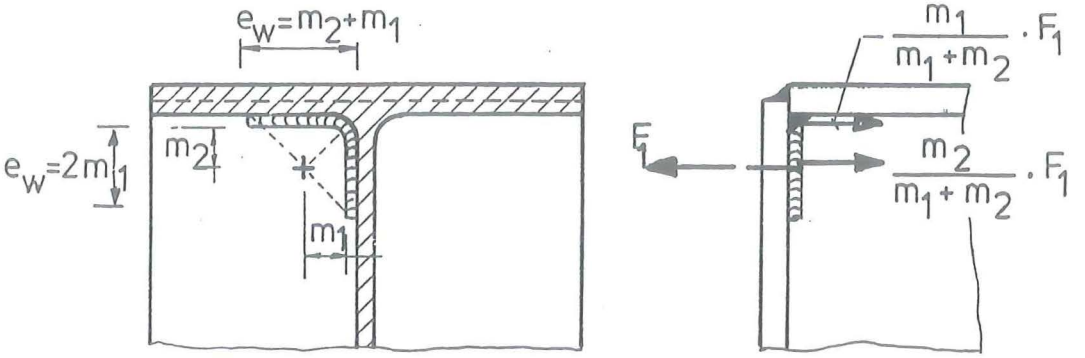

e_w = effective width of the weld

Fig. 19.: The distribution of force F_1 over the welds is taken as inversely proportional to the distances m_1 and m_2.

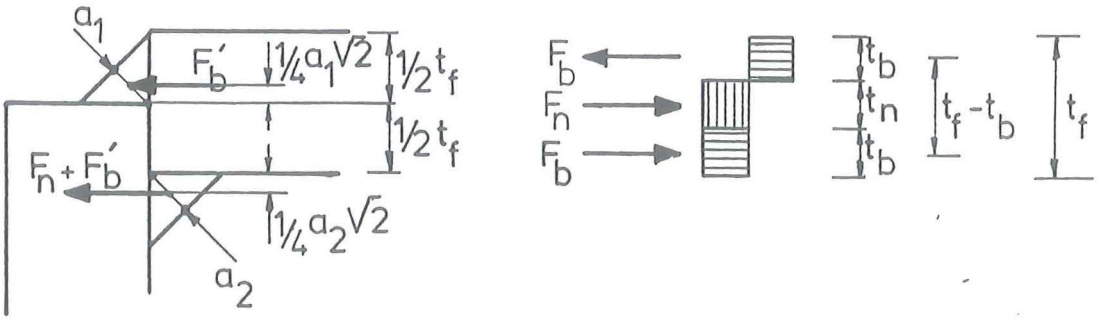

$$\Sigma M = 0 \rightarrow (F_n + F_b') \left(\tfrac{1}{2}t_f + \tfrac{1}{4}a_1\sqrt{2} + \tfrac{1}{4}a_2\sqrt{2}\right) - F_b\,(t_f - t_b) - F_n\,\tfrac{1}{4}a_1\sqrt{2} = 0$$

Fig. 20.: Assumed force equilibrium in the welds and the beam-flange when the flange yields due to a combination of tension and bending.

Assuming various values of the tensile force F_n as a fraction α_1 of the bending force F_b, the α_i-values of table 4 can be calculated with an iterative process.

In table 4 the required weld dimensions are given as a fraction of the flange thickness t_f.

$F_n = \alpha_1 F_b$	$t_b = \alpha_2 t_f$	$F_b' = \alpha_3 F_b$	$a_1 = \alpha_4 t_f$	$a_2 = \alpha_5 t_f$
α_1	α_2	α_3	α_4	α_5
(1)	(2)	(3)	(4)	(5)
0.0	0.5	0.685	0.343	0.343
0.1	0.476	0.633	0.301	0.349
0.2	0.454	0.577	0.262	0.353
0.3	0.434	0.519	0.225	0.356
0.4	0.417	0.458	0.191	0.358
0.5	0.400	0.395	0.158	0.358
0.6	0.385	0.330	0.127	0.358
0.7	0.370	0.265	0.098	0.357

Table 4.: Results of the formula of fig. 20 reached with an iterative process.

In the computation of the values of table 4, the Dutch code of practice [7] is used, which takes into account that the weld material is better than the parent material with a factor 0.7.
It is evident, that it is very unfavourable assuming the normal force F_n completely transferred by the weld at the lower side. Thus a smaller value for the dimension of a_2 is tolerable, provided that a_1 is enlarged corresponding. However, $a_2 > a_1$ is more in agreement with the transfer of forces.
A connection between end-plate and beam-flange, where the edge of the end-plate is higher than the flange-centre, is more favourable because the lever-arm between the fillet welds increases.

The dimensions of the fillet welds between end-plate and beam-web should be taken equal to half of the web-thickness, because a complete connection is assumed in the computation; if yielding of the beam-web due to tension is the governing failure mechanism.

4.2.4. Failure of the beam-web due to tension

Similar formulae as used for the computation of the limit state design strength of the column-web are used for the computation of the beam-web. For the uppermost bolts, the same situation exists as explained for the uppermost bolts in the column-flange.

However, mostly the beam-flange has a smaller plastic moment than the end-plate has. This implies that the plastic moment at the edge of the end-plate can never be higher than the plastic moment of the beam-flange because it is assumed that the beam-web yields completely. This is the same situation, as shown in figure 18.

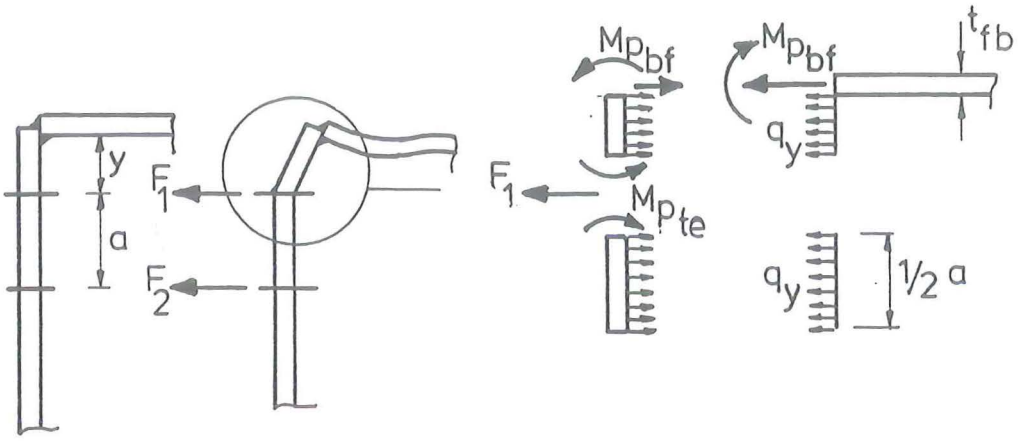

Fig. 21.: Failure of the beam-web due to tension of the uppermost bolt

This results in the following formula:

$$F_1 = (Mp_{te} + Mp_{fb})/y + \{\tfrac{1}{2}a + \tfrac{1}{2}(y-\tfrac{1}{2}t_f)\}q_y \qquad (8)$$

Where:

Mp_{te} = plastic moment of the end-plate

Mp_{fb} = plastic moment of the beam-flange

y = distance between the centres of the uppermost bolt and the beam-flange

a = distance between the centres of the bolts

$q_y = t_{wb} * \sigma_y$

in which:

t_{wb} = thickness of the beam-web

σ_y = actual yield stress of the beam-web

4.2.5. Failure of the beam-web due to shear

The forces present at the interface of column and end-plate should be distributed into the beam by the cooperation of end-plate and beam-web. Owing to the philosophy of the design method used for the end-plate, this occurs partly by bending of the end-plate, but the main part should be transferred by the beam-web.
The cross-section of the beam-web just above the uppermost bolt should be checked against shear (see figure 22).

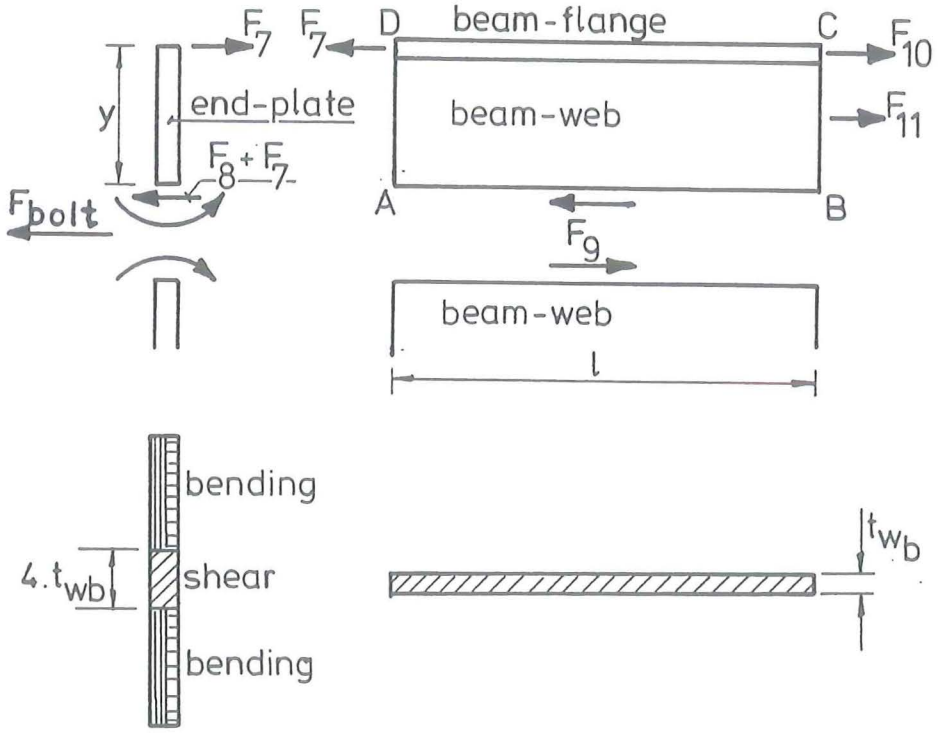

Fig. 22.: The forces $F_{10}+F_{11}$ should be transferred mainly by shear in the web.

From the deformed situation it may be decided that the failure mechanism is caused by:
-shear in the beam-web (force F_9)
-shear in the end-plate (force F_8)
-bending of the end-plate(force F_7)
The sum of the forces F_7,F_8 and F_9 can never be larger than the sum of the forces F_{10} + F_{11} present in the beam-flange and beam-web in the cross-section where the haunch flange is connected to the beam-flange.

This results in the following formula:

$$F_{10} + F_{11} = F_7 + F_8 + F_9 \qquad (9)$$

Where:

F_7 = force transferred by bending of the end-plate

For simplicity it is proposed to apply the total width of the end-plate for the computation of the force transferred by bending but to take into account only the bending moment on one side of the deformed plate.

Thus:

$$\hat{F}_7 = \frac{\frac{1}{4} t_e^2 \, b \, \sigma_y}{y} \qquad (10)$$

in which: t_e = thickness of the end-plate
b = width of the end-plate
σ_y = actual yield stress of the end plate
y = centre distance between bolt and flange

F_8 = force transferred by shear of the end-plate

It is not easy to decide which part of the end-plate transfers the force by bending or by shear.
The proposal of taking a width of four times the web thickness as effective width for shear of the end-plate seems to be a good one.

Thus:

$$\hat{F}_8 = 4 t_{w_b} * t_e * 0.58 \, \sigma_y \qquad (11)$$

in which: t_{w_b} = thickness of the beam-web
t_e = thickness of the end-plate
σ_y = actual yield stress of the end-plate

F_9 = force transferred by shear of the beam-web

$$\hat{F}_9 = t_{w_b} * l * 0.58 \, \sigma_y \qquad (12)$$

in which: t_{w_b} = thickness of the beam-web
l = length of the haunch
σ_y = actual yield stress of the beam-web

The sum of the forces F_7, F_8 and F_9 determines the magnitude of the stresses in the beam-section where the flange is connected to.
These stresses are represented by forces F_{10} and F_{11}
where:

F_{10} = represents the force in the beam-flange
F_{11} = represents the force in the part of the beam-web between boltline and beam-flange

If the forces F_{10} and F_{11} remain below the limit state design loads determined by complete yielding of the beam, it is supposed that bending of the beam occurs symmetrically with respect to the axis of gravity, thus the neutral axis coincides with the axis of gravity.
Thus an elastic redistribution is supposed.
The resulting bending moment is converted into a bending moment at the interface of end-plate and column-flange as described in chapter 4.1.2.

4.2.6. Failure of the beam due to bending

The forces F_{10} and F_{11} as discussed for the failure of the beam-web are restricted by the yielding of the beam-flange and the beam-web due to bending.
If the sum of the forces F_7, F_8 and F_9 is large enough to reach this situation, the bending moment is restricted by the plastic force distribution in the beam.
The resulting plastic moment is also converted into a moment at the interface of endplate and column-flange.

4.2.7. Failure of the column-web on the compression-side

The limit state design load of the compression side is determined by buckling of the column-web. This limit state design load is computed with the formula

$$\hat{F} = 5(r_c + r_{f_c}) + t_{f_h} * t_{w_c} * \sigma_{y_{w_c}} \qquad (13)$$

where: r_c = radius of the root of the column
t_{f_c} = thickness of the column-flange
t_{f_h} = thickness of the flange of the haunch
t_{w_c} = thickness of the column-web
$\sigma_{y_{w_c}}$ = actual yield stress of the column-web

This formula is the same as used in |4| and |5| for bolted-connections with extended end-plates.
It is thought to be unadvisable to apply a formula which takes into account the spreading effect of the end-plate, because the flange of the haunch is connected to the edge of the end-plate.
Moreover, shrinkage of the welds caused bending of the end-plate.
This unfavourable effect for the deformation of the connection was minimized in tests 1 and 2 by inserting a shim in the gap between end-plate and column. The shim had a width of 20 mm.
In tests 3 through 5 the end-plate was counter-bended before welding so as to give a straight alignment of the end-plate after shrinkage occurs.

The limit state design loads of the column-webs with doubler plates are computed with a formula which takes into account half the plate thickness as described in |4| and |5|.

Thus $\hat{F} = \{5(r_c + t_{f_c}) + t_{f_h}\} \; t_{w_c} * \sigma_{y_{w_c}} + \frac{t_{p_{w_c}}}{2} \; \sigma_{y_{p_c}}$ (14)

where: $t_{p_{w_c}}$ = thickness of the web doubler.

4.2.8. Failure of the haunch

4.2.8.1. Haunch with flange

The force on the compression side of the column should be transferred by the haunch into the beam.
For the haunches stiffened with flanges this is assumed to occur by means of axial forces through the haunch-flange and the end-plate as indicated in figure 23.

It should be checked whether:
- the force $\frac{Fc}{\cot \alpha}$ can be transferred by the end-plate
- the force $\frac{Fc}{\cos \alpha}$ or $\frac{Fb}{\cos \alpha}$ can be transferred by the haunch-flange
- the force $\frac{Fb}{\cot \alpha}$ can be applied at the beam-web without failure due to buckling.

The latter check will be discussed in chapter 4.2.9.

The possibility whether the force $\frac{Fc}{\cos \alpha}$ or $\frac{Fb}{\cos \alpha}$ may be transferred by the haunch-flange depends not only on the flange-thickness and yield-strength but also on the effective width of the haunch-flange.
Without stiffeners in column or beam it is not possible to assume a complete contribution of the haunch-flange.
In |7| a formula is given to determine the limit state load of the connection as shown in figure 24.

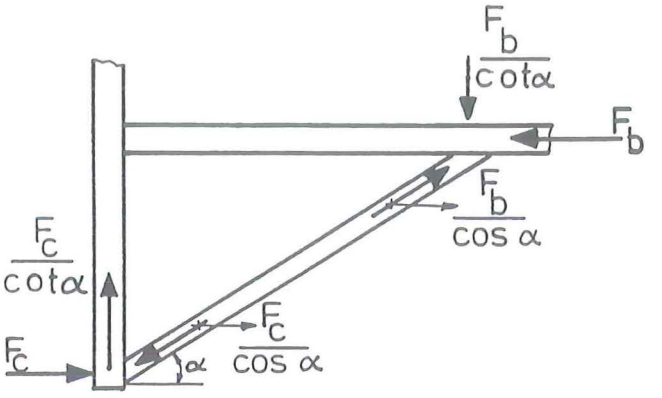

Fig. 23.: Distribution of the compressive force into the haunch-flange and the end-plate

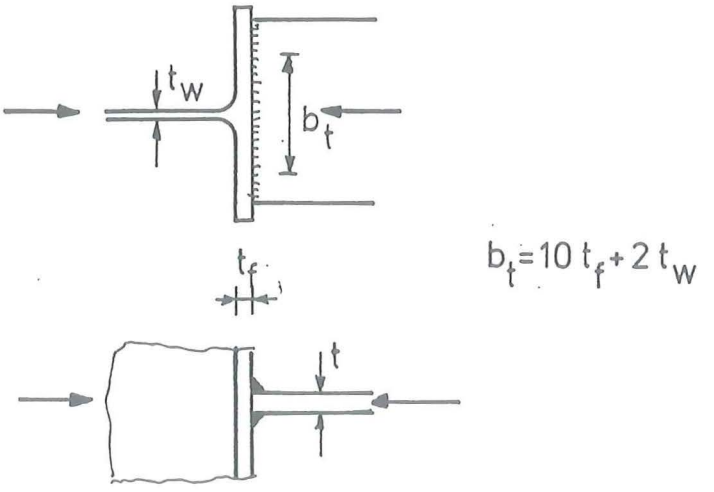

Fig. 24.: Effective width of haunch-flange according to |7|

This same formula may be used for the effective width of the haunch-flange on the beam-side.
This results in:

$$\hat{F}_b = \{10t_{f_b} + 2t_{w_b}\}\ t_{f_h} * \sigma_{y_{f_h}} * \cos\alpha \qquad (15)$$

where:

t_{f_b} = thickness of the beam-flange
t_{w_b} = thickness of the beam-web
t_{f_h} = thickness of the haunch-flange
$\sigma_{y_{f_h}}$ = actual yield stress of the haunch-flange
$\hat{F}_b$ = limit state design load of the haunch at the beam-side.

On the column-side, the effective width may be increased with the thickness of the end-plate, thus:

$$\hat{F}_c = \{10(t_{f_c} + t_e) + 2t_{w_c}\}\ t_{f_h} * y_{f_h} * \cos\alpha \qquad (16)$$

where:

t_{f_c} = thickness of the column-flange
t_e = thickness of the end-plate
t_{w_c} = thickness of the column-web

Naturally, the effective width can never be larger than the width of the haunch itself, thus:

$$\hat{F}_c = \hat{F}_b = b_{f_h} * t_{f_h} * \sigma_{y_{f_h}} * \cos\alpha \qquad (17)$$

where: b_{f_h} = width of the haunch-flange.

4.2.8.2. Haunch without a flange

For haunches which are not stiffened with flanges, the following aspects hold true.
The compression force introduces forces in part of the haunch as indicated in figure 25.

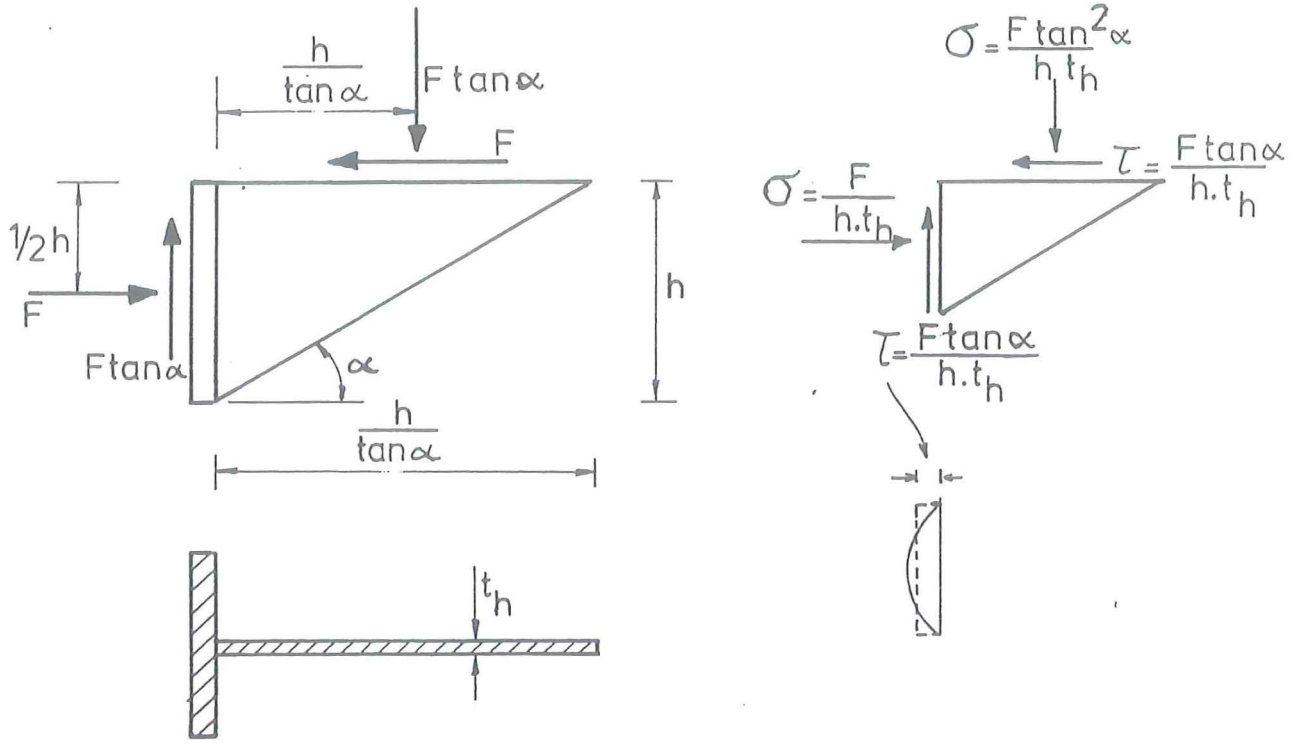

Fig. 25.: Force and stress distribution for a haunch without a flange.

This force distribution introduces shear and normal stresses in the haunch which may be approached with the following formulae:

$$\tau = \frac{F \tan \alpha}{h * t_h}$$

$$\sigma_x = \frac{F}{h * t_h} \qquad \sigma_y = \frac{F \tan^2\alpha}{h * t_h}$$

where the definitions of the parameters are given in figure 25.

Thus:
$$\sigma_{yh} = \sqrt{\left(\frac{F}{h*t_h}\right)^2 + 3\left(\frac{F*\tan\alpha}{h*t_h}\right)^2} + \left(\frac{F\tan^2\alpha}{h*t_h}\right)^2 - \left(\frac{F\tan\alpha}{h*t_h}\right)^2$$

$$\hat{F} = \frac{h*t_h*\sigma_{yh}}{\sqrt{1+ 2\tan^2\alpha + \tan^4\alpha}} \qquad (18)$$

$$\hat{F} = (h * t_h * \sigma_{yh})\cos^2\alpha$$

To give an impression of the values for $\hat{F}$ with various slopes of the haunch some values are given.

$\tan \alpha = 1$ $\quad \hat{F} = 0.5h * t_h * \sigma y_h$

$\tan \alpha = \frac{1}{2}$ $\quad \hat{F} = 0.80 * t_h * \sigma_{yh}$

$\tan \alpha = \frac{1}{3}$ $\quad \hat{F} = 0.90 * t_h * \sigma_{yh}$

$\tan \alpha = \frac{1}{4}$ $\quad \hat{F} = 0.94 * t_h * \sigma_{yh}$

An additional load transferred by bending of the end-plate may be taken into account because complete yielding of the haunch is assumed.

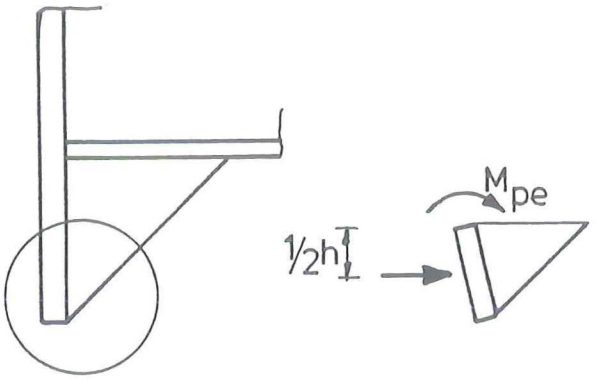

Fig. 26.: Bending of the end-plate restrains yielding of the haunch

Thus: $$\hat{F} = \frac{h.t_h.\sigma_{yh}}{\sqrt{1+3\tan^2\alpha}+\tan\alpha} + \frac{2M_{pe}}{h} \qquad (19)$$

$$\hat{F} = (h\ t_h.\sigma_{yh})\cos^2\alpha + \frac{2M_{pe}}{h}$$

Because the limit state design load mainly depends on the assumed height h, formula (19) determines where the resultant of the compressive force should be taken.

The absolute value of the limit state design load is determined by the forces transferred by the bolts or by the limit state design load due to buckling of column-web.

At the beam-side of the haunch another situation exists.
The force computed with the failure mechanism due to shear of the web on the tension side should be in balance with the force transferred

by the haunch as shown in figure 27.

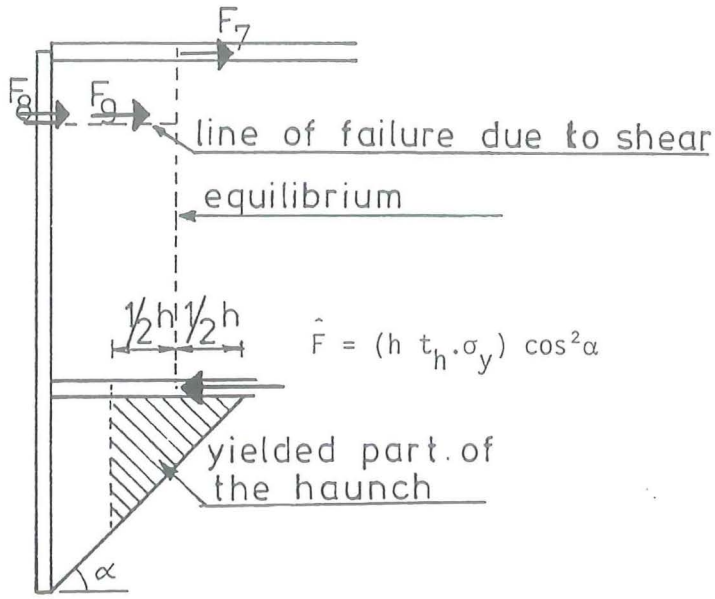

Fig. 27.: Equilibrium between the forces on the compression- and tension-side determines the magnitude of the forces

The length of the distance, h, should be computed such that equilibrium between the force on the tension-side and compression-side is reached. Thus the computation of the forces is an iterative process in which the length h should be chosen such that the value F computed with formula (18) should be balanced by the sum of the forces F_7, F_8 and F_9 as described in chapter 4.2.5.

4.2.9. Failure of the beam-web due to compression

Formula (13) used for buckling of the column-web may also be applied to check failure of the beam-web due to the vertical component of the force transferred by the haunch.
Tests carried out earlier |8| showed, however, an influence of the bending stress on the failure of the web.

The limit state design load will be computed with and without reduction due to bending moment.

The computation with reduction can only be carried out iteratively, because the reduction formula is:

$$\hat{F} = (1.25 - 0.5 \frac{\sigma}{\sigma_y}) \hat{F}_w \qquad (20)$$

where:

σ = a bending stress which depends on the value of $\hat{F}$
$\hat{F}_w$ = limit state design load of the web without reduction
σ_y = actual yield stress of the beam-flange
$\hat{F}$ = limit state design load of the web with reduction

Formula (13) and (20) can be reduced to a single formula by resolving the force components as shown in figure 23.

$$\hat{F}_b = (1.25 - 0.5 \frac{\hat{Fb}}{Fy_f}) \cot\alpha \ \{5(tf_b + r_b) + tf_h\} \ \sigma y_w * t_{wb} \qquad (21)$$

where:

$\hat{F}_b$ = limit state design load of the beam-flange
F_{y_f} = yield force of the beam-flange
$\cot\alpha$ = slope of the haunch
tf_b = thickness of the beam-flange
r_b = radius of the root of the beam
tf_h = thickness of the haunch-flange
σy_w = actual yield stress of the beam-web
t_{wb} = thickness of the beam-web

Thus the computation of the limit state design load due to buckling of the beam-web with reduction induced by bending is an iterative process.

4.2.10. Failure of the beam-flange

In the failure mechanism of the tension-side it is assumed that in the beam-section where the haunch starts, a linear strain distribution is present.
Thus the actual load of the beam-flange on the compression side is assumed to be equal to that of the beam-flange on the tension-side. The limit state design load of the beam-flange on the compression side is taken equal to the load which causes yielding of the beam-flange. This is done despite the situation, that buckling of the beam-flange may be initiated by the deformation caused by the haunch-flange if no stiffeners are used(see fig
Thus the chance of buckling depends on the dimensions of the haunch-flange.

However, this is the same situation as exists in the column-flange of the unstiffened welded beam-to-column connection.
The limit state design bending moment of this situation is governed by the limit state design loads of the failure mechanisms due to buckling of the beam-web and/or yielding of the haunch.

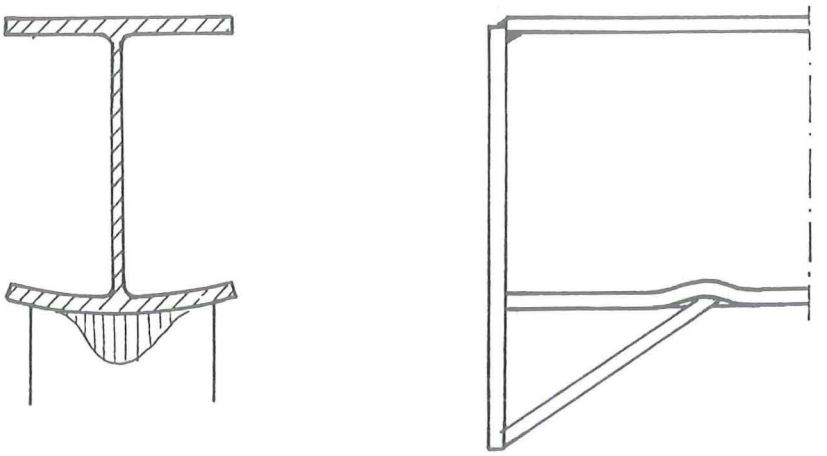

Fig. 28.: The haunch-flange may initiate buckling of the beam-flange if no stiffeners are used.

Test number and end-plate thickness	Limit state design moments		Actual ultimate moment.	Determining failure mechanisms and remarks.
	Column and end-plate	Beam and haunch		
	kNm	kNm	kNm	
(1)	(2)	(3)	(4)	
1 - 15,3	249	212	287 310	Shear of the beam-web 310kNm was ultimately reached after strengthening of beam and column web
1 - 20	257	240	293 330	Shear of the beam-web 330 kNm was ultimately reached after strengtening of beam and column web
2 - 13	142	179	235	Tension beam - web uppermost bolt Bending end-plate other bolts.
2 - 20	178	220	235	Tension column-web uppermost bolt Bending end-plate other bolts.
3 - 18	272	398	380	Tension beam-web uppermost bolt Bending end-plate second bolt Bending column-flange other bolts. (Shear of the beam-web).
3 - 21	300	412	382	Bending column-flange uppermost bolt. Bending end-plate second bolt. Bending column-flange other bolts. (Shear of the beam-web).
4 - 18	235	226	322	Shear of the beam-web.
4 - 21	235	262	315	Bending column-flange.
5 - 18	302	250	345	Shear of the beam-web and the haunch.
5 - 21	356	285	328	Shear of the beam-web and the haunch.

Table 4. Limit state design moments at interface of column and beam with determining failure mechanisms.

Failure mechanism with component of the connection.	Test number and end-plate thickness.									
	1-15	1-20	2-13	2-20	3-18	3-21	4-18	4-21	5-18	5-21
(1)	(2)	(3)	(4)	(5)	(6)	(7)	(8)	(9)	(10)	(11)
1. Tension column-web.										
Uppermost bolt	0.66	0,62	1,58	1,32	1,05	0,97	0,66	0,65	0,36	0,32
Second bolt	0,45	0,66	0,50	0,84	0,36	0,52	0,66	0,65	0,38	0,33
Other bolts	0,61	0,66	0,62	0,76	0,68	0,63	0,66	0,65	0,35	0,33
2. Bending column-flange.										
Uppermost bolt	1,15	1,14	1,32	1,10	1,38	1,27	1,37	1,34	1,04	0,92
Second bolt	0,78	1,14	0,78	1,32	0,47	0,69	1,37	1,34	0,78	0,92
Other bolts	1,05	1,14	1,08	1,32	1,40	1,27	1,37	1,34	0,98	0,92
3. Bending end-plate										
Uppermost bolt	0,87	< 0,81	1,36	< 1,14	0,90	< 0,83	0,67	< 0,65	0,74	< 0,65
Second bolt	1,15	0,99	1,65	1,18	1,40	1,27	1,34	0,82	1,14	0,85
Other bolts	1,15	0,75	1,65	0,87	1,09	0,63	1,07	< 0,82	1,14	< 0,85
4. Tension beam-web.										
Uppermost bolt	1,05 0,97	1,01** 0,90	1,65	1,05	1,40	1,11	1,03	0,87	1,14	0,87
Second bolt	0,59	0,64	0,50	0,49	0,69	1,00	0,66	0,64	0,71	0,67
Other bolts	0,59	0,64	0,62	0,76	0,67	0,62	0,66	0,64	0,71	0,67
5. Shear beam-web	1,35 1,46*	1,22 1,40**	1,31	1,07	0,95	0,84	1,42	1,20	1,17	0,98
6. Beam Tension-side.	0,88	0,91	0,58	0,58	0,95	0,93	0,98	0,96	1,00	0,96
7. Buckling column -web	1,15	1,14	1,22	1,26	0,89	0,87	0,77	0,76	0,81	0,77
8a. Haunch at column	1,02	1,00	0,56	0,53	0,87	0,85	0,77	0,57	1,14	0,92
8b. Haunch at beam	0,94	0,97	0,89	0,89	0,81	0,79	0,67	0,66	n.a	n.a
9. Buckling beam-web.	1,02*	1,03*	0,66	0,66	0,71	0,69	n.a	n.a	n.a	n.a
10. Beam Compression -side.	0,88	0,91	0,58	0,58	0,95	0,93	0,98	0,96	1,00	0,96

Remarks: * Without strengthening-plate added during testing and computed with reduction due to bending.

** after strengthening.

Table 5. Ratios between actual ultimate loads and limit state design loads.

5. RESULTS

5.1. Computation

The results of the computation are given in appendix A2 (page 83).
Tables 2 and 3 at pages 21 and 22 give a summary of the computation.
Table 4 at page 45 gives the failure mechanism which determine finally the limit state design bending moment of a test-specimen.
However, the actual moments were larger than the limit state design loads
This implies that more failure mechanisms came successively into being during the increase of load.

That is why the ratios between the actual loads and limit state design loads of all possible mechanisms are summarized in table 5 at page 46.
The ratios are computed as follows.
The limit state design loads used in the computation of the limit state design bending moments are multiplied by the ratio between the actual bending moment and the limit state design moment. The loads found in this way are then divided by the limit state design loads of the failure modes concerned. Table 5 gives the possibility to check which failure modes occurred successively provided that the design formulae used are the appropriate ones.

5.2. Boltforces

The results of the boltforce measurements are given in figures A3.1; A3.2 and A3.3. (pp. 115-117).
In figures A3.1 and A3.2 the moment-boltforce curves of the cornerbolts and additional bolts of testspecimens 1 and 2 are given.
The boltforces are averaged values of two bolts on both sides of the column-web.
The moment-boltforce curves of the other specimens are not given, because they are not important for the review of the behaviour of the testspecimens.

Instead of the moment-boltforce curves, figure A3.3, gives a review of the boltforce distribution at specific bending moments. Again these boltforces are averaged values of two bolts on both sides of the column-web.

5.3. Deformations

The deformations are presented in moment-deformation graphs in figures A3.4 through A3.19. (pp. 118-128).
The deformations are averaged of the two values measured at either side of the column-web.
In each figure it is indicated which deformation the graph refers to.

Figures A3.4 through A3.8 give all the moment-deformation relationships of the deformations measured.(pp. 118-122)

Figures A3.9 through A3.13 give an impression of the rotations of the connections. (pp. 123-125)
These rotations are converted from the deformations measured between the centre line of the column and the end-plate at the centre height of the upper- and lower beam-flanges.
The actual rotations of the connections were larger due to the deformations over the haunched part of the beam, but those were not measured.
The limit state design loads of the connections are indicated in these moment rotation curves.

Figures A3.14 through A3.19 give the moment-deformation curves related to specific failure modes. (pp. 126-128)
These moment-deformation curves are converted from the deformations measured. The curves of all specimens are gathered in one figure to facilitate comparisons.
The limit state design load of the failure mechanism which the curve refers to is also indicated.

6. DISCUSSION OF THE RESULTS

6.0. General

Firstly a review of the failure modes is given on the basis of the moment-deformation curves in figures A3.14 through A3.19.

This is followed by a review of the behaviour of the tests using the ratios between actual and limit state loads summarized in table 5.

Next the measured boltforces are compared with the computed ones.
Finally the limit state design bending moments are compared with the moment-rotation curves and the values computed with a former design method [5].

6.1. Comparison of limit state design loads with deformation curves

6.1.1. Column-web (tension side at first boltrow) (Figure A3.14, page 126)

Figure A3.14 gives moment-deformation curves measured on the uppermost boltline.
A comparison of these curves with the limit state design loads (indicated in the figures) shows no good agreement between the test-results and the computation method.
This is especially true for test 2 and test 4.

According to table 5 the ratio between actual load and limit state design load of test 2 is such that yielding of the column web should have occurred. The photograph of test 2 in figure 4 shows that crumbling of the white-wash occurred in the column-web, but mainly between the innermost bolts. This suggests that a redistribution occurred whereby the forces of the innermost bolts increased.
This might be caused by a decrease of the uppermost boltforces as a result of shear in the beam web. This is suggested by the ratios in table 5.

The photograph of test 4 in figure 4 shows that an extremely large bending of the column-flange occurred which was probably partly included in the measurement of the deformation of the web as given in figure A3.14.

6.1.2. Column-flange (bending) (Figure A3.15, page 126)

Figure A3.15 gives moment-deformation curves measured on the uppermost boltline. A comparison of the curves with the limit state design loads for bending gives the impression that the computation methods is in good

agreement with the actual situation, with the exception of test 3.
This can be explained by the fact that the distance between bolt-head and stiffener was so small that the load caused flange deflections due to shear and not due to bending.
This phenomenon has already been observed in other tests |2| , and is confirmed by the fact that crumbling of the whitewash was slightly present as shown in the photograph of fig. 4.(page 10)
Figure A3.16 gives the sum of the deformations due to tension of the column-web and bending of the column-flange on the uppermost boltline
It is evident that the deformations of the column-components on the uppermost boltline are smaller, with smaller thickness of the end plate.
This confirms the idea that redistribution occurs when the uppermost bolts have reached the limit state load of the end plate.

6.1.3. Tension or shear in the beam-web (Figure A3.17, page 127)

The mechanisms of tension and shearfailure in the beam-web are not separable. They interact and measurement of the deformations due to one of the mechanisms is impossible.
Despite this phenomenon the limit state design load of large deformations may be approached computing the failure mechanisms separately (see figure A3.17).
Apparently the lower limit state load initiates the large deformations.

6.1.4. Buckling of the column-web (Figure A3.18).

Comparison of the moment-deformation curves of test 3, 4 and 5 with that of test 1 in figure A3.18 shows an improvement of the strength capacity due to the web doubler plates welded according to the simple method as described in the introduction.
However, improvement occurs only when plates are applied on both sides of the column-web as it is shown in the result of test 2.
In that test the plate was only present on one side. Buckling occurred at a load which was 26% higher than the limit state load computed without taking into account the plate, but 74% lower than the value computed with

an assumed contribution of the plate.
Theoretically the plate on one side of the column-web may even initiate a buckling because the transfer of the load occurs eccentrically with respect to the centre of gravity of the cross-section.
Former tests |9| showed this unfavourable effect would not be harmful when the plate was welded as shown in figure 2.

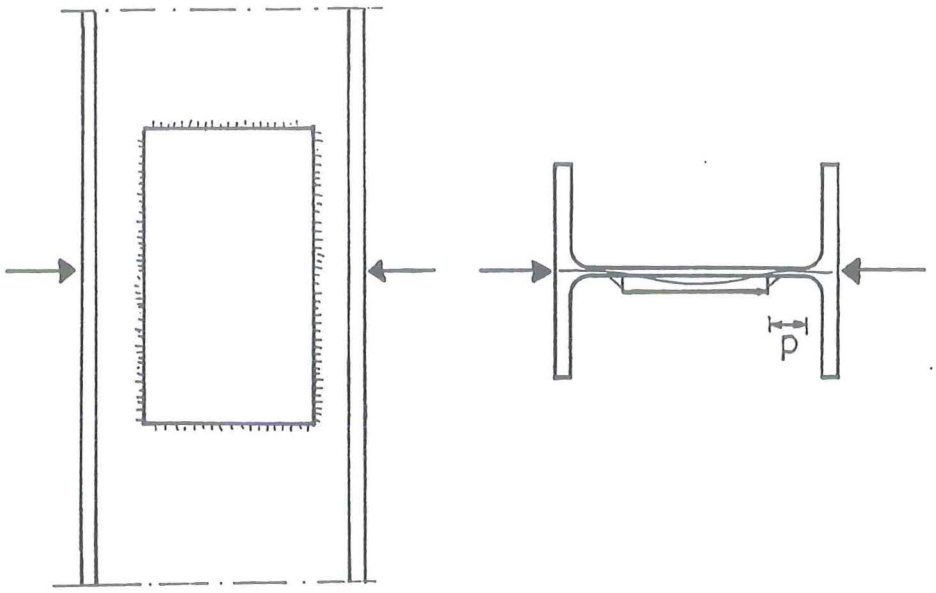

Fig. 29.: The transfer of load occurs eccentrically with respect to the centre of gravity if one plate is attached.

The influence of the distance p (see figure 29) is questionable because the development of large deformations had already started in test 3, 4, and 5 before the limit state design load was reached.
For a thoroughly research in this behaviour, it may be better checked with detail tests.
It is evident that deformations of other parts of the connections influence the behaviour as is shown by the result of test 4 where the larger deformations occurred probably because the beam-web was stiffened.

6.1.5. Haunch-flange on the column-side (A3.19, page 128).

In figure A3.19 the difference between the deformations of the column-web and the end-plate are given.
It is true that in these deformations the closure of the gap between end-plate and column are also incorporated.
Despite this phenomenon the curves give an impression of the deformations of the haunch-flange by comparing them with the results of test 5 where no haunch-flange was present.
The limit state design loads due to yielding of the haunch are too large with respect to the loading, so, no conclusion can be drawn about the adequacy of the computation method.

6.2. Comparison of the ratios of table 5 with the testresults

6.2.0. General

As already stated, table 5 gives the possibility to check which failure modes occurred successively provided that the formulae used to determine the limit state design loads are the appropriate ones.
A ratio larger than unity means that the actual ultimate bending moment was that factor larger than the bending moment present at the instant that the limit state design load was reached.

It appears from the table e.g. that the limit state design loads for bending of the column-flange at the corner bolt are exceeded for all specimens except of test 5.

However, for test 2-13 tensile failure in the column-web was obviously more harmful than failure due to bending of the column-flange, whereas failure at the corner bolt due to tension in the beam-web together with bending of the end-plate on the second and other bolts ultimately determined the limit state moment.
This conclusion is drawn by checking column (4) of table 5 where all the factors of test 2-13 are summarized.

6.2.1. Testspecimen 1

Strengthening of the beam was necessary at a bending moment of about 260 kNm because crumbling of the whitewash gave the impression that buckling of the beam-web might occur.

This situation is shown in figure 4.

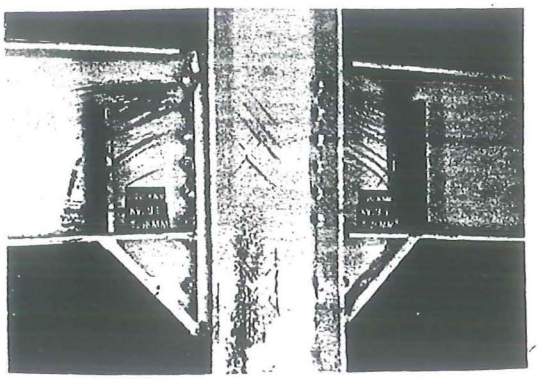

Fig. 30.: The beam-webs of test 1 have been strengthened to avoid web-buckling (~260 kNm).

The strengthening of the beam-web is shown in figure 30.
After strengthening, the bending moment was increased until buckling of the column-web at the compression-side prevented a further increase of the load (~290 kNm).
After unloading, the column-web was strengthened on the compression as well as on the tension-side by means of plates welded directly between the column-flanges.
Furthermore the beam-flanges were strengthened to avoid buckling which had already started to occur. This situation is shown in the photograph of figure 31.

The phenomenon of flange buckling whereas yielding of the flanges had not started theoretically will be discussed with test 4 where the same effect was observed.

After strengthening it was tried to increase the load again, however, this is not shown in the moment-deformation graphs. The increase of loading was possible until a bending moment of about 310 kNm.
At that moment failure of the beam-web occurred due to shear and fracture of the weld between the 15 mm thick end-plate and the beam-flange as shown in fig. 32.

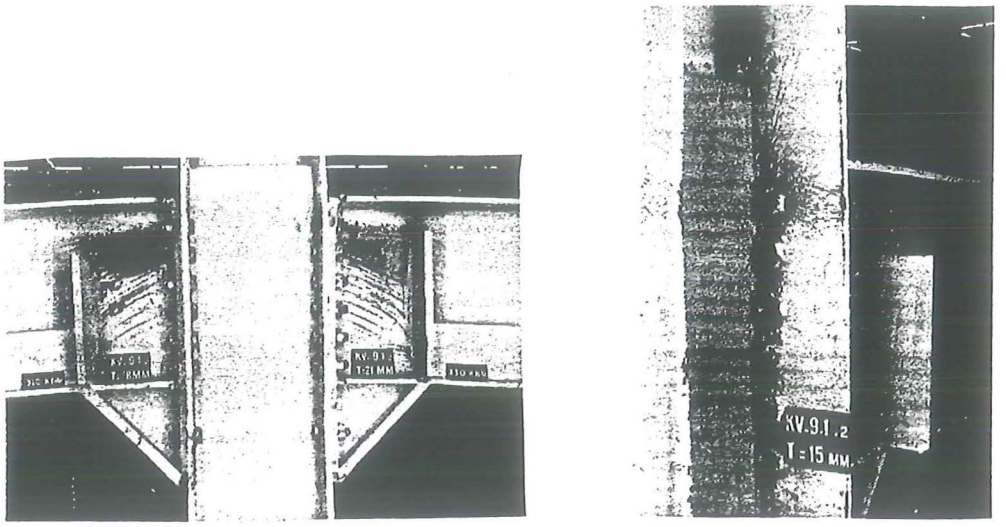

Fig. 31.: The column-web as well as the beam flanges of test 1 have been strengthened.

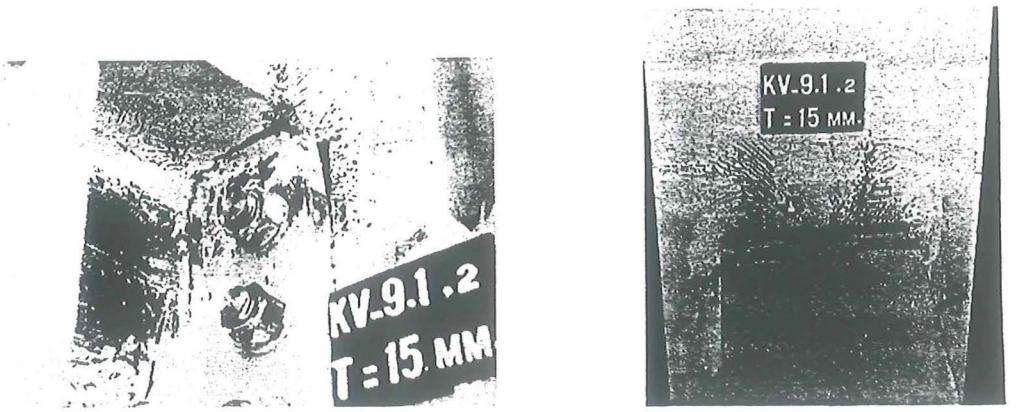

Fig. 32.: Fracture of the weld between the end-plate and the beam-flange occurred after complete yielding of the flange (M = 310 kNm).

The ratio between actual load and limit state design load of the welds computed according to chapter 4.2.3.2. was 1.05 at that moment.
The rotation of the connection was certainly more than 0.04 radians, thus sufficient rotational-capacity was reached at that moment.
This result and the results of the other tests gave the indication that sufficient rotational-capacity is reached when the dimensions of the welds are chosen according to chapter 4.2.3.2.
In the other tests the welds did not fracture at bending moments larger than 310 kNm.
The crumbling of the whitewash from the beam-web as visible in the photographs in figure 31 and 32 shows the presence of the failure mechanism due to shear in the beam web.

The behaviour of test 1 proves the actuality of the described failure modes as is shown by the photographs.

6.2.2. Test specimen 2

As appears from table 5, tension in the beam-web at the corner bolt and bending of the end-plate at the other bolts was theoretically the determining factor for the connection with the 13 mm - thick end-plate, but not for the connection with the 20 mm - thick end-plate.
The photographs in figure 33 show the situation of the end-plates after finishing the test and these pictures confirm the behaviour as

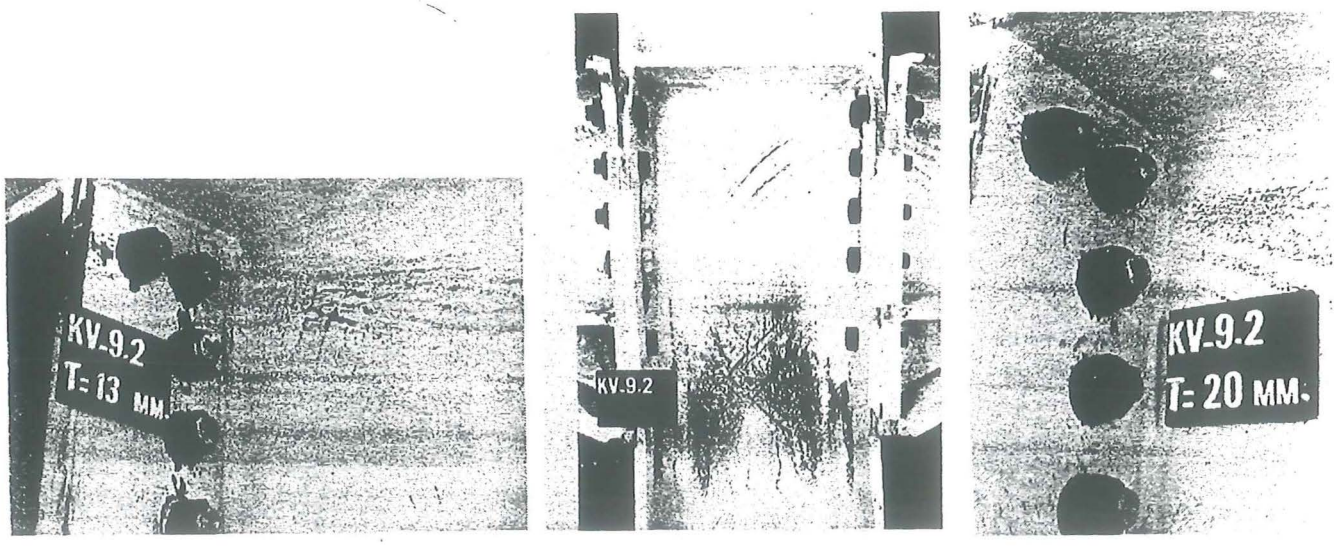

Fig. 33.: The 13mm-thick end-plate of test 2 failed whereas with the 20mm thick end-plate failure occurred due to bending of the column-flange.

expected from table 5 and described previously.
The photographs of figure 34 show the failure of the various components of the column to be in agreement with the ratios indicated in table 5.

As already shown in figure 18 and here in figure 34, the welds which are designed according to chapter 4.2.3.2. have a large deformation capacity.

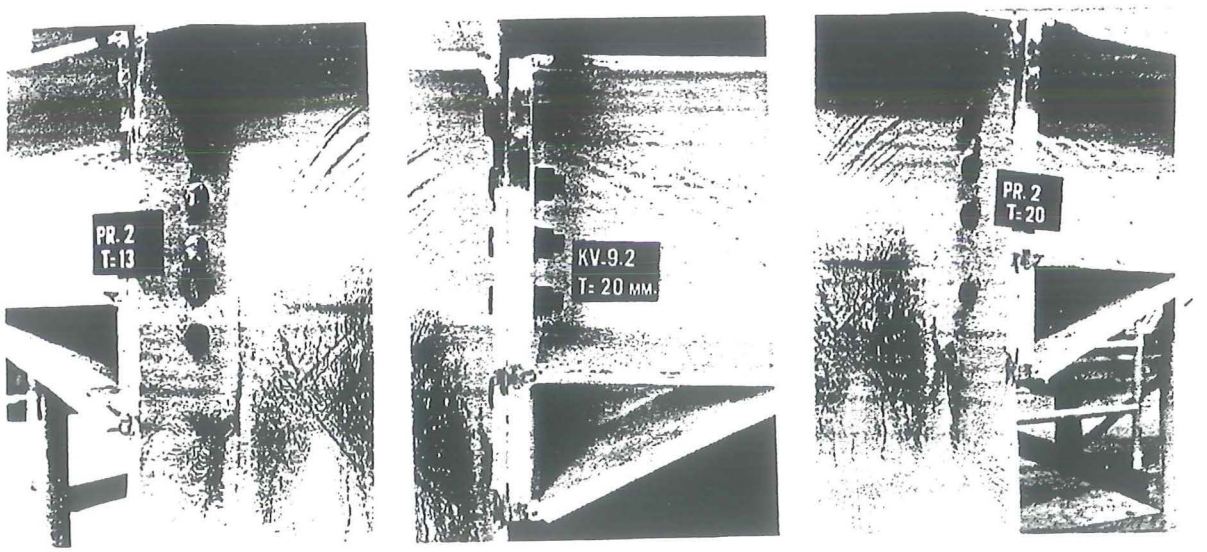

Fig. 34.: The yielding of the column-components shown by crumbling of the whitewash.

6.2.3. Testspecimen 3

The photograph in figure 35 shows that failure occurred ultimately by buckling of the beam-flange on the compression side.

This seems to be in contradiction with the ratios stated in table 5. According to this table test 3-18 should have failed due to a combination of tension in the beam-web at the uppermost bolt, bending of the end-plate at the second bolt and bending of the column-flange at the other bolts.

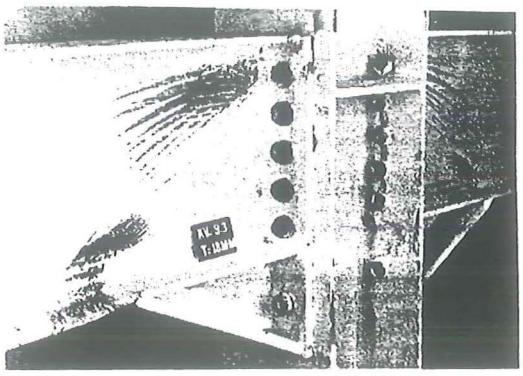

Fig. 35.: Failure of test 3 by buckling of the beam-flange.

The photograph shows that yielding of the beam-web occurred significantly. It is possible that due to this yielding a redistribution of stresses occurred in the beam-section where the haunch flange is connected to. The result might be a sinking of the neutral-axis and an increase of the stresses in the beam-flange.
Thus the conclusion is that failure occurred due to buckling of the beam-flange introduced by yielding of the beam-web which was caused by a combination of tension and shear.
This behaviour is however sufficiently limited by the limit state design load for tension in the beam web.

The failure of the connection with the 21 mm thick end-plate is already discussed in the chapter concerning the failure mode of the column-flange due to bending (6.1.2.).
It was concluded there, that the column-flange may transfer a larger load owing to the small distance between bolt-heads and column-stiffener.
In that case failure occurs due to tension of the beam-web.

6.2.4. Testspecimen 4

The failure modes of buckling of the column-web and beam-web were prevented from the beginning by strengthening with plates.
This is why the behaviour of this testspecimen should be comparable with the results of test 1 as far as buckling of the beam flange is concerned.
This behaviour was confirmed.

Buckling of the beam-flange occurred at a bending moment at the interface of about 280 kNm.
This corresponds with a stress of about 225 N/mm^2 at the most stressed fibre of the beam if a linear stress distribution is assumed(see fig. 37).
The latter assumption is however questionable.
According to table 5 failure due to shear in the beam-web at the uppermost boltline was already present before buckling occurred.
This is not only theoretically true but also proved by the crumbling of the whitewash as shown in the photograph in figure 4 and in the photographs in figure 36.

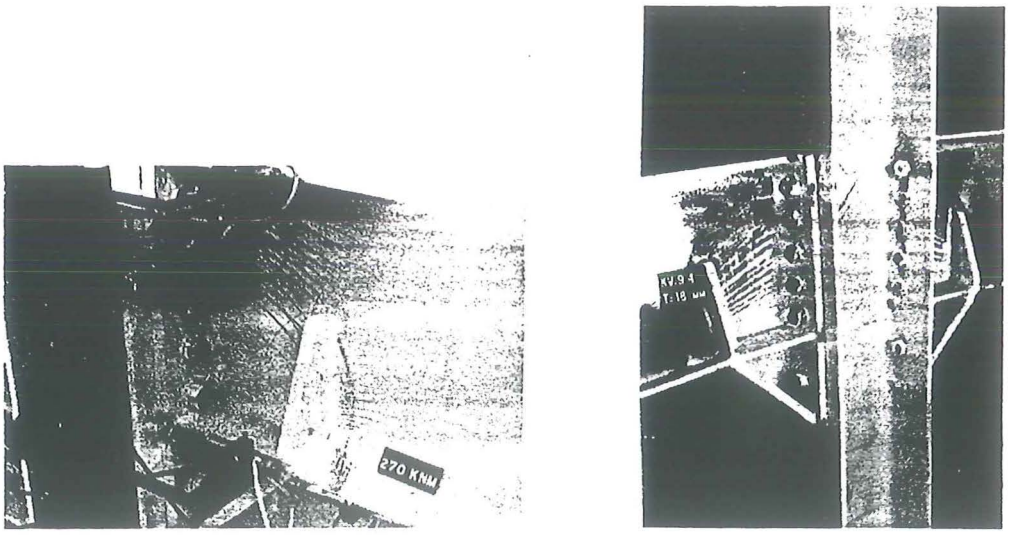

Fig. 36.: Yielding of the beam-web due to a combination of shear and tension with buckling of the beam-flange on the compression-side.

It is evident that it is not correct to assume an elastic stress distribution when the web has already yielded.
In order to get a general idea about the force distribution in the haunched part of the beam an approximation of the shear and tensile forces has been made as shown in figure 37.
The assumptions are a linear stress distribution in the beam-section where the haunch starts and equilibrium of the forces in the horizontal direction.
The limit state loads due to shear are indicated in brackets.

It follows from the figure that the limit state loads are exceeded.
This implies a redistribution whereby the stresses on the tension-side should decrease in the vicinity of the flange and should increase in the centre of gravity of the cross-section.

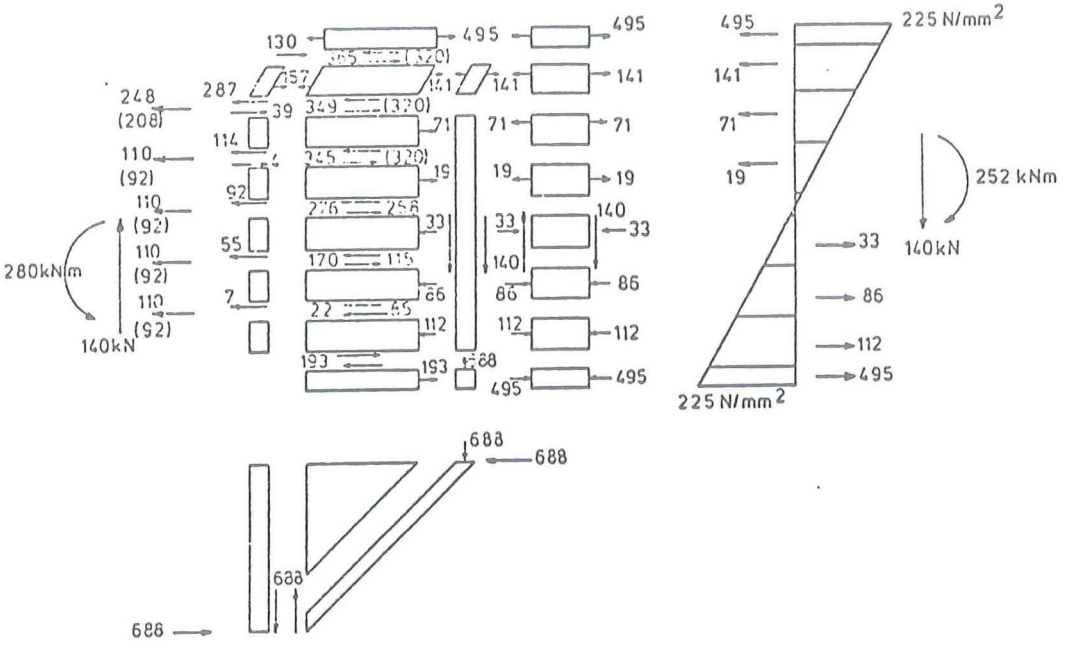

Fig. 37.: Assumed force-distribution in the haunched part of the beam when buckling of the beam-flange occurred.

The result is that the lever-arm between the forces on the compression- and tension-side decreases.
An increase of the stresses on the compression-side is necessary to reach a balance of forces.
Thus the stresses in the beam-flange might be much higher than the assumed ones.
Again, as already stated with test 3, it could be concluded that failure due to buckling of the flange is introduced by failure on the tension-side due to shear in the beam-web.
The limit state load is ultimately restricted by the latter failure mode.

The crumbling of the whitewash on the tension-side of the column-web, as can be seen in the photographs, can also be explained by the previous analysis.
Owing to the redistribution, the uppermost bolt does not get the force as assumed. This implies that the other bolts should transfer more.

6.2.5. Testspecimen 5

The photograph in figure 4 shows that yielding occurred in the haunch-plates and in the beam-web.
This is completely in agreement with the assumptions made in the computation.

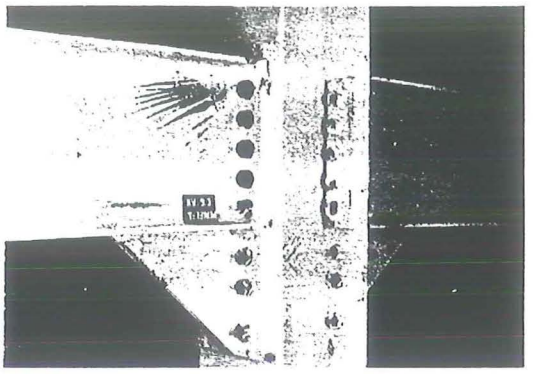

Fig. 38.: Yielding patterns of test 5.

Failure due to the bending of the end-plate as suggested by the computation of the limit state design load of the other bolts is not confirmed by crumbling of the whitewash as is shown in figure 38.

The crumbling of the whitewash on the compression-side of the column-web just above the web doubler plate (see figure 4) shows that the location of the reaction force has risen due to the yielding of the haunch-plate as assumed in the computation.

The crumbling of the whitewash from the beam-web just above the start of the haunch indicates that the force, introduced from the haunch, is not concentrated. This is favourable in order to avoid buckling of the beam-web. It seems to be a good approach when the thickness of the haunch-plate is chosen such that the limit state design loads per unit length of the haunch and that of the beam-web are balanced.

6.3. Boltforces

The review of boltforces measured at specific bending moments as given in fig. A3.1. shows that:

- there is no linear relationship between the boltforce and its distance to the reaction point (as expected before the tests were carried out), and
- the second bolt from the upperside has often got a lower boltforce than the other bolts.

The linear force distribution was expected because the distance p between bolthead and the toe of the root was smaller than 1.25 times the thickness of the column-flange, as described in chapter 1.0.

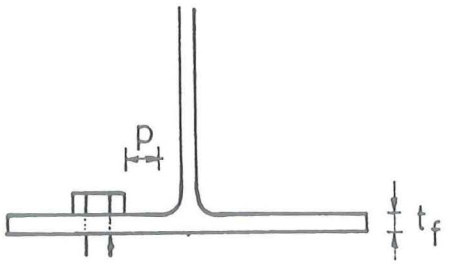

Fig. 39 : The distance p between bolthead and toe of the root was smaller than 1.25 * t_f

The result shown in figure A.3.1. was the reason to compute the limit state design loads of flange and end-plate in combination with the bolt in accordance with formulae (4) and (5).
In figure 40, a comparison is made between the measured boltforces and the boltforces computed according to formulae (4) and (5) or formula (7).

	Measured boltforce in kN		Computed boltforce in kN	
	247 145 150 138 96 68	196 121 99 92 95 37	180(175) 57 78 78 78 54	156(147) 68 68 68 68 12
Testnumber	1-15	1-20	1-15	1-20
Actual moment	280 kNm	273 kNm	280 kNm	273 kNm
	137 242 92	80 190 108	48 216 51	52 162 82
Testnumber	2-13	2-20	2-13	2-20
Actual moment	235 kNm	235 kNm	235 kNm	235 kNm
	290 124 167 164 139	275 200 140 163 117	194(228) 99 92 92 92	177(228) 144 84 84 84
Testnumber	3-18	3-21	3-18	3-21
Actual moment	380 kNm	382 kNm	380 kNm	382 kNm
	298 148 170 147 142	278 129 225 157 152	200(228) 88 88 88 88	196(228) 86 86 86 86
Testnumber	4-18	4-21	4-18	4-21
Actual moment	322 kNm	325 kNm	322 kNm	315 kNm
	295 148 190 228 188	290 132 206 185 156	252(231) 77 101 101 101	213(231) 98 98 98 98
Testnumber	5-18	5-21	5-18	5-21
Actual moment	345 kNm	328 kNm	345 kNm	328 kNm

Fig. 40. Comparison of measured and computed boltforces.

The computed boltforces are the limit state design loads either of column flange or end plate, increased with the prying action according to the computed values multiplied by the factor between actual bending moment and limit state design moment.
The values in brackets are the limit state design strengths of the bolts (0.7 times the actual fracure load).
Obviously the actual loads are much higher than the computed boltforces.
Apparently the prying action is much higher than that assumed in the computation.
This may be explained by the effect of strain-hardening in the plastic hinge formed in the boltline or a smaller distance from the boltline to the assumed point of action of the prying force.
This effect might be harmful for the connection if a large rotational capacity is required. However, it appeared,e.g. from the result of test 1,that a redistribution of forces occurred when the uppermost bolt reached the region of plastic deformations in the vicinity of the fracture load.
The uppermost bolts in the other tests did not reach the fracture load but evidently they reached the region of plastic deformations independent of what end-plate thickness was used.
This favourable behaviour might only be reached with grade 8.8 bolts.

6.4. Limit state design moments

In the moment-rotation curves in figures A3.9 through A3.13 the limit state design bending moments are indicated.
All limit state design bending moments are at the end of the elastic state of the connection while already some plastic deformation has occurred.
They have definitely not too high values for limit state design.

The limit state design moments are also compared with the limit state design moments computed according to the method described in |5|.
At the moment that the latter method was developed, only the testresults of |10| were available.
It was then decided to base the limit state design moment on the limit state design strength of the second bolt and to assume a linear distribution of forces over the bolts as shown in figure 41.

These assumptions were made, because it was expected that the uppermost bolt could transfer more load than the second bolt, due to the support of beam-flange and beam-web.
However a method to compute this load was not known.
Table 6 gives the limit state design bending moments of this former method and the method used in this report, the difference is expressed as a ratio between the values.

It is evident that the new method gives better results.

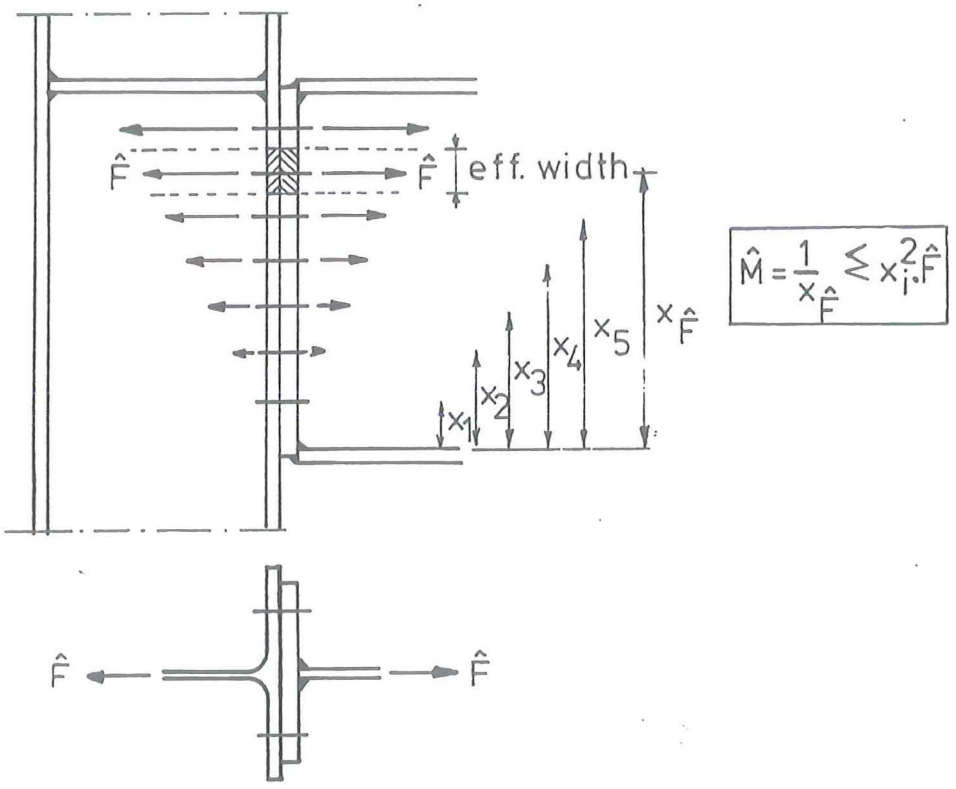

Fig. 41.: Computation method according to |5|.

Test no with end-plate thickness	Limit state moments old method kNm	Limit state moments new method kNm	Difference Ratio New / Old
(1)	(2)	(3)	(4)
1-15	166	212	1.28
1-20	182	240	1.32
2-13	64	142	2.22
2-20	98	178	1.82
3-18	157	272	1.73
3-21	157	300	1.91
4-18	157	226	1.44
4-21	157	235	1.50
5-18	206	250	1.21
5-21	242	285	1.18

Table 6.: Comparison of the old and new design methods.

6.5. Conditions for the use of the design chart

The testresults show that the chart used for the design of stiffened column-flanges (figure 16), can only be used for flush-end-plates when the beam-web and flange do not fail.
This is why a check against shear failure or tensile failure of the beam-web with bending of the beam-flanges should be included in the design-method.
The results of tests 2 and 3 indicate that the check against tensile failure of the beam-web is satisfactory with the computation method as given in chapter 4.2.4.
The check against shear failure is only necessary with haunched beams.
This statement is proved with the help of figure 42.

6.5.1. Haunched beams

With haunched beams, the bending moment-capacity increases with the increase of the depth of the haunched part. Theoretically, this may be as indicated by the dotted line in the moment-capacity diagram of fig. 42a.
In practice, the bending moment at the end of the beam is determined by the moment-capacity of the end-plate and the material directly behind it.
In the haunched part, the moment-capacity is determined by the current of the forces which depends on the strength of the end-plate, the bolt configuration and last but not least the shear force capacity of the beam-web.

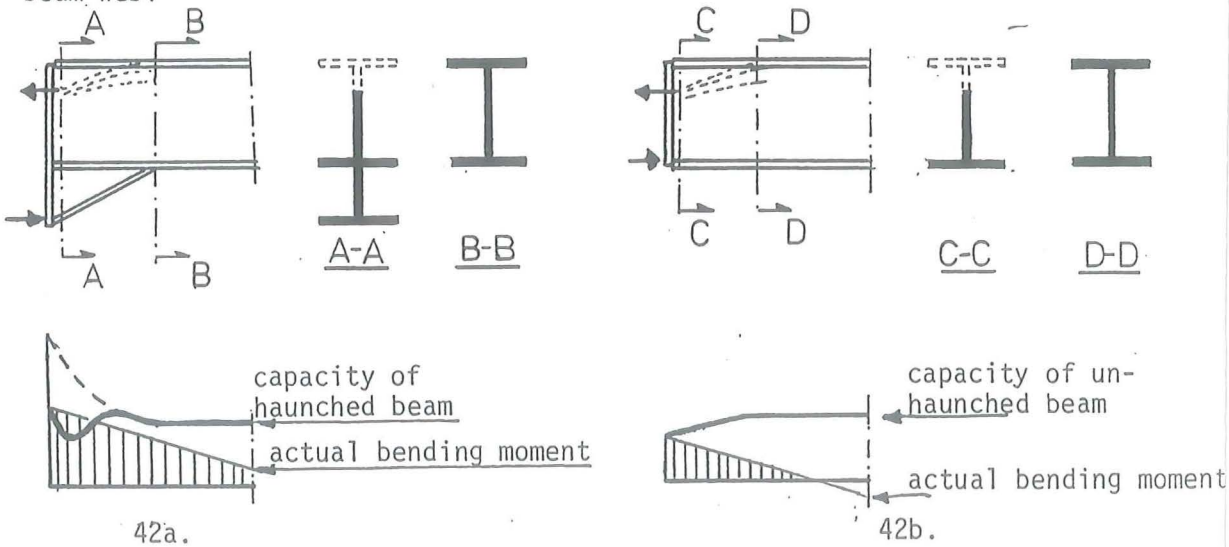

Fig.42: Comparison of active cross-sectional areas of haunched and unhaunched beams

Owing to this current of the forces, it is possible that the moment-capacity of the haunched part has the behaviour as indicated by the solid line in figure 42a. Initially an increase of the moment-capacity will occur due to the increase of the depth, but then a decrease occurs, because the upper flange of the beam does not contribute anymore in the transfer of the forces.

Finally the moment-capacity will increase again, because the influence of the increased depth becomes larger than that of the decrease of the active beam-web area.
The test results indicate that this behaviour is checked satisfactory with the computation method as given in chapter 4.2.5.

6.5.2. Unhaunched beams

The moment capacity of a connection of a beam without a haunch is completely determined by the moment-capacity of the end-plate with the material directly behind it (see fig. 42b).
In other cross-sections of the beam the difference between the moment-capacity and the actual bending moment is always larger.
Thus in that case a check of shear failure can be neglected.

6.6. Pre-tensioning, stiffness and rotational capacity.

6.6.1. Pre-tensioning

In some standards |12| and |13|, controlled tightening of the bolts is required as moreover the limit state design load is made dependent on the magnitude of the pre-tensioning.
This requirement is mainly meant to govern the deformation of the connection. Research of Bouwman |14| , showed that this purpose may only be reached with specific measures.
This is especially true with the use of flush-end-plates. This will be explained in the following sections.

6.6.1.1. Unfavourable situation

It is possible that the end-plates have the shape, as shown in figure 43, after pre-tensioning. This shape may have come into being after shrinkage of the welds.

The contact stresses due to the pre-tensioning are concentrated between the bolts.

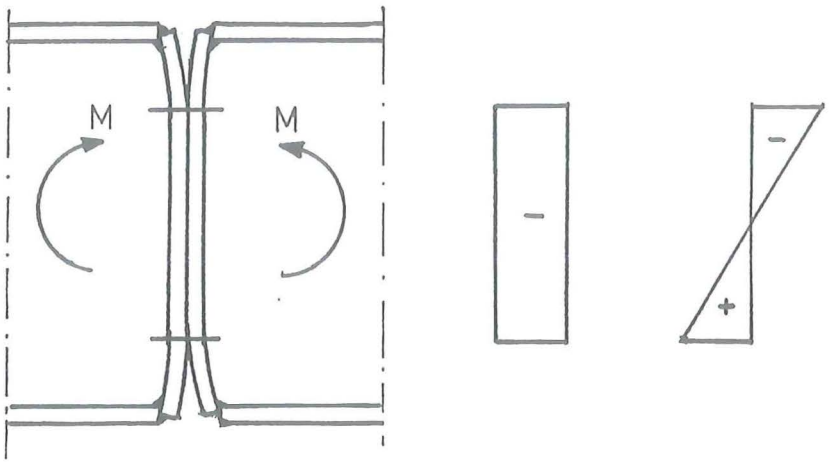

(a) (b) (c)

(a) Deformation of the end-plate after pretensioning.
(b) Contact stresses due to pretensioning.
(c) Stress distribution due to bending.

Fig. 43.: Unfavourable situation after pretensioning.

A bending moment acting on the connection is transferred by a change of the contact stresses.
An increase of the rotation between the boltlines occur when the contact stresses on the tension side are exceeded by the stresses due to bending or the yield stress on the compression side is exceeded.
In the outlined situation this will already occur with a small bending moment because the lever-arm between the resultants of the stresses is small. Moreover an additional rotation occurs due to bending of the end plates.

6.6.1.2. Favourable situation

A more favourable situation exists when the contact stresses are concentrated in line with the flanges as shown in figure 44. Because the limit state bending moment may be determined by the addition of the contact and bending stresses in the compressed side of the connection, the shim on the compression side has been made larger than on the tension side.
As long as contact forces are present between the end plates, whereas the yield stress is not exceeded on the compression side, then the moment rotation characteristics of the connection and any part of the beam agree with each other. But the agreement depends on the magnitude of the pretension. This will be shown later on with an example (see figure 46).

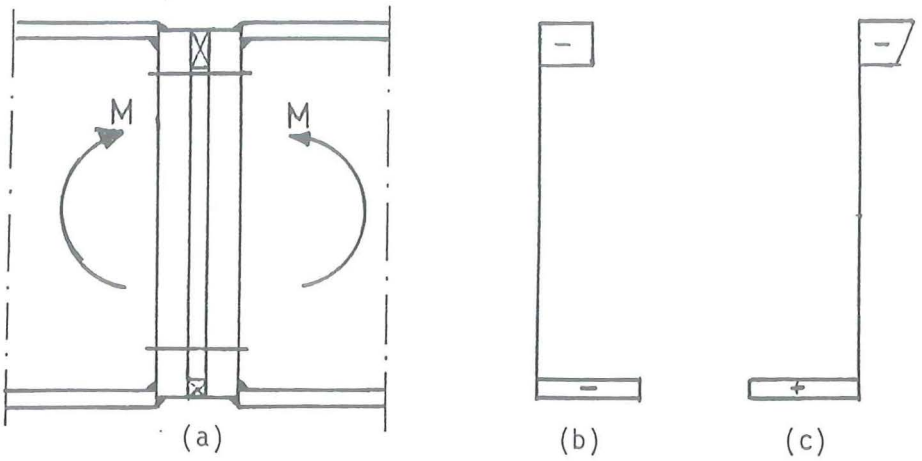

(a) End-plates with shims
(b) contact stresses due to pretensioning
(c) Stress distribution due to bending

Fig. 44.: Favourable situation.

6.6.1.3. Agreement between connection and beam behaviour

It is possible that the pre-tension is sufficient to reach the plastic moment of the beam. In that case the end-plate should have sufficient thickness so that a redistribution of the local forces is possible and a complete restrain of the beam may be assumed. This thickness is reached with the design method proposed by Mc Guire |11|. In this method the end plate thickness is determined by the bending moment at the bolt line caused by the force concentrated in the beam-flange (see figure 45). This is a very simple way of design which agrees with the actual situation. A support of the beam-web cannot be expected because complete yielding of the beam is assumed in the limit state situation.

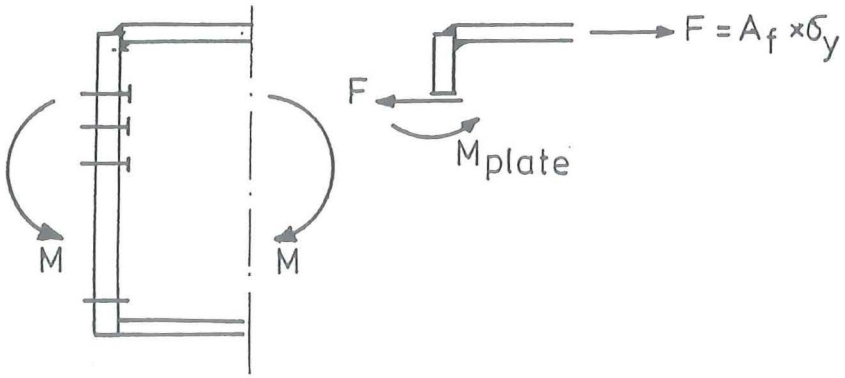

Fig. 45.: Analytical model of end-plate according to Mc Guire |11|

It should be noticed that a complete agreement of moment-rotation behaviour of beams and flush-end-plate connections is only possible with a small portion of the European rolled sections.
This is explained with the connection of two beam-sections HE-300A as shown in figure 46.
With four M27 bolts of grade 10.9, a pre-tension of 1320 kN may be accepted. With a bending moment above 310 kNm the pretension is exceeded.
An increase of the moment above this value causes a gap between the end-plate on the tension-side. This increase of the moment is then transferred by tension of the bolts.
The bolts remain elastic until a bending moment of 362 kNm and fails theoretically at a bending moment of 403 kNm. The beam-section has a plastic moment of 332 kNm.

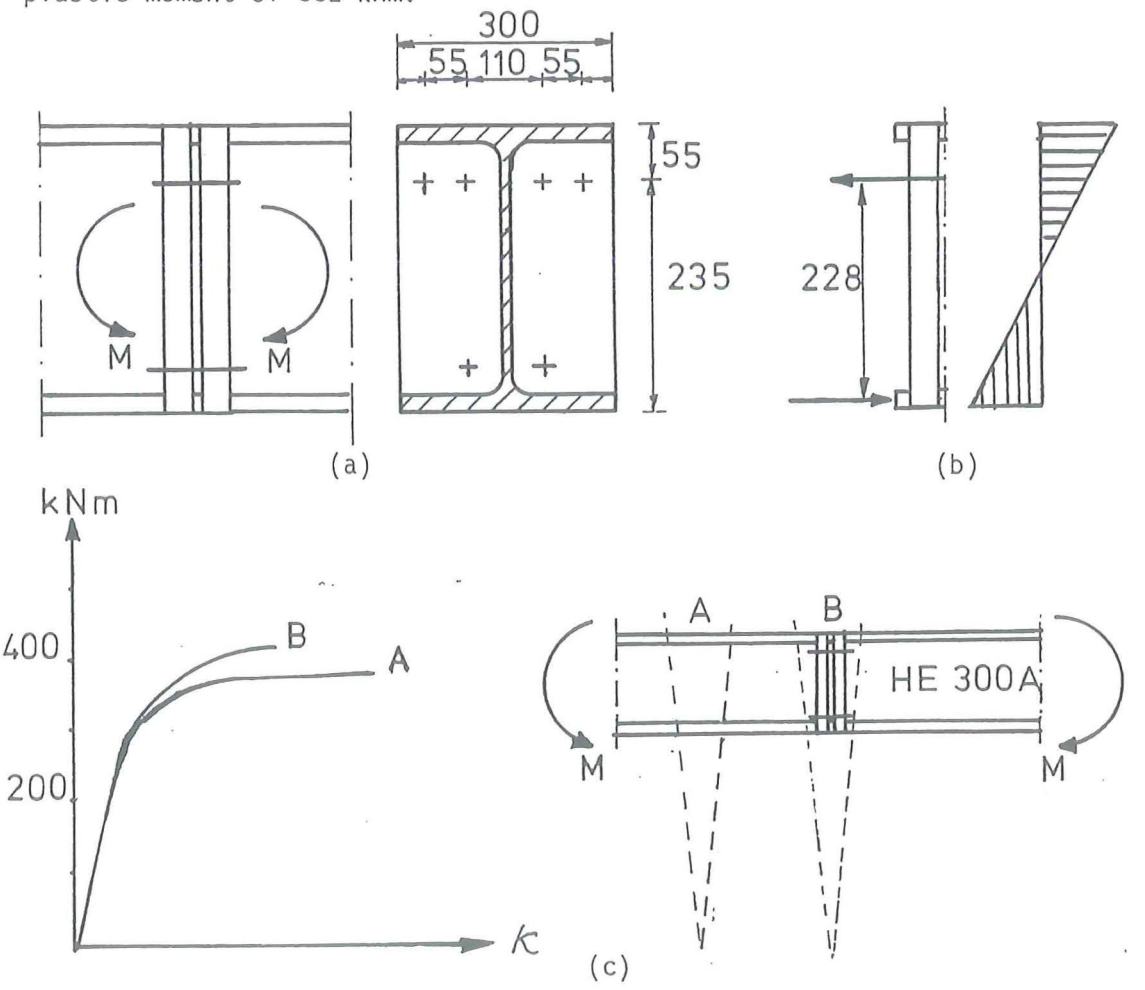

(a) End-plate connection with shims
(b) Force and stress distribution when pre-tensioning is cancelled
(c) Comparison of moment-deformation characteristics

Fig. 46.: Connection where agreement between beam- and connection behaviour occurs due to the pre-tensioning.

In the beam-section itself yielding starts theoretically with a bending moment of 302 kNm.
The rotational capacity is then delivered by yielding of the beam.
With larger flange thicknesses yielding cannot be reached with this bolt configuration. In that case the rotational capacity should be delivered by the bolts, but that is impossible with bolts of grade 10.9.

This example shows that it is impossible to reach an agreement in the behaviour of the beam and the connection with flush end-plates and European rolled sections larger than HE 300A.
More bolts cannot be used due to the restricted width of the flanges and the fact that the effect of bolts located under the first boltline is rather small. Moreover, the increase of the contact stresses on the compression side enlarges the possibility of prematurely yielding.
Then the only possibility to reach agreement of connection and beam behaviour is the use of end-plates extended beyond the flanges.

The design method of the end-plate extended beyond the tension side is already developed in |6| . The behaviour of this type of connection is mostly favourable because the contact forces are concentrated between the bolts on both sides of the flange in tension.
The rotational capacity is delivered by bending of the end-plate.

The design method of the end-plate extended beyond the compression side is developed in this report. It is advised to follow this method because the end-plate should not be made too thick, when yielding may not occur in the beam.
For the rotational capacity cannot be delivered by yielding of the beam and deformation capacity cannot be expected of bolts grade 10.9., whereas the plastic deformation of bolts grade 8.8. is max. 2 mm.

The disadvantage of the described design method is that it is time-consuming and not economic when the connection is used a few times.
In the latter situation it may be more economic to use a less sophisticated way of design in which no rotational capacity of the connection is desired.

6.6.2. Check of a stiffness formula

The previous arguments show that controlled tightening of the bolts does only make sense when specific measures are taken to concentrate the contact forces at the centres of the beam-flanges.
In all other cases the stiffness of the connection depends on coincidences and controlled tightening is not advised.
Despite these circumstances a formula is developed |2| for the deformation of the end-plate if the bolt is tightened with hand-wrenches without specific measures.

$$\delta = \frac{T}{210} * 24 * \lambda_2 \left(\frac{T}{\hat{B}_t}\right)^2 * \frac{m_1^2}{t_e^3} \qquad (22)$$

where:

δ = deformation of the end-plate at the corner bolt
T = load of the corner bolt
$\hat{B}_t$ = limit state design strength of the corner bolt
m_1 = distance m_1 as defined in figure 16
λ_2 = parameter as defined in figure 16
t_e = thickness of the end-plate

This formula is checked for various loads with the moment deformation curves of test 2.
The results are summarized in table 7.

Test end-plate thickness	Bending moment	Deformations				Limit state moment
		column-flange		End-plate		
		measured	computed	measured	computed	
	kNm	mm	mm	mm	mm	kNm
	(2)	(3)	(4)	(5)	(6)	(7)
2-13	102	0	0.16	0.10	0.52	
	153	0	0.55	0.45	1.75	142
	223	1.7	1.71	4.65	5.43	
2-20	122	0.1	0.16	0.20	0.20	
	183	1.0	0.55	0.90	0.68	178
	225	3.3	1.01	1.75	1.25	

Table 7.: Computed and measured deformations of test 2

Test 2 is chosen, because the column-flange is stiffened and formula (22) may also be applied for the computation of the deformation of this part of the connection.
The results of the computation are not very promising as might have been expected if the previous considerations were taken into account.
With the 13 mm end-plate the computed values are too large and with the 20 mm end-plate they are too small.

6.7. Rotational capacity

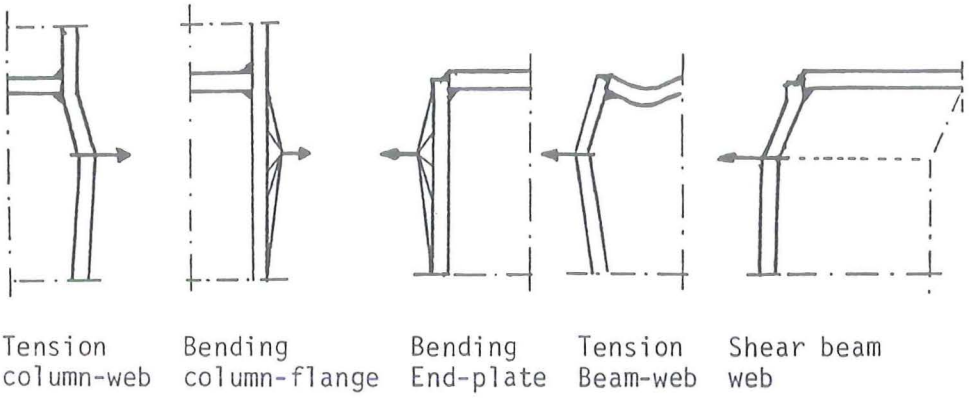

Fig. 47.: Failure mechanisms with deformation capacity.

Figure 47 shows schematically which failure mechanisms on the tension-side of the connection may deliver the rotational capacity. It is important to know which increase of forces in bolts or welds are necessary to reach sufficient rotational capacity after that the limit state load of a specific failure mode is exceeded.
This knowledge may be used in giving the bolts and welds such dimensions that rotation of the connection may occur without fracture.

As appears from figure 47 this is especially true for:

- the weld between column-flange and diaphragm
- the welds between end-plate and beam-flange
- the weld between end-plate and beam-web

If the limit state strength of these welds is enough to cause yielding of the connected material then their dimensions are sufficient.

This happens to be with the welds designed in accordance with the failure modes due to tension of column-web and beam-web (chapter 4.2.3.2.).
But this is not the case if these welds are designed proportional to the limit state design strength of the corner bolt.
From table 5 it appears that the ratio between the actual load and the limit state design strength for bending of the column flange or the end plate at the uppermost bolt has never been larger than 1.38.
This value belongs to the result of test 3 with the 18 mm thick end-plate which has got a rotational capacity which is sufficient for a connection in a braced frame with a spanlength of more than 200 times the beam-depth.

On the basis of these results the conclusion may be drawn that an extra strength of welds and bolts of 38% is sufficient to reach sufficient rotational capacity.

7. CONCLUSIONS

7.1. Design chart and check of the beam-web

The use of the chart in figure 16 is allowed for the design of flush-end-plates, provided that the beam-flange and beam-web do not fail prematurely.
This is why a check against shear failure or tensile failure of the beam-web with bending of the beam-flanges should be included in the design method.
This check may be executed with the methods described in chapter 4.
The results calculated with these methods agree with the test results.

7.2. Contribution of the additional bolt

The contribution of the additional bolt in the uppermost bolt-line of a flush-end-plate may be determined with the design method used for one side of a T-stub (formulae (4) and (5)). However, the limit state design moment of the flange of a T-stub is replaced by the limit state design moment of the beam flange.

7.3. Contribution of the other bolts

The limit state design strengths of the boltrows below the first row may be determined with the design method of T-stubs.
The contribution of these bolts is not proportional with the distance to the reaction point on the compression-side.
In the tests, a minimum of deformation was sufficient to reach the limit state design strength determined by bending of the column flanges.

7.4. Fillet welds

The dimensions of the fillet welds between the end-plate and the beam-flange are determined by the limit statedesign load, either of the end plate due to bending or of the beam-web due to tension.
In the first case, the dimensions should be enlarged with a factor which depends on the desired rotational capacity of the connection.
From these tests it appears that this factor isnot larger than 38% of the computed dimensions.

In the latter case, the rotational capacity is reached by yielding of the beam-flange whereas the fillet welds have dimensions equal to 30% and 35% of the flange thickness.

7.5. Web doublers

A web doubler on one side of the column-web does not give a higher strength capacity on the compression-side of the connection when a simple way of welding is used.
It does when plates are welded on either side of the column-web.
However, a design method could not be checked with the test results because other parts of the connection failed prematurely.
Research with detailed tests are necessary.

7.6. Haunch without a flange

The haunch without a flange has several advantages. The force transferred by the haunch is not concentrated at a small area of the beam- and column-web as it is with a haunch-flange.
The use of tightening equipment is facilitated. The welding labour is minimized. The disadvantage is that a larger haunch is necessary to get the same lever-arm as with a haunch with a flange.
Further research is advised to confirm the proposed design-method.

7.7. Controlled tightening

Controlled tightening does not make sense if no specific measures are taken to concentrate the contact forces in the centre plane of beam and column.
The stiffness of the connection depends on the location of the contact forces.

7.8. Rotational capacity

Agreement between connection and beam behaviour until failure cannot be reached with beam-sections larger than HE-300A and end-plates which do not extend beyond the flanges.
When yielding of the beam can not be reached, the end-plate should not be made too thick in order to reach sufficient rotational capacity.

8. REFERENCES

|1| Doornbos, L.M.;(1979)
Design method for the stiffened column-flange.
Developed with yield line theory. Checked with experimental results (in Dutch).
Thesis, Delft University of Technology.

|2| Zoetemeijer, P.; (1981)
Semi Rigid Beam-to-column connections with stiffened column-flanges and flush end-plates.
Proceedings of the International Conference held at Teesside Polytechnic Middlesbrough, Cleveland, 6-9 April 1981.

|3| Van Douwen, A.A.; (1981)
Design for economy in bolted and welded connections.
Proceedings of the International Conference held at Teesside Polytechnic Middlesbrough, Cleveland, 6-9 April 1981.

|4| Bijlaard, F.S.K.; (1981)
Requirements for welded and bolted beam-to-column connections in Non-Sway Frames.
Proceedings of the International Conference held at Teesside Polytechnic Middlesbrough, Cleveland, 6-9 April 1981.

|5| Van Bercum, J.Th; Bijlaard, F.S.K. and Zoetemeijer, P. (1978)
Design rules for bolted beam-to-column- connections. (in Dutch)
Staalbouwkundig Genootschap, P.O.B. 20714, 3001 JA, Rotterdam.

|6| Zoetemeijer, P.; (1974)
A design method for the tension side of statically loaded beam-to-column connections.
Heron, Vol. 20, 1974, No. 1.

|7| NEN 2062 (1977) Arc Welding
Calculation of welded joints in unalloyed and low-alloy steel with up to and including Fe 510 which are predominantly statically loaded (1977).
Unofficial translation. Netherlands Standards Institution.

|8| Zoetemeijer, P.; (1980)
The interaction of normal-, bending- and shear stresses in the web of European rolled sections.
Report 6-80-5, Stevin Laboratory, Delft University of Technology.

|9| Voorn, W.J.M.; (1971)
Welded beam-to-column connections in Non-Sway Frames (in Dutch)
Report IBBC - TNO, Nr. BI71-24.

|10| Zoetemeijer, P.; Kolstein, M.H. (1975)
Bolted beam-to-column connections with flush end-plates.
Tests and computation methods (in Dutch).
Report 6-75-20, Stevin-Laboratory, Delft University of Technology.

|11| Mc Guire, W. (1968)
Steel Structures, Prentice Hall Inc.

|12| DSTV/DAST (1978)
Moment end-plate connections with HSFG bolts (in German) IHE 1.

|13| Norme Francaise. NF P22-460 Juin 1979 (in French)
Jointing by means of bolts with controlled tightening

|14| Bouwman, L.P.; (1981)
The Structural Design of Bolted Connections Dynamically Loaded in Tension.
Proceedings of the International Conference held at Teesside Polytechnic Middlesbrough, Cleveland, 6-9 April 1981.

|15| Technical principles for the design and calculation of building structures T.G.B. 1972, Steel NEN 3851.
Netherlands Standards Institution.

|16| Witteveen, J.; Stark, J.W.B.; Bijlaard, F.S.K.; Zoetemeijer, P.
Design rules for welded and bolted beam-to-column connections in non-sway frames.
Paper presented at the ASCE Convention and Exposition held at Portland, April 14-18, 1980.

APPENDIX 1

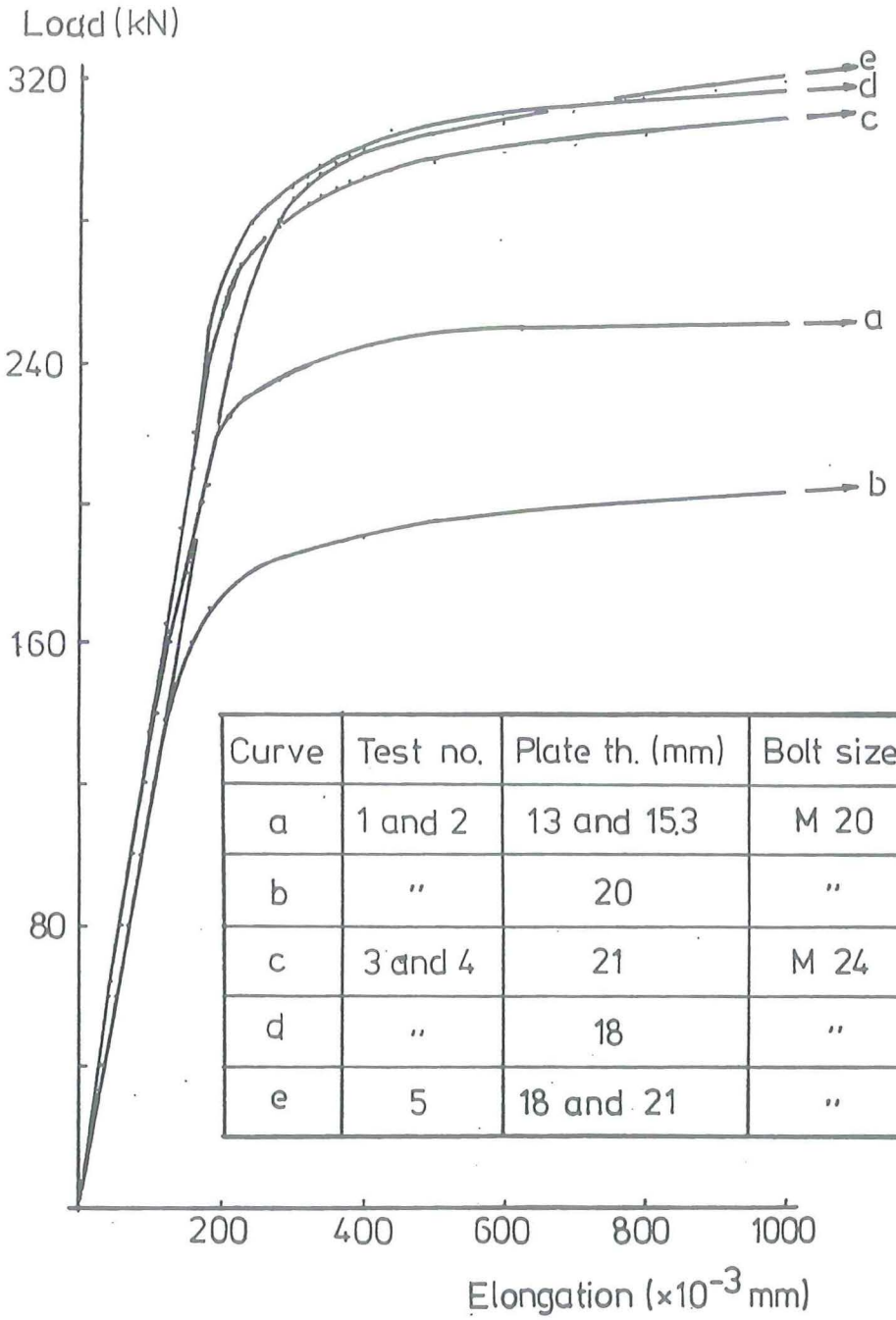

Curve	Test no.	Plate th. (mm)	Bolt size	Fracture load
a	1 and 2	13 and 15.3	M 20	250 kN
b	"	20	"	210 "
c	3 and 4	21	M 24	326 "
d	"	18	"	336 "
e	5	18 and 21	"	332 "

Load - elongation characteristics of the bolts measured in the tests

APPENDIX 2

Appendix 2 Column-web

Computation of the limit state design loads

The limit state design loads due to a specific failure mechanism are computed for all tests. The processing, from limit state design loads to limit state design moments, is given in tables 2 and 3.

1. Tension in the column-web

1.1. Column-web uppermost bolt

1.1.1. Unstiffened column-flange

Test 1

Effective length 147 mm (see computation of column-flange)

$F_1 = 147*9*296 \rightarrow F_1 = 394$ kN

Test 4 and 5

Effective length 159 mm (see computation of column-flange)

$F_1 = 159*9*296 \rightarrow F_1 = 431$ kN

1.1.2. Stiffened column-flange

Test 2

$$F_1 = \frac{2}{4}*13^2*257*\frac{300}{46} + \frac{1}{2}*46*9*296 + 30*9*296 \rightarrow F_1 = 286 \text{ kN}$$

Test 3

$$F_1 = \frac{2}{4}*13^2*257*\frac{300}{28} + \frac{1}{2}*28*9*296 + 35*9*296 \rightarrow F_1 = 366 \text{ kN}$$

1.2. Column-web second bolt

The computation of the limit state design load of the second bolt is the same as that of the other bolts with the exception of test 3. In test 3, the computation of the second bolt is equal to that of the uppermost one.

1.3. Column-web other bolts

Test 1 and 2

$F_i = 60*9*296 \rightarrow F_i = 160$ kN

Test 3, 4 and 5

$F_i = 70*9*296 \rightarrow F_i = 190$ kN

2. Bending of the column-flange with failure of the bolt

2.1. Uppermost bolt

2.1.1. Unstiffened-column flange

Test 1

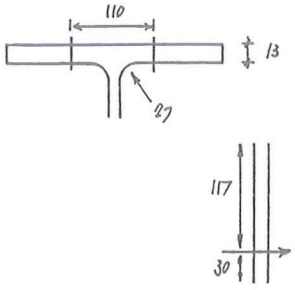

$n' = \frac{300-110}{2} = 95$ $\qquad n = 35$

$m = \frac{110-9-2 * 0.8 * 27}{2} = 28.9$

effective length: $30+2 * 28.9+0.625 * 95$

$= 147$ mm

$T*m = M_p + M_p' \rightarrow T*28.9 = 2*\frac{1}{4}*147*13^2*262 \rightarrow T = 113$ kN $\quad F_1 = 226$ kN

$T*m = (\Sigma \hat{B}_t - T)*n = M_p \rightarrow T.(28.9+33) = \frac{1}{4}*147*13^2*262 + 0.7*250000*35$

with end-plate 15.3 mm $\hat{B}_t = 0.7*250000 \rightarrow T = 120$ kN

with end-plate 20 mm $\hat{B}_t = 0.7*210000$

$T = 107$ kN $\quad F_1 = 214$ kN

Distribution of the forces in the limit state design situation.

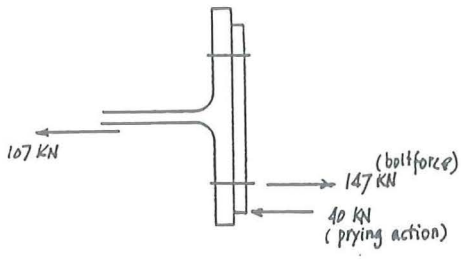

Test 4

$n' = \frac{300-120}{2} = 90$ mm $\qquad n = 50$ mm

$m = \frac{120-9,0-0.8 * 2 * 27}{2} = 33.9$ mm

$n = 1.25 * 33.9 = 42.4$ mm

effective length: $35+2 * 33.9 + 0.625 * 90 = 159$ mm

$T*m = M_p + M_p' \rightarrow T*33.9 = 2*\frac{1}{4}*159*13^2*262 \rightarrow T = 104$ kN

$T*m - (\Sigma \hat{B}t - T)*n = Mp \rightarrow T(33.9+42.4) = \frac{1}{4}*159*13^2*262+0.7\ 320.000*42.4$

$T = 148$ kN

$$B = 104+\frac{\frac{1}{4}*159*13^2*262}{42.4} = 104+42 = 146 \text{ kN}$$

$$F_1 = 208 \text{ kN}$$

Distribution of the forces in the limit state

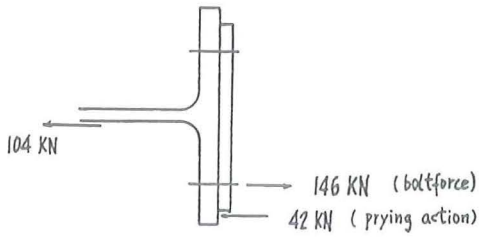

Test 5

The column-flange has been stiffened with backing plates with a thickness of 16 mm.
This results in a larger value for $\hat{M}_p'$. Because the yield strength of the material is not determined, the value of $\hat{M}_p'$ is chosen equal to twice the yield moment of the unstiffened column-flange.
The bolt configuration is the same as in test-specimen 4.
Thus:

$$T*m = M_p+M_p' \rightarrow T*33.9 = 3*\tfrac{1}{4}*159*13^2*262 \rightarrow T = 156 \text{ kN}$$

$$T*m = (\Sigma\hat{B}_t-T)n = T(33.9+42.4) = \tfrac{1}{4}*159*13^2*262+0.7*330000*42.4$$

$T = 151$ kN $F_1 = 302$ kN
$B = 231$ kN

Distribution of forces in the limit state design situation.

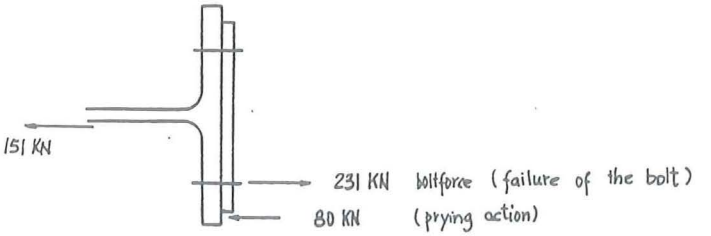

2.1.2. Stiffened-column flange

Test 2

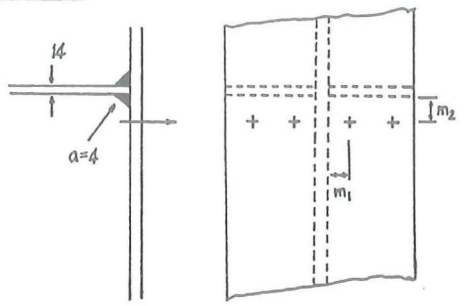

$m_1 = \frac{110-9-2*27}{2} = 23{,}5$

$m_2 = 60-14-4\sqrt{2} = 40.3$ mm

$m_1+n' = 23.5 + 95 = 118.5$ mm

$\lambda_1 = 0.2 \qquad \lambda_2 = 0.34$

$T = 4\pi*\frac{1}{4}*13^2*262 = 139$ kN

$F_1 = 278$ kN $\quad 2B_t = 0{,}7x500=350$kN

Bolt adjacent to uppermost bolt :

$m = 60 - \frac{13}{2} - 0.8*4\sqrt{2} = 48.9$ mm

effective width or width available $95 - 23.5 = 71.5$ mm

$T*m = M_p+M_p' \rightarrow T*48.9 = 2*\frac{1}{4}+71{,}5*13^2*262 \rightarrow T = 32$ kN

$F_1=278 + 64$ kN

Test 3 (uppermost and second bolt stiffened)

$m_2 = \frac{70-14}{2} = 28$ mm:

$m_1 = \frac{120-9-2*27}{2} = 28.5$ mm $\qquad m_1 + n' = 28.5 + 90 = 118.5$ mm

$\lambda_1 = \frac{28}{118{,}5} = 0.24 \qquad \lambda_2 = \frac{28.5}{118.5} = 0.24$

$T = 4\pi * \frac{1}{4} * 13^2 * 262 = 139$ kN $\qquad F_1 = F_2 = 278$ kN

2.2. Bending of the column flange

Second and innermost bolts :

Test 1

Effective width 60 mm

$m = 28.9$ mm (see uppermost bolt) $n' = \frac{300 - 110}{2} = 95$ mm

$T * m = M_p + M_p' \rightarrow T * 28.9 = 2 * \frac{1}{4} * 60 * 13^2 * 262 \quad T = 46$ kN

$F_i = 92$ kN

Distribution of forces in the limit state design situation.

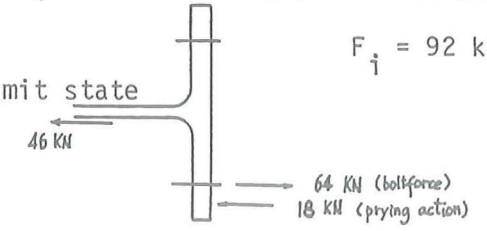

Test 2

Second bolt :

Width available: 30 + 60 - 23.5 = 66.5 mm

m = 28.9 (see test specimen 1)

$T * m = M_p + M_p' \rightarrow T * 28.9 = 2 * \frac{1}{4} * 66.5 * 13^2 * 262 \rightarrow T = 51$ kN

$F_2 = 102$ kN

All other bolts :

$T * m = M_p + M_p' \rightarrow T = \frac{60}{66.5} * 51 = 46$ kN $\rightarrow$ $F_i = 92$ kN

Test 3

Third bolt :

Width available = 35 + 60 - 23 = 72 mm

$m = 28.5 + \frac{1}{5} * 27 = 33.9$ mm $\qquad n' = 50$ mm

$T * m = M_p + M_p' \rightarrow T * 33.9 = 2 * \frac{1}{4} * 72 * 13^3 * 262 \rightarrow T = 47$ kN

$F_3 = 94$ kN

All other bolts : $T = \frac{70}{72} * 47 = 46$ kN $\qquad F_i = 92$ kN

$$B = 46 + \frac{\frac{1}{4} * 70 * 13^2 * 262}{33.9 * 1.25} = 46 + 18 = 64 \text{ kN}$$

Test 4

Effective width 70 mm

m = 33.9 mm (see uppermost bolt)

$T * m = M_p + M_p' \rightarrow T * 33.9 = 2 * \frac{1}{4} * 70 * 13^2 * 262 \rightarrow T = 46$ kN

$F_i = 92$ kN

B = 64 kN

Test 5

All other bolts:

$T * 33.9 = 3 * \frac{1}{4} * 70 * 13^2 * 262 \rightarrow T = 69$ kN $\quad B = 69 + 37 = 106$ kN

Column-flange
End-plate

$T * m - (B_t - T) n = M_p \quad T (33.9 + 42.4) = \frac{1}{4} * 70 * 13^2 * 262 + 07\ 330.000 *$

$T (33.9 + 42.4) = \frac{1}{4} * 70 * 13^2 * 262 + 0.7 * 330{,}000 * 42.4$

$T = 139$ kN

$F_i = 138$ kN

3. Bending of the end-plate with failure of the bolt

3.1. Uppermost bolt

Test 1

Endplate: thickness 15.3 mm $\quad \sigma_y = 270$ N/mm^2

$m_1 = \frac{110 - 9.5 - 8\sqrt{2}}{2} = 44.6$

$m_2 = 60 - 12{,}2 - 4\sqrt{2} = 42.1$

$m_1 + n' = 44.6 + 35 = 79.6$

$\lambda_1 = 0{,}56 \quad \lambda_2 = 0.53$

$T = 9.5 * \frac{1}{4} * 15.3^2 * 270 \rightarrow \quad T = 150$ kN

$F_1 = 300$ kN

Endplate thickness 20 mm $\quad F_1 > 300$ kN

Test 2

Endplate: thickness 13 mm $\quad \sigma_y = 270$ N/mm^2

$m_1 = \frac{110 - 9.5 - 8\sqrt{2}}{2} = 44.6$ mm

$m_2 = 60 - 13 - 4\sqrt{2} = 41.3$ mm

$m_1 + n' = 41.3 + 95 = 136.3$ mm

$\lambda_1 = 0.33 \qquad \lambda_2 = 0.30$

$T = 4\pi * \frac{1}{4} * 13^2 * 270 = 143$ kN

Bolt adjacent to uppermost bolt :

$m = 60 - \frac{13}{2} = 53.5$ mm

Effective width or width available $95 - 41.3 = 53.7$ mm

$T * m = M_p + M_p' \rightarrow T * 53.5 = 2 * \frac{1}{4} * 53.7 * 13^2 * 270 \rightarrow T = 23$ kN

$F_1 = 286 + 46$ kN

End-plate: thickness 20 mm $\sigma_y = 270$ N/mm^2

Comparison of the limit state design loads of column flange and end plate with a thickness of 13 mm shows that a small increase in thickness makes the column flange the determining factor.

Thus: $F_1 > 286 + 46$

Test 3, 4 and 5

End-plate thickness 18 mm $\sigma_y = 266$ N/mm^2

Uppermost bolt $m_1 = \frac{120 - 9.5 - 8\sqrt{2}}{2} = 49.6$ mm

$m_2 = 70 - 14 - 4\sqrt{2} = 50.3$ mm

$m_1 + n' = 49.6 + 50 = 99.6$ mm

$\lambda_1 = 0.50 \quad \lambda_2 = 0.50$

$T = 9.9 * \frac{1}{4} * 18^2 * 266 = 213$ kN

$F_1 = 426$ kN

End-plate thickness 21 mm $F_1 > 426$ kN

3.2. Second and other bolts

Test 1 End-plate thickness 15.3 mm $\sigma_y = 270$ N/mm^2

Second bolt: effective length $60 - 44.6 + 30 = 45.4$ mm

$m = 44.6 + 4\sqrt{2} * \frac{1}{5} = 45.7$ mm

$T * m = M_p + M_p' \rightarrow T * 45.7 = 2 * \frac{1}{4} * 45.4 \quad 15.3^2 * 270 \rightarrow T = 31$ kN

$F_2 = 62$ kN

All other bolts :

$T * m = M_p + M_p' \rightarrow T = \frac{60}{45.4} * 31 = 42$ kN $\qquad F_i = 84$ kN

$T * m = (\Sigma B_t - T)\, n = M_p \rightarrow T\,(45.7 + 35) = \frac{1}{4} * 60 * 15.3^2 * 270 + 0.7\ 250.000 * 35$

$T = 87$ kN

Distribution of forces in the limit state design situation.

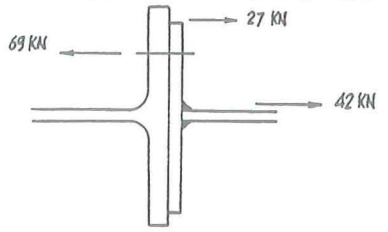

End-plate thickness 20 mm: $\sigma_y = 266\ N/mm^2$

Second bolt: available length = 45.4 mm

m = 45.7 mm

$T * m = M_p + M_p' \rightarrow T = 45.7 = 2 * \frac{1}{4} * 45.4 * 20^2 * 266 \rightarrow T = 53\ kN$

$F_2 = 106\ kN$

All other bolts :

$T * m = M_p + M_p' \rightarrow T = \frac{60}{45.7} * 53 = 70\ kN$ $\qquad F_i = 140\ kN$

Test 2

Endplate thickness - 13 mm: $\sigma_y = 270\ N/mm^2$

Second bolt:

Width available 30 + 60 - 41.3 = 48.7 mm

$m = 44.6 + \frac{1}{5} * 4\sqrt{2} = 45.7$ mm

$T * m = M_p + M_p' \rightarrow T * 45.7 = 2 * \frac{1}{4} * 48.7 * 13^2 * 270 \rightarrow T = 24\ kN$

$F_2 = 48\ kN$

All other bolts :

$T * m = M_p + M_p' \rightarrow \frac{60}{48.7} * 24 \rightarrow T = 30\ kN$ $\qquad F_i = 60\ kN$

End-plate thickness 20 mm : $\sigma_y = 266\ N/mm^2$

Width available 48.7 mm

m = 45.7 mm

$T * m = M_p + M_p' \rightarrow T * 45.7 = 2 * \frac{1}{4} * 48.7 * 20^2 * 266 \rightarrow T = 57\ kN$

$F_2 = 114\ kN$

All other bolts :

$T * m = M_p + M_p' \rightarrow \frac{60}{48.7} * 57 \cdot T = 70$ $\qquad F_i = 140\ kN$

Test 3, 4 and 5

End-plate thickness 18 mm $\quad \sigma_y = 266\ N/mm^2$

Second bolt :

Width available $35 + 70 - 49.6 = 55.4$ mm

$$m = 49.6 + \frac{1}{5} * 4\ 2 = 50.7 \quad n' = n = 50 \text{ mm}$$

$$T * m = M_p + M_p' \rightarrow T * 50.7 = 2 * \tfrac{1}{4} * 55.4 \quad 18^2 * 266 \rightarrow T = 47 \text{ kN}$$

$$F_2 = 94 \text{ kN}$$

$$B = 47 + \frac{\frac{1}{4} * 55.4 * 18^2 * 266}{50} = 71 \text{ kN}$$

All other bolts :

$$T * m = M_p + M_p' \rightarrow T = \frac{70}{55.4} * 47 = 59 \text{ kN} \qquad F_i = 118 \text{ kN}$$

$$B = 59 + \frac{\frac{1}{4} * 70.4 \quad 18^2 * 266}{50} = 93 \text{ kN}$$

End-plate thickness 21 mm $\quad \sigma_y = 310\ N/mm^2$

Width available 55.4 mm

$$m = 50.7 \text{ mm}$$

$$T * m = M_p + M_p' \rightarrow T * 50.7 = 2 * \tfrac{1}{4} * 55.4 * 21^2 * 310 \rightarrow T = 75 \text{ kN}$$

$$F_2 = 150 \text{ kN}$$

$$n = 50 \rightarrow B = 75 + 38 = 113 \text{ kN}$$

All other bolts :

$$T * m = M_p + M_p' \rightarrow T = \frac{70}{55.4} * 75 = 95 \text{ kN} \rightarrow F_i = 190 \text{ kN}$$

4. Tension in the beam-web with bending of the end-plate

4.1 Uppermost bolt

Test 1-15.3

$$F_1 = (\tfrac{1}{4} * 15.3^2 * 270 + \tfrac{1}{4} * 12.2^2 * 256)\frac{181}{53} + \frac{1}{2} * 47.8 * 9.5 * 287 + 30 * 9.5 * 2$$

$$= 86 + 147 = 233 \text{ kN}$$

Test 1-20

$$F_1 = (\tfrac{1}{4} * 20^2 * 266 + \tfrac{1}{4} * 12.2^2 * 256)\frac{181}{53} + \tfrac{1}{2} * 47.8 * 9.5 * 287 + 30 * 9.5 * 2$$

$$= 123 + 147 = 270 \text{ kN}$$

Test 2-13

$$F_1 = (\tfrac{1}{4} * 13^2 * 270 + \tfrac{1}{4} * 13.5^2 * 266)\frac{300}{53} + \tfrac{1}{2} * 46.5 * 9 * 294 + 30 * 9 * 29$$

$$= 133 + 141 = 274 \text{ kN}$$

Test 2-20

$$F_1 = (\tfrac{1}{4} * 20^2 * 266 + \tfrac{1}{4} * 13.5^2 * 266)\frac{300}{53} + \tfrac{1}{2} * 46.5 * 9 * 294 + 30 * 9 * 294$$

$$= 219 + 141 = 360 \text{ kN}$$

Test 3-18, 4-18, 5-18

$$F_1 = \tfrac{1}{4} * 18^2 * 266 * \frac{220}{64} + \tfrac{1}{4} * 12.2^2 * 256 * \frac{181}{64} + \tfrac{1}{2} * 57.8 * 9.5 * 287 + 35 *$$

$$9.5 * 287 = 74 + 27 + 174 = 275$$

Test 3-21, 4-21, 5-21

$$F_1 = \tfrac{1}{4} * 21^2 * 310 * \frac{220}{64} + \tfrac{1}{4} * 12.2^2 * 256 * \frac{181}{64} + \tfrac{1}{2} * 57.8 * 9.5 * 287 +$$

$$35 * 9.5 * 287 = 117 + 27 + 174 = 319 \text{ kN}$$

4.2. All other bolts

Test 1

$F_i = 60 * 9.5 * 287 \rightarrow F_i = 163$ kN

Test 2

$F_i = 60 * 9 * 294 \rightarrow F_i = 159$ kN

Test 3, 4 and 5

$F_i = 70 * 9.5 * 287 \rightarrow F_i = 190$ kN

5. Shear in the beam-web over the length of the haunch

Test 1

Bending of the 15.3 mm end-plate

$F_7 = \frac{1}{4} * 181 * 15.3^2 * 270/54$ $F_7 = 53$ kN

Shear in the 15.3 mm end-plate

$F_i = 4 * 9.5 * 0.58 * 15.3 * 270$ $F_8 = 91$ kN

Shear in the beam-web

$F_9 = 200 * 9.5 * 0.58 * 290$ $F_9 = 319$ kN

$F_{10} + F_{11} = 463$ kN

Bending of the 20 mm end-plate

$F_7 = \frac{1}{4} * 181 * 20^2 * \frac{266}{54}$ $F_7 = 90$ kN

Shear in the 20 mm end-plate

$F_8 = 4 * 9.5 * 0.58 * 20 * 266$ $F_8 = 117$ kN

Shear in the beam-web

$F_9 = 319$ kN

$F_{10} + F_{11} = 526$ kN

Test 2

Bending of the 13 mm end-plate

$F_7 = \frac{1}{4} * 300 * 13^2 * \frac{270}{54}$ $F_7 = 64$ kN

Shear in the 13mm end-plate

$F_8 = 4 * 9 * 0.58 * 13 * 270$ $F_i = 73$ kN

Shear in the beam-web

$F_9 = 270 * 9 * 0.58 * 294$ $\quad F_9 = 414$ kN

$F_{10} + F_{11} = 551$ kN

Bending of the 20 mm end-plate

$F_7 = \frac{1}{4} * 300 * 20^2 * \frac{266}{54}$ $\quad F_7 = 150$ kN

Shear in the 20 mm end-plate

$F_8 = 4 * 9 * 0.58 * 20 * 266$ $\quad F_8 = 111$ kN

Shear in the beam-web

$F_9 = 414$ kN

$F_{10} + F_{11} = 675$ kN

Test 3

Bending of the 18 mm end-plate

$F_7 = \frac{1}{4} * 220 * 18^2 * \frac{266}{64}$ $\quad F_7 = 75$ kN

Shear in the 18 mm end-plate

$F_8 = 4 * 9.5 * 0.58 * 18 * 266$ $\quad F_8 = 106$ kN

Shear in the beam-web

$F_9 = 370 * 9.5 * 0.58 * 290$ $\quad F_9 = 591$ kN

$F_{10} + F_{11} = 772$ kN

Bending of the 21 mm end-plate

$F_7 = \frac{1}{4} * 220 * 21^2 * \frac{310}{64}$ $\quad F_7 = 118$ kN

Shear in the 21 mm end-plate

$F_8 = 4 * 9.5 * 0.58 * 21 * 310$ $\quad F_8 = 143$ kN

Shear in the beam-web $\quad F_9 = 591$ kN

$F_{10} + F_{11} = 852$ kN

Test 4

Bending of the 18 mm end-plate

see test 3 $\quad F_7 = 75$ kN

Shear in the 18 mm end-plate
see test 3 $F_8 = 106$ kN

Shear in the beam-web
see test 1 $F_9 = 320$ kN

$F_{10} + F_{11} = 501$ kN

Bending of the 21 mm end-plate
see test 3 $F_7 = 118$ kN

Shear in the 21 mm end-plate
see test 3 $F_8 = 143$ kN

Shear in the beam-web
see test 1 $F_9 = 320$ kN

$F_{10} + F_{11} = 581$ kN

Test 5

Bending of the 18 mm end-plate
see test 3 $F_7 = 75$ kN

Shear in the 18 mm end-plate
see test 3 $F_8 = 106$ kN

Shear in the beam-web
$F_9 = 228 * 9.5 * 0.58 * 290$ $F_9 = 362$ kN

$F_{10} + F_{11} = 543$ kN

The length of 228 mm is related to the computation of the haunch as explained in section 4.2.8.2 of the report.

Bending of the 21 mm end-plate
see test 3 $F_7 = 148$ kN

Shear in the 21 mm end-plate
see test 3 $F_8 = 143$ kN

Shear in the beam-web
$F_9 = 228 * 9.5 * 0.58 * 290$ $F_9 = 361$ kN

$F_{10} + F_{11} = 622$ kN

6. Tension in the beam section where the haunch flange is connected to

It ought to be checked whether the forces $F_7 + F_8 + F_9$ can be transferred by the beam section where the haunch flange is connected to.
If this is not possible, the bending moment at the interface of end-plate and column-web should be reduced proportionally (test 3-20).
On the other hand, the stresses in the beam section to where the haunch is connected can never be larger than the stresses caused by the sum of the forces F_7, F_8 and F_9 .
To facilitate the computation, a stress distribution is first assumed. The forces and the bending moment corresponding with this specific stress distribution are calculated. The actual situation is computed by taking the forces $F_7+F_8+F_9$ into account. The bending moment at the interface is converted from the latter computed bending moment.

Test 1

Elastic

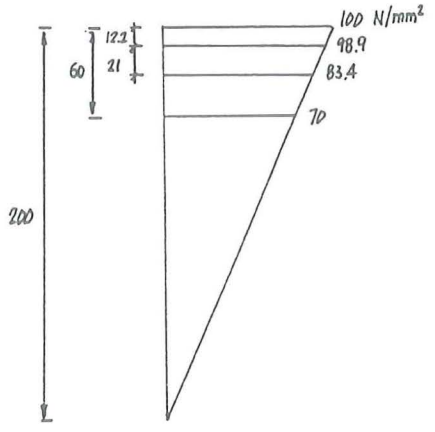

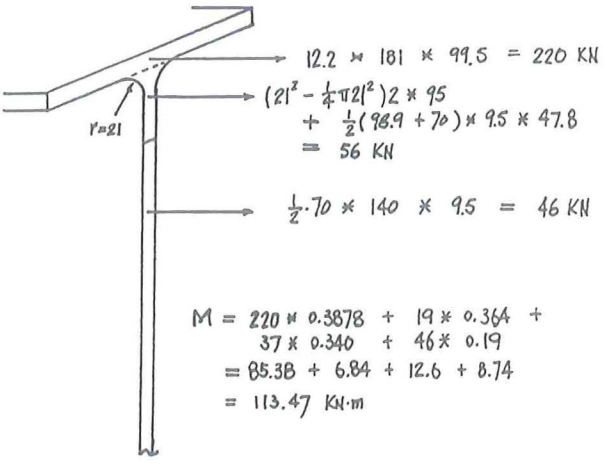

With end-plate 15.3 mm

$F_7 + F_8 + F_9 = 463$ kN

$\sigma = \frac{463}{276} * 100 = 167$ N/mm^2 < 256 N/mm^2

$F_{10} = \frac{463}{276} * 220 = 369$ kN

$F_{11} = \frac{463}{276} * 56 = 94$ kN

463 kN

$M = \frac{463}{276} * 113 = 189$ kNm

At the interface $M = \frac{2}{1.8} * 189 = 212$ kNm

With 20 mm end-plate

$F_7 + F_8 + F_9 = 526$ kN

$\sigma = \frac{526}{276} * 100 = 190$ N/mm^2 < 256 N/mm^2

$M = \frac{526}{276} * 113 = 216$ kN

At the interface: $M = \frac{2}{1.8} * 216 = 240$ kNm

Test 2

Elastic

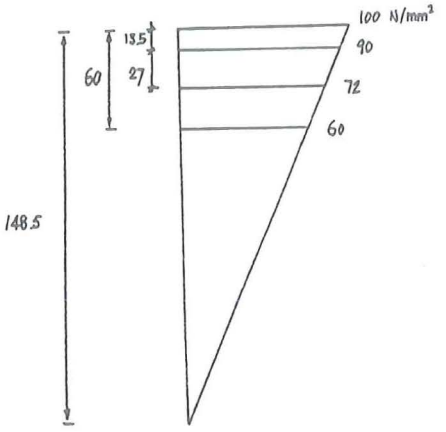

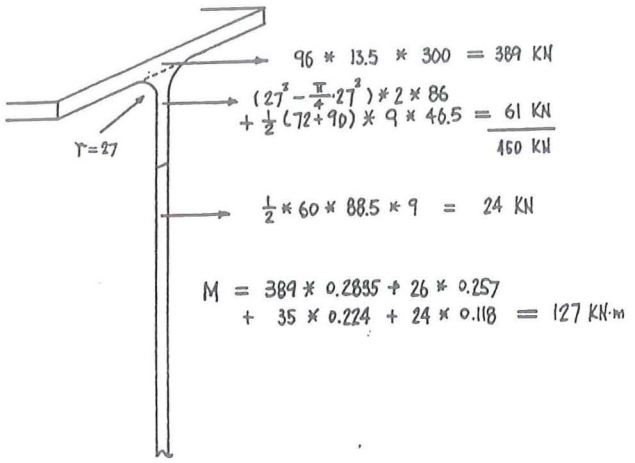

With 13 mm end-plate

$F_7 + F_8 + F_9 = 551$ kN

$\sigma = \frac{551}{450} = 100 = 122$ N/mm^2 < 266 N/mm^2

$M = \frac{551}{450} * 127 = 156$ kNm

At the interface: $M = \frac{2}{1.73} * 156 = 180$ kNm

With 20 mm end-plate

$F_7 + F_8 + F_9 = 675$ kN

$\sigma = \frac{675}{450} * 100 = 150$ N/mm^2 < 266 N/mm^2

$M = \frac{675}{450} * 127 = 190$ kN

At the interface $M = \frac{2}{1.73} * 190 = 220$ kNm

Test 3

Elastic

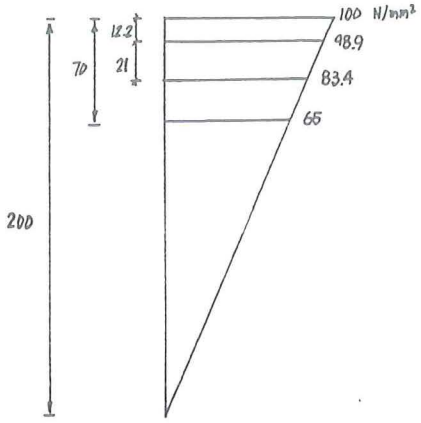

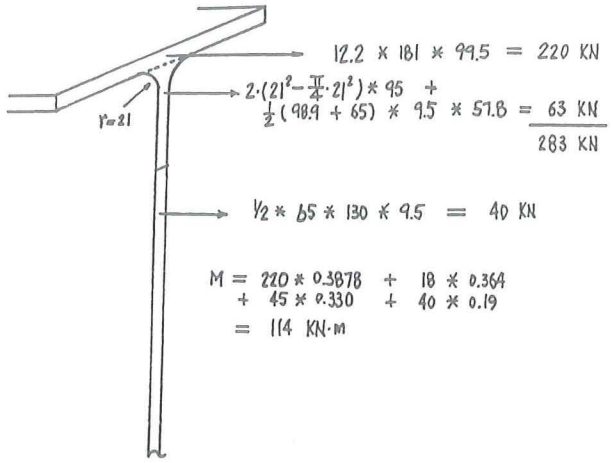

With end-plate 18 mm

$F_7 + F_8 + F_9 = 772$ kN

$$\sigma = \frac{772}{283} * 100 = 273 \text{ N/mm}^2 > 256 \text{ N/mm}^2$$

thus yielding of the flange.

Plastic

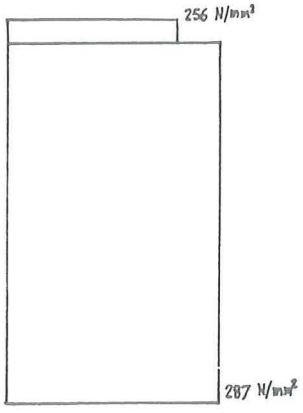

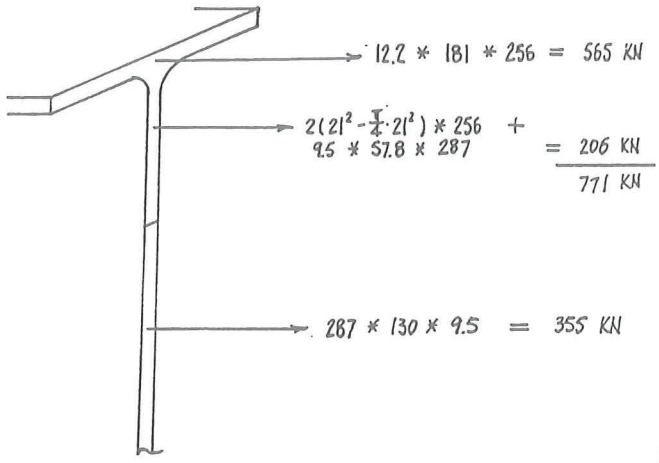

From the above figure, it can be seen that yielding of the part above the boltline is sufficient to transfer the loads $F_7 + F_8 + F_9$.
In that case:

M = 565 * 0.3878 + 48 * 0.364 + 158 * 0.33 + 177 * 0.19 = 324 kNm

At the interface $M = \frac{2}{1.63} * 324 = 398$ kNm

With end-plate 21 mm

$F_7 + F_8 + F_9 = 852$ kNm

In this case the failure mechanism due to shear in the beam-web cannot be reached, owing to the yielding of the beam section where the haunch is connected to. If complete yielding of the beam is assumed:

$M = 324$ kNm $+ 177 * 0.09 = 339$ kNm

At the interface

$M = \frac{2}{1.63} * 335 = 416$ kNm

Test 4

For elastic force distribution see test 3.

With 18 mm end-plate

$F_7 + F_8 + F_9 = 501$ kN

$\sigma = \frac{501}{283} * 100 = 177$ N/mm^2 < 256 N/mm^2

$M = \frac{501}{283} * 114 = 203$ kNm

At the interface $M = \frac{2}{1.8} * 203 = 226$ kNm

With 21 mm end-plate

$F_7 + F_8 + F_9 = 581$ kN

$\sigma = \frac{581}{283} * 100 = 205$ N/mm^2 < 256 N/mm^2

$M = \frac{581}{283} * 114 = 236$ kNm

At the interface: $M = \frac{2}{1.8} * 236 = 262$ kNm

Test 5

For elastic force distribution see test 3.

For the magnitude of the forces $F_7 + F_8 + F_9$ see the computation of the haunch-force with end-plate 18 mm

$\sigma = \frac{543}{283} * 100 = 191$ N/mm^2 < 256 N/mm^2

$M = \frac{543}{283} * 114 = 221$ kNm

At the interface $M = \frac{2}{1.78} * 221 = 250$ kNm

With 21 mm end-plate

$\sigma = \frac{622}{283} * 100 = 220$ N/mm^2 < 256 N/mm^2

$M = \frac{622}{283} * 114 = 252$ kNm

At the interface $M = \frac{2}{178} * 252 = 285$ kNm

7. Failure of the column web due to buckling or yielding

Test 1

$F = \{5(27 + 13) + 20\} * 9 * 302 \rightarrow F = 598$ kN

Test 2

$F = \{5(27 + 13) + 20\} * \{9 * 302 + 4 * 240\} = 809$ kN

If the plate welded on one side of the column-web does not contribute then F = 598 kN as computed with test 1.

Test 3, 4 and 5

$F = \{5(27 + 13) + 20\} * \{9 * 302 + 8 * 240\} = 1020$ kN

8. Failure of the haunch-flange due to yielding

The following formulae are used to compute the forces F_b and F_c as far as failure of the haunch is concerned.
For the definitions of the parameters, see the figure below.

$$F_b = \{10 * t_{fb} + 2\ t_{wb}\}\ t_{fh} * \sigma_{yfh} * \cos\alpha$$

$$F_b = b_{fh} * t_{fh} * \sigma_{yfh} * \cos\alpha$$

$$F_c = b_{fh} * t_{fh} * \sigma_{yfh} * \cos\alpha$$

$$F_c = \{10\ (t_{fc} + t_e) + 2\ t_{wc}\}\ t_{fh} * \sigma_{yfh} * \cos\alpha$$

$$F_c = b_{fh} * t_e * \sigma_{ye} * \cot\alpha$$

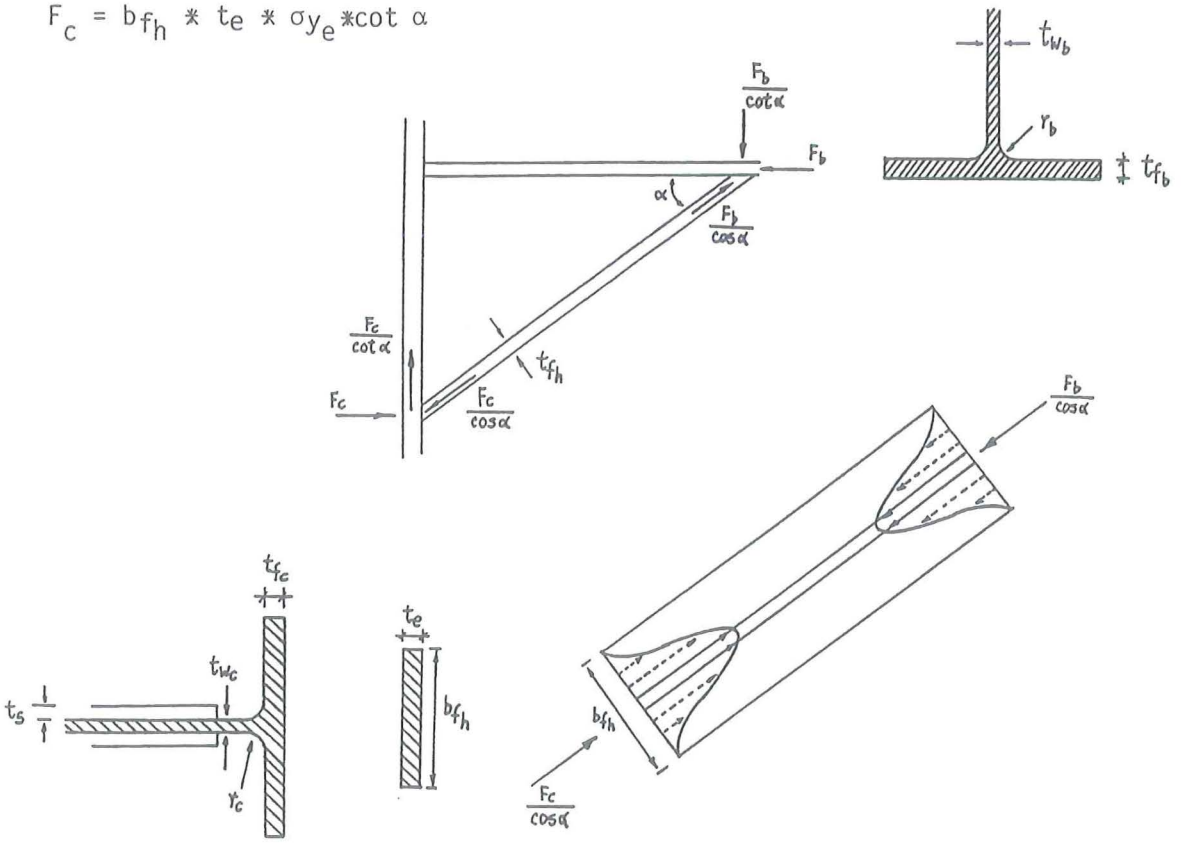

The force, F_b, determines the limit state situation when it is lower than the limit state force of the flange itself. In all other cases, the force F_c is the determining factor because it has to transfer the sum of the forces of beam-flange and beam-web.

Test 1

$\alpha = 45^o$ $\cot \alpha = 1$ $\cos \alpha = 0.707$

$r_b = 21$ mm $r_c = 27$ mm $b_{f_h} = 180$ mm

$t_{f_b} = 12.2$ mm $t_{f_c} = 13$ mm $t_{f_h} = 20$ mm

$t_{w_b} = 9.5$ mm $t_{w_c} = 9$ mm $\sigma_{y f_h} = 266$ N/mm^2

$\sigma_{y b_w} = 293$ N/mm^2 $t_s = 0$ mm $t_e = 15.3 - 20$ mm

$\sigma_{y_c} = 302$ N/mm^2 $\sigma_{y_e} = 270 \quad 266$ N/mm^2

$F_b = \{10 * 12.2 + 2 * 9.5\}\ 20 * 266 * 0.707 \rightarrow F_b = 530$ kN

$F_b = 180 * 20 * 266 * 0.707 \rightarrow F_b = 677$ kN

$F_c = 180 * 20 * 266 * 0.707 \rightarrow \boxed{F_c = 677 \text{ kN}}$

With 15.3 mm end-plate

$F_c = \{10\ (13 + 15.3) + 2 * 9\}\ 20 * 266 * 0.707 \rightarrow F_c = 1046$ kN

With 20 mm end-plate

$F_c = \{10\ (13 + 20) + 2 * 9\}\ 20 * 266 * 0.707 \rightarrow F_c = 1309$ kN

With 15.3 mm end-plate

$F_c = 181 * 15.3 * 270 * 1 \rightarrow F_c = 744$ kN

With 20 mm end-plate

$F_c = 181 * 20 * 266 * 1 \rightarrow F_c = 958$ kN

Test 2

$\alpha = 27.4$ $\cot \alpha = 1.93$ $\cos \alpha = 0.888$

$r_b = 27$ $r_c = 27$ $b_{f_h} = 300$

$t_{f_b} = 13$ $t_{f_c} = 13$ $t_{f_h} = 20$

$t_{w_b} = 9$ $t_{w_c} = 9$ $y_{f_h} = 266$ N/mm^2

$\sigma_{y b_w} = 296$ $t_s = 0$ $t_e = 13 - 20$

$\sigma_{y_c} = 302$ N/mm^2 $\sigma_{y_e} = 270 \quad 266$ N/mm^2

$F_b = \{10 * 13 + 2 * 9\}\ 20 * 266 * 0.888 \rightarrow F_b = 699$ kN

$F_b = 300 * 20 * 266 * 0.888 \rightarrow F_b = 1417$ kN

$F_c = 300 * 20 * 266 * 0.888 \rightarrow \boxed{F_c = 1417 \text{ kN}}$

With end-plate: 13 mm

$F_c = 10\ (13 + 13) + 2.9\ \ 20 * 266 * 0.888 \rightarrow \boxed{F_c = 1301 \text{ kN}}$

With end-plate: 20 mm

$F_c = 10\ (13 + 20) + 2.9\ \ 20 * 266 * 0.888 \rightarrow F_c = 1644 \text{ kN}$

With end-plate: 13 mm

$F_c = 300 * 13 * 270 * 1.93 \rightarrow F_c = 2032 \text{ kN}$

With end-plate: 20 mm

$F_c = 300 * 20 * 266 * 1.93 \rightarrow F_c = 3080 \text{ kN}$

Test 3

$\alpha = 27.4$	$\cot \alpha = 1.95$	$\cos \alpha = 0.889$
$r_b = 21$	$r_c = 27$	$b_{f_h} = 220$ mm
$t_{f_b} = 9.5$	$t_{f_c} = 13$	$t_{f_h} = 20$ mm
$\sigma_{y b_w} = 293$	$t_s = 8$	$\sigma_{y f_h} = 266$ N/mm^2
	$\sigma_{y_c} = 302$ N/mm^2	$\sigma_{y_e} = 266 - 310$ N/mm^2

$F_b = \{10 * 12.2 + 2 * 9.5\}\ 20 * 266 * 0.889 \rightarrow F_b = 666 \text{ kN}$

$F_b = 220 * 20 * 266 * 0.889 \rightarrow F_b = 1040 \text{ kN}$

$F_c = 220 * 20 * 266 * 0.889 \rightarrow \boxed{F_c = 1040 \text{ kN}}$

With end-plate: 18 mm

$F_c = \{10\ (13 + 18) + 2*9\}\ 20 * 266 * 0.889 \rightarrow F_c = 1551 \text{ kN}$

With end-plate: 21 mm

$F_c = \{10\ (13 + 21) + 2*9\}\ 20 * 266 * 0.889 \rightarrow F_c = 1693 \text{ kN}$

With end-plate: 18 mm

$F_c = 220 * 18 * 266 * 1.95 \rightarrow F_c = 2054 \text{ kN}$

With end-plate: 21 mm

$F_c = 220 * 21 * 310 * 1.95 \rightarrow F_c = 2793 \text{ kN}$

st 4

e same data as in test 1

= 220 * 20 * 266 * 0.707 → F_b = 827 kN

= 220 * 20 * 266 * 0.707 → F_c = 827 kN

th end-plate: 18 mm

= {10 (13 + 18) + 2.9} 20 * 266 * 0.707 → F_c = 1233 kN

th end-plate: 21 mm

= {10 (13 + 21) + 2.9} 20 * 266 * 0.707 → F_c = 1346 kN

th end-plate: 18 mm

= 220 * 18 * 266 * 1 → F_c = 1053 kN

h end-plate: 21 mm

= 220 * 21 * 310 → F_c = 1432 kN

t 5

t-specimen 5 has no haunch-flange. Failure of the haunch
urs by yielding due to shear-forces.
magnitude of the part which will yield depends on the magnitude
the force necessary to react the boltforces.
t is why failure of the haunch will be contemplated with the com-
ation of the limit state bending moment.
n the computation of the boltforces, the following force distributions
the end-plates were found.

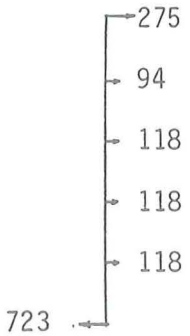

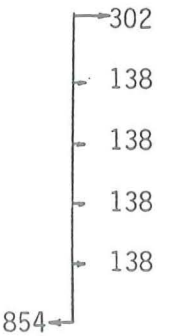

plate :18 mm

end-plate 21 mm

The required reaction of the compression side is much lower than the buckling load of the stiffened column-web.

Applying the formula: (as explained in chapter 4.2.8.2. of the report)

$$\hat{F} = h * t_h * \sigma_{yh} \cos^2\alpha + \frac{2M_{pe}}{h} \qquad (19)$$

gives the following tables of resultant reaction forces at different locations.

End-plate 18 mm

$$\hat{F} = \frac{20 * 266}{2 * 1000} h + \frac{\frac{2}{4} * 18^2 * 220 * 266}{1000\ h} =$$

$$= 2.66 + \frac{4740}{h} \text{ kN}$$

h	2.66 h		$\frac{4740}{h}$	$\hat{F}$
100	266	+	94.8	360
200	532	+	47.4	579
250	665	+	37.9	702
269	715	+	35	750

End-plate 21 mm

$$\hat{F} = \frac{25 * 240 * h}{2 * 1000} + \frac{\frac{2}{4} * 21^2 * 220 *}{1000\ h}$$

$$= 3h + \frac{15038}{h}$$

h	3h		$\frac{15038}{h}$		$\hat{F}$
100	300	+	150	=	450
200	600	+	75	=	675
250	750	+	60	=	810
266	798	+	56	=	854

In combination with the boltforces this results in the following lever-arms for the uppermost bolts.

End-plate 18 mm $\qquad 730 - 70 - \frac{269}{2} = 526$ mm

End-plate 21 mm $\qquad 730 - 70 - \frac{266}{2} = 525$ mm

and the following limit state moments.

$\hat{M} = 275 * 0.526 + 94 * 0.456 + 118 * 0.386 + 118 * 0.316 + 118 * 0.246 =$

$= 302$ kNm

$\hat{M} = 302 * 0.525 + 138 * 0.455 + 138 * 0.385 + 138 * 0.315 + 138 * 0.245 =$

$= 356$ kNm

The computation of the forces on the beam-side is an iterative process (see chapter 4.2.8.2.).

With end-plate 18 mm

h = 100 → F_7 (see test 3) = 75 kN

F_8 (see test 3) = 106 kN

F_9 = 280 * 9.5 * 0.58 * 290 = 447 kN

$F_{10} + F_{11}$ = 628 kN

h = 100 → F_{haunch} = 266 kN

h = 200 → $F_7 + F_8 + F_9$ = 75 + 106 + 230 * 9.5 * 0.58 * 290 = 551 kN

h = 200 → F_{haunch} = 532 kN

h = 210 → $F_7 + F_8 + F_9$ = 75 + 106 + 225 * 9.5 * 0.58 * 290 = 540 kN

h = 210 → F_{haunch} = 558 kN

h = 205 → $F_7 + F_8 + F_9$ = 75 + 106 + 227.5 * 9.5 * 0.58 * 290 = 536 kN

h = 205 → F_{haunch} = 545 kN

h = 204 → $F_7 + F_8 + F_9$ = 75 + 106 + 228 * 9.5 * 0.58 * 290 = 543 kN

h = 204 → F_{haunch} = 543 kN

With end-plate 21 mm

h = 200 → F_7 (see test 3) = 118 kN

→ F_8 (see test 3) = 143 kN

→ F_9 = 230 * 9.5 * 0.58 * 290 = 367 kN

628 kN

h = 200 → F_{haunch} = 600 kN

h = 208 → $F_7 + F_8 + F_9$ = 118 + 143 + 226 * 9.5 * 0.58 * 290 = 622 kN

h = 208 → F_{haunch} = 624 kN

9. Failure of the beam-web due to compression

The computation is in accordance with chapter 4.2.9 of the report.

$$F_{w_b} = \{5(t_{f_b} + r_b) + t_{f_h}\}\ \sigma_{y_{w_b}} * t_{w_b}$$

$$F_{w_b} = \{5(12.2 + 21) + 20\} * 293 * 9.5 \rightarrow F_w = 517 \text{ kN}$$

Formula (13) and (20) can be reduced to a single formula by resolving the force components as shown in figure 23.

$$F_b = (1.25 - 0.5 \frac{F_f}{F_{y_f}})\ \cot\alpha\ \{5(t_{f_b} + r_b) + t_{f_h}\}\ \sigma_{y_w} * t_{w_b}$$

where: F_b = force in the beam-flange
F_{y_f} = yield force of the beam-flange
$\cot\alpha$ = slope of the haunch
t_{f_b} = thickness of the beam-flange
r_b = radius of the fillet of the beam
t_{f_h} = thickness of the haunch flange
σ_{y_w} = actual yield stress of the beam-web
t_{w_b} = thickness of the beam-web

Test 1

$$F_w = \{5(t_{f_b} + r_b) + t_{f_h}\}\ \ \sigma_{y_w} * t_{w_b}$$

$$F_w = \{5(122 + 21) + 20\}\ \ 293 * 9.5 \rightarrow F_w = 517 \text{ kN}$$

$\cot\alpha = 1$ $\qquad F_{y_f} = 12.2 * 181 - 256 = 565$ kN

Suppose $F_b = 480$ kN

Check $\quad F_b = (1.25 - 0.5 \frac{480}{565}) * 1 * 517 \rightarrow F_b = 426$ kN

Suppose $F_b = 460$ kN

Check $\quad F_b = (1.25 - 0.5 \frac{460}{565}) * 1 * 517 \rightarrow F_b = 435$ kN

Suppose $F_b = 445$ kN

Check $\quad F_b = (1.25 - 0.5 \frac{440}{565}) * 1 * 517 \rightarrow F_b = 444$ kN

Thus $\quad F_b = 442$ kN

Test 2

$F_w = \{5(14 + 27) + 20\} * 296 * 9 \rightarrow F_w = 599$ kN

$\cot\alpha = 1.93 \quad F_{yf} = 13.8 * 300 * 266 \rightarrow F_{yf} = 1101$ kN

Suppose $F_b = 800$ kN

Check $F_b = (1.25 - 0.5 \frac{800}{1101}) * 1.93 * 599 \rightarrow F_b = 1025$ kN

Suppose $F_b = 950$ kN

Check $F_b = (1.25 - 0.5 \frac{950}{1101}) * 1.93 * 599 \rightarrow F_b = 946$ kN

Thus $F_b = 948$ kN

Test 3

$F_w = 517$ kN (see test 1)

$\cot\alpha = 1.95$

If the flange yields thus $F_b = 565$ kN, then

$$F_w = 565 / 1.95 = 290 \text{ kN}$$

This latter value is smaller than $0.75 * 517 = 388$ kN thus okay.

Test 4

Not applicable due to the stiffening.

Test 5

Not applicable due to the spreading effect caused by yielding of the haunch.

10. Failure of the beam-flange due to buckling

This will be contemplated in the discussion.

11. Computation of the welds

11.1 In accordance with chapter 4.2.3.2 of the report.

Test 1

Distribution of the minimum limit state load of the uppermost bolt over the welds between end-plate and beam gives:

$$\frac{m_1}{m_1 + m_2} * F_1 = \frac{44.6}{44.6 + 42.1} * 113 = 58 \text{ kN}$$

$$\frac{m_2}{m_1 + m_2} * F_1 = \frac{42.1}{44.6 + 42.1} * 113 = 55 \text{ kN}$$

Effective length $a_3 : 2 * m_1 = 89.2$ mm

$a_2 : 2 * m_2 = 84.2$ mm

Weld dimension $a_2 = \frac{58000}{240 * 84.2} = 2.87$ mm

$a_3 = \frac{55000}{240 * 89.2} = 2.56$ mm

The mechanism of tensile failure of the beam web requires:

$a_1 = 0.3 * 12.2 = 3.66 \rightarrow$ practical 4 mm

$a_2 = 0.35 * 12.2 = 4.27 \rightarrow$ " 5 mm

Test 2

$$\frac{m_1}{m_1 + m_2} * F_1 = \frac{44.6}{41.3 + 44.6} * 139 = 72 \text{ kN}$$

$$\frac{m_2}{m_1 + m_2} * F_1 = \frac{41.3}{44.3 + 44.6} * 278 = 67 \text{ kN}$$

Effective length weld $a_3 : 2m_1 = 89.2$ mm

" " " $a_2 : 2m_2 = 82.6$ mm

Weld dimension $a_2 = \frac{72000}{240 * 82.6} = 3.63$ mm

" " $a_3 = \frac{67000}{240 * 89.2} = 3.12$ mm

The mechanism of tensile failure of the beam-web requires:

$a_1 = 0.3 * 13.5 = 4.05$ mm $\rightarrow$ practical 4 mm

$a_2 = 0.35 * 13.5 = 4.72$ mm $\rightarrow$ practical 5 mm

Test 3, 4 and 5

The largest minimum limit state load is taken

$$\frac{m_1}{m_1 * m_2} * F_1 = \frac{49.6}{49.6 + 50.3} * 151 = 75 \text{ kN}$$

$$\frac{m_2}{m_1 + m_2} * F_1 = \frac{50.3}{49.6 + 50.3} * 151 = 76 \text{ kN}$$

Effective length weld $a_3 : 2m_1 = 99.2$ mm

" " " $a_2 : 2m_2 = 100.6$ mm

Weld dimension $a_2 = \frac{75000}{240 * 100.6} = 3.10$ mm

Weld dimension $a_3 = \frac{76000}{240 * 99.2} = 3.19$ mm

The mechanism of tensile failure of the beam-web requires the same dimensions of the welds as in test 1 (i.e. 4 and 5 mm).

APPENDIX 3

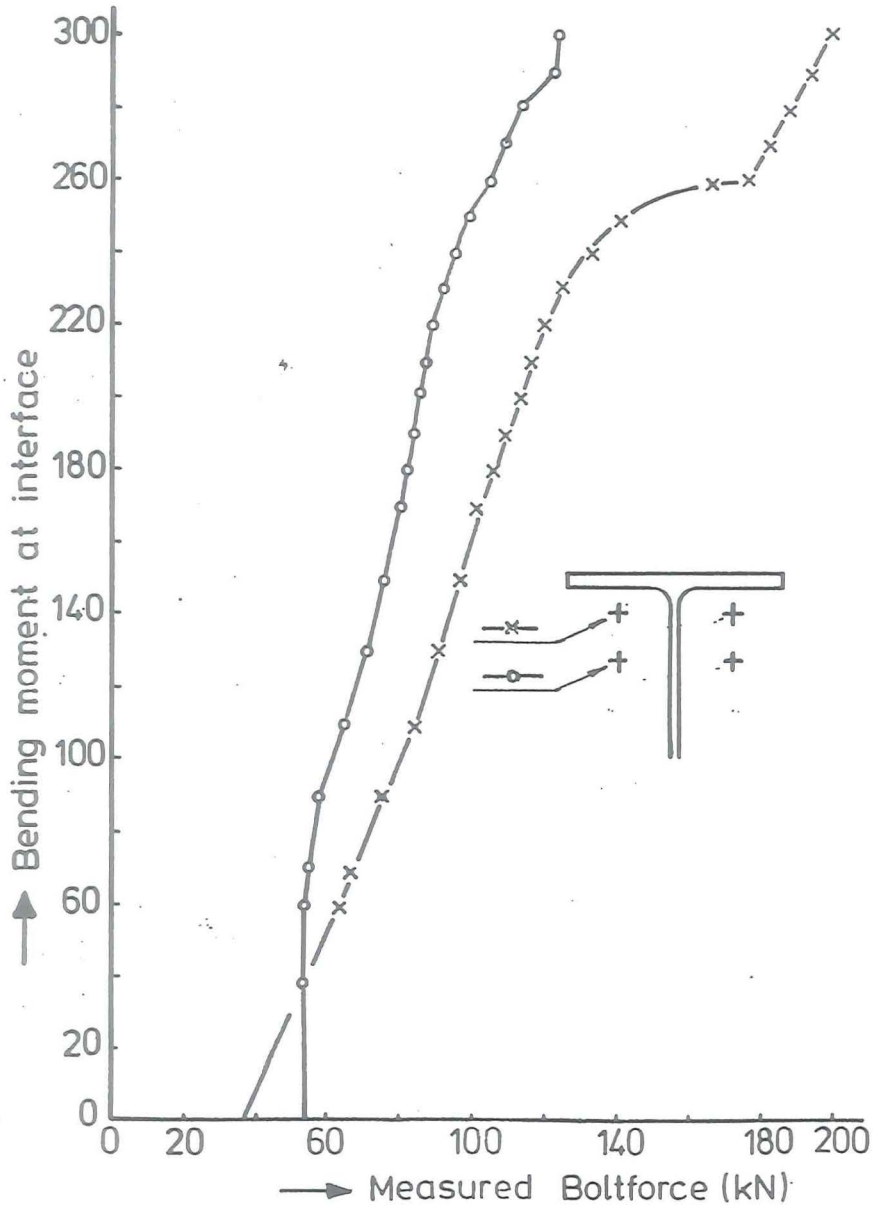

Testspecimen 1 End-plate 20 mm

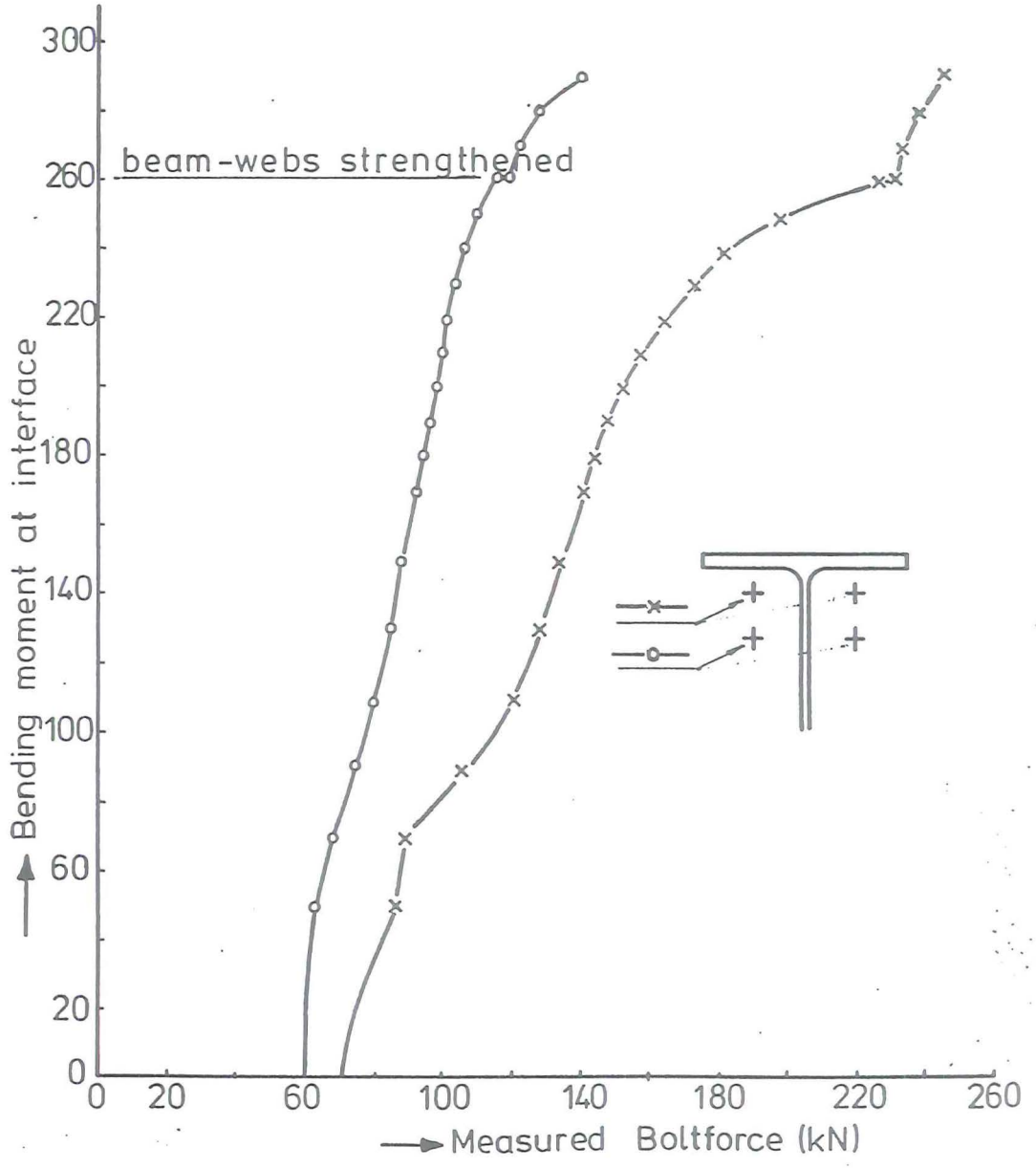

Testspecimen 1 End-plate 15,3 mm

Fig.A3.1 Moment-boltforce curves of testspecimen 1

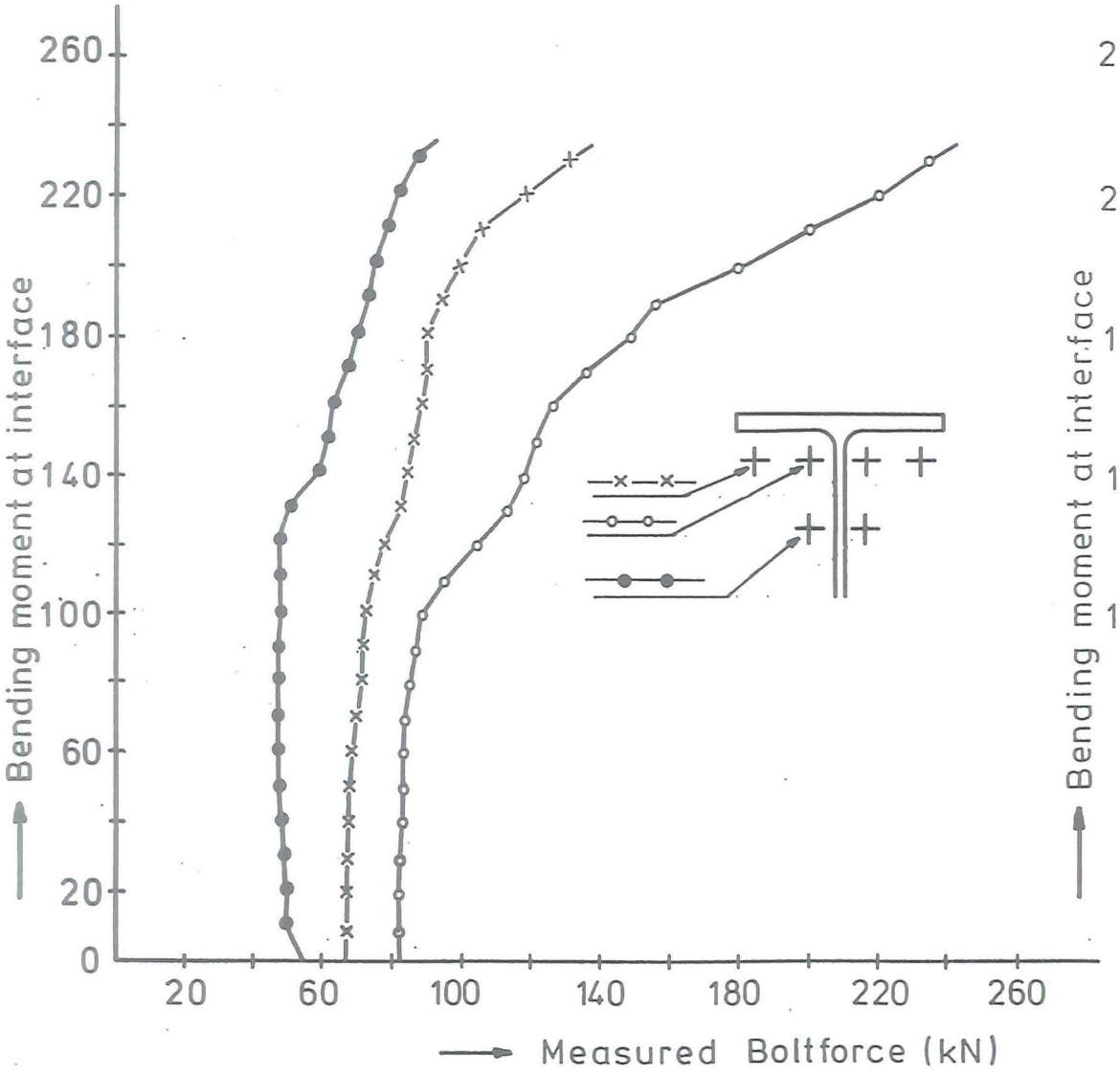

Testspecimen 2 End-plate 13 mm

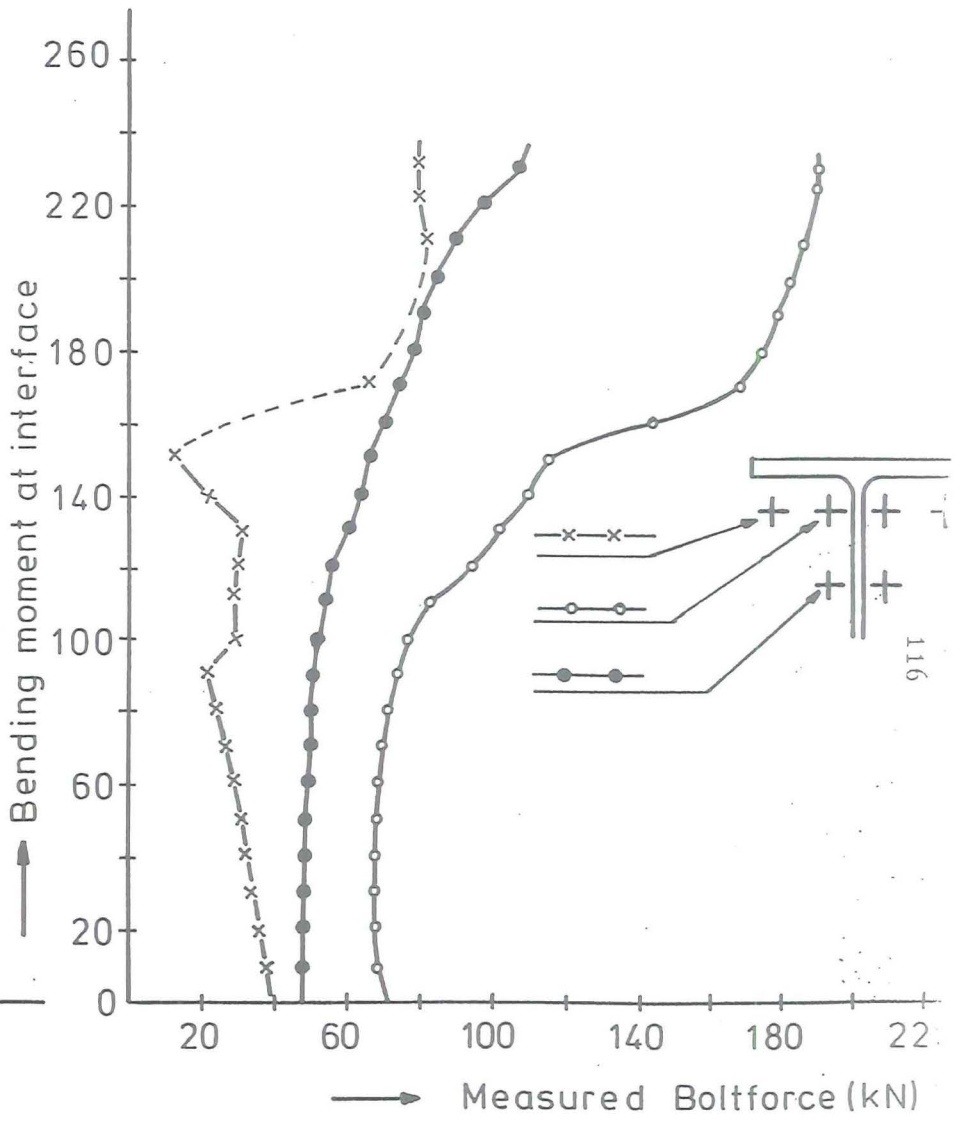

Testspecimen 2 End-plate 20 mm

Fig.A3.2: Moment-boltforce curves of testspecimen 2

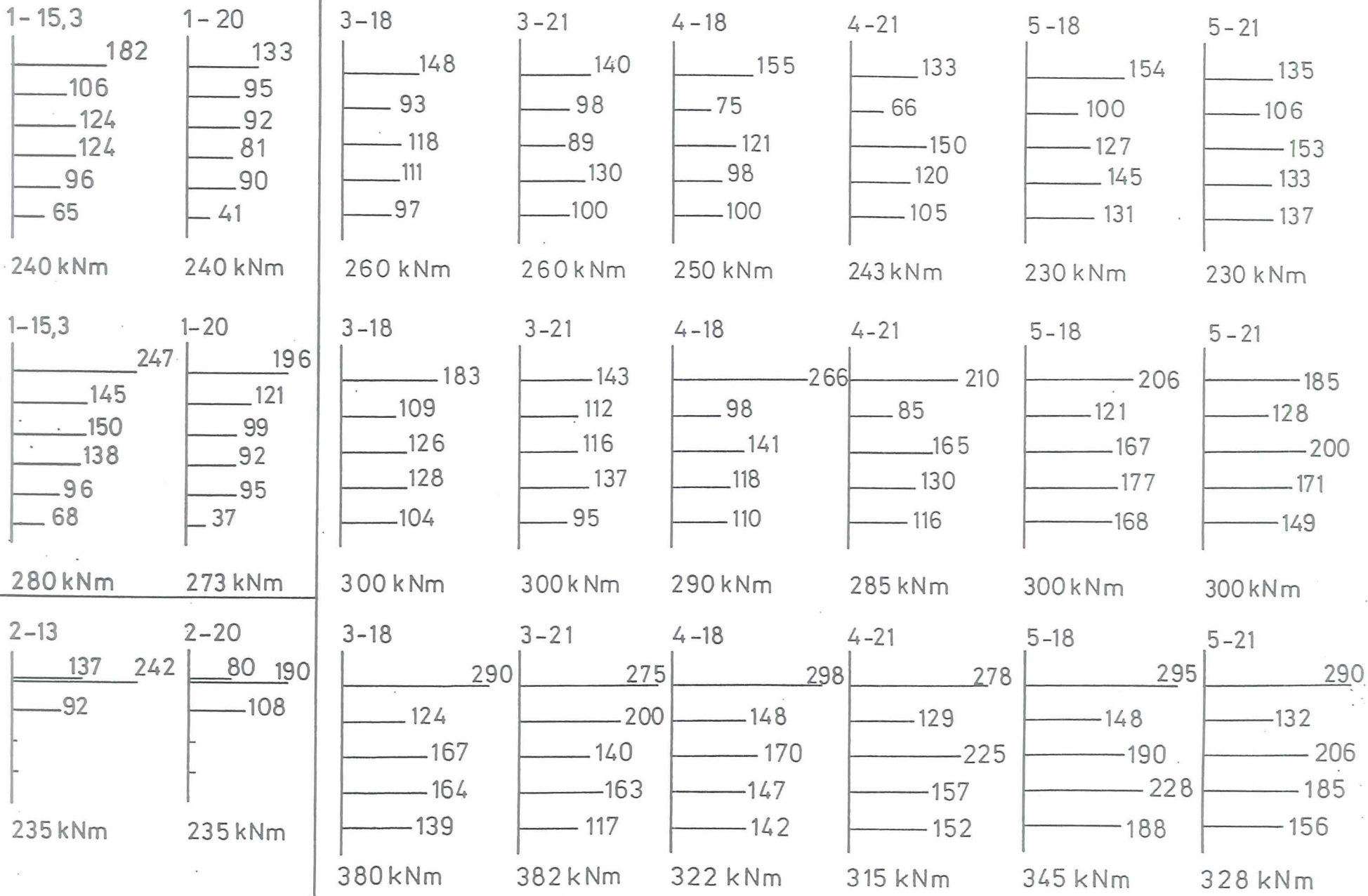

Fig. A.3.3.

Measured boltforces at specific bending moments

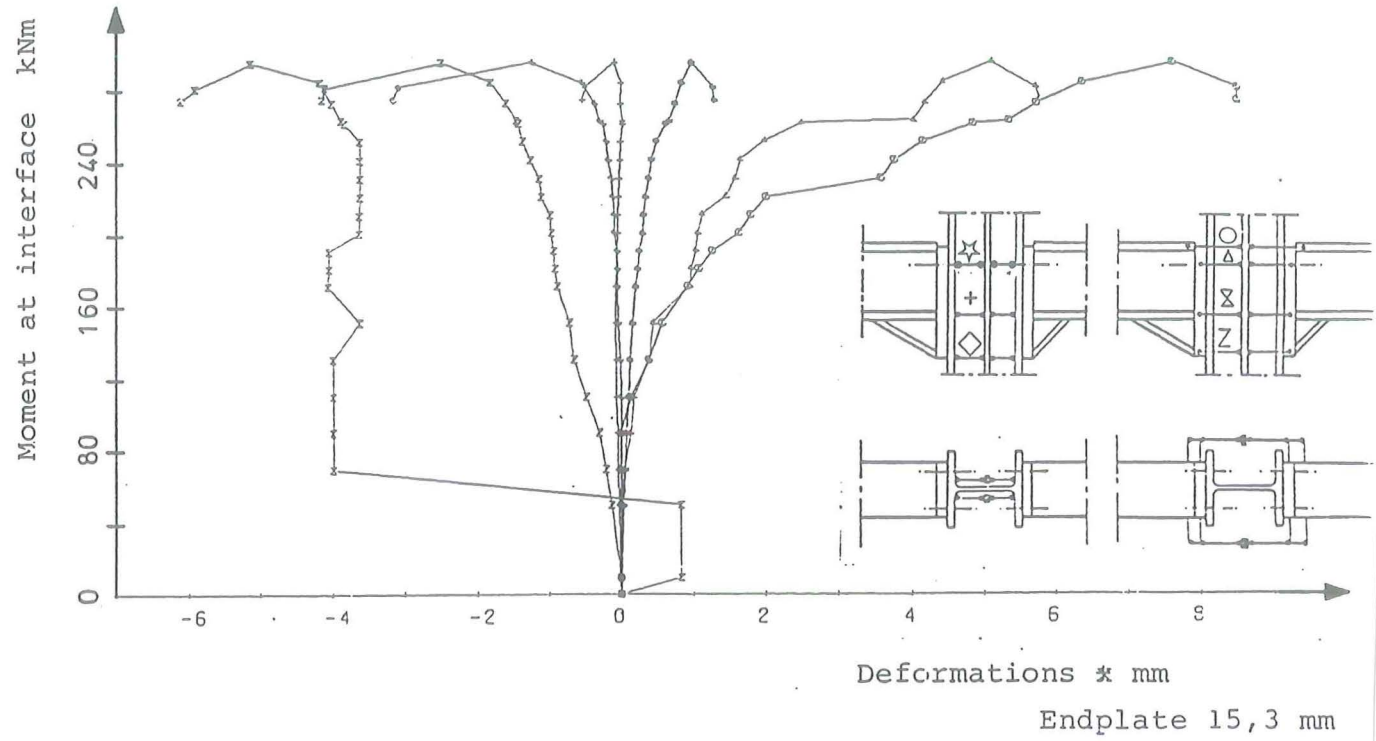

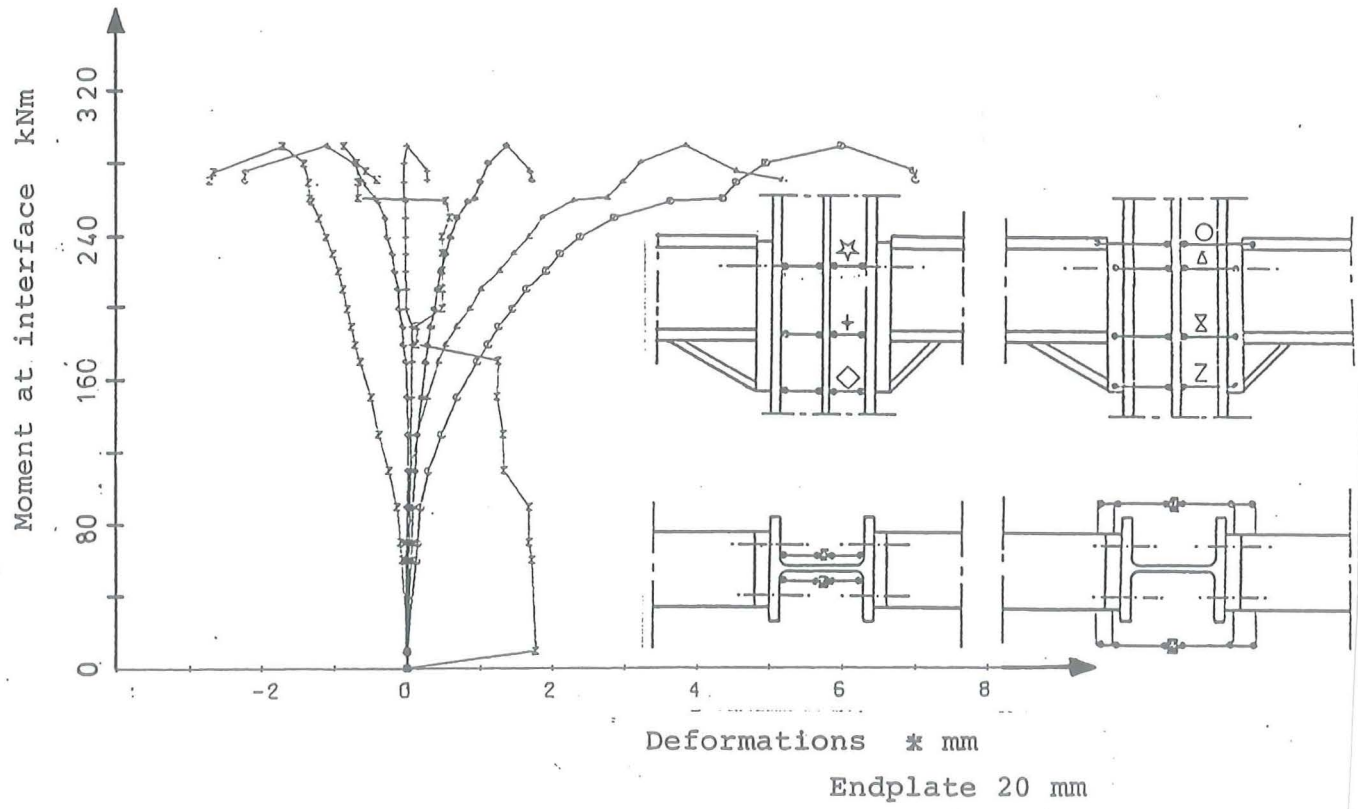

Fig. A.3.4. Moment - deformation curves of test 1

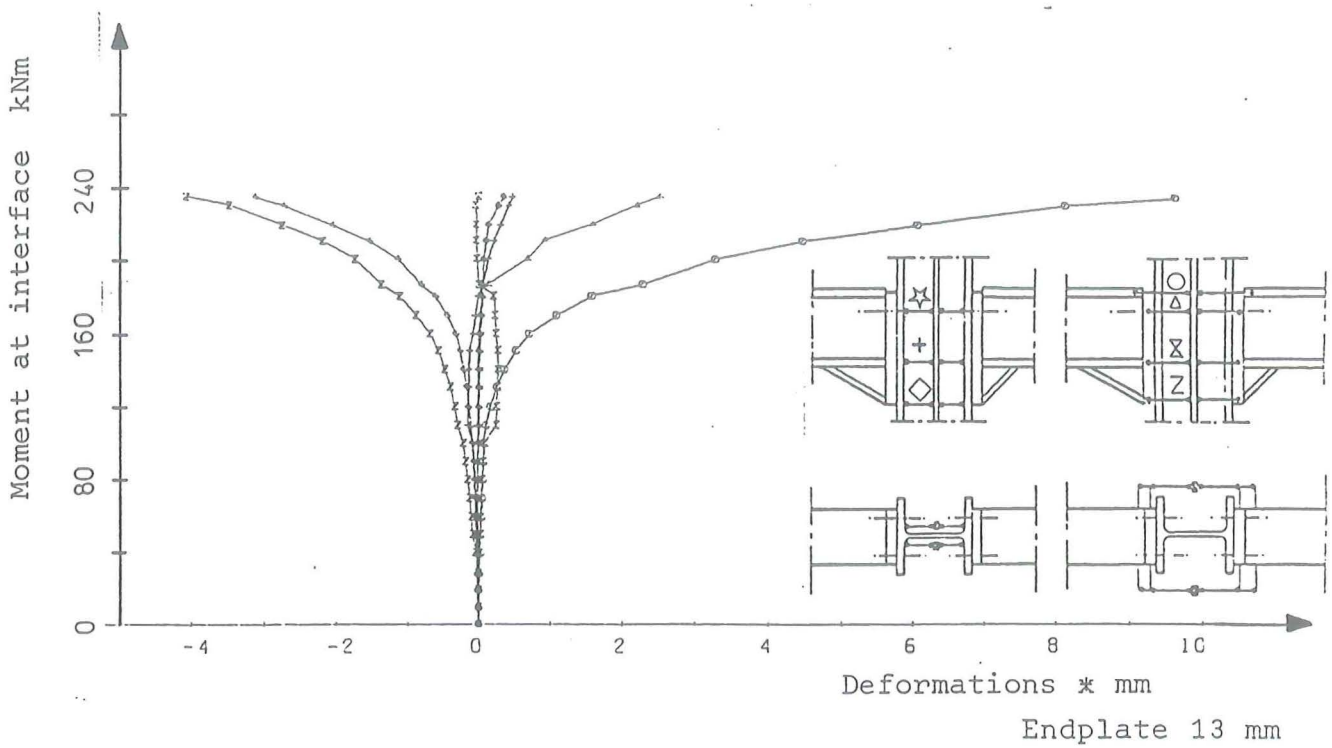

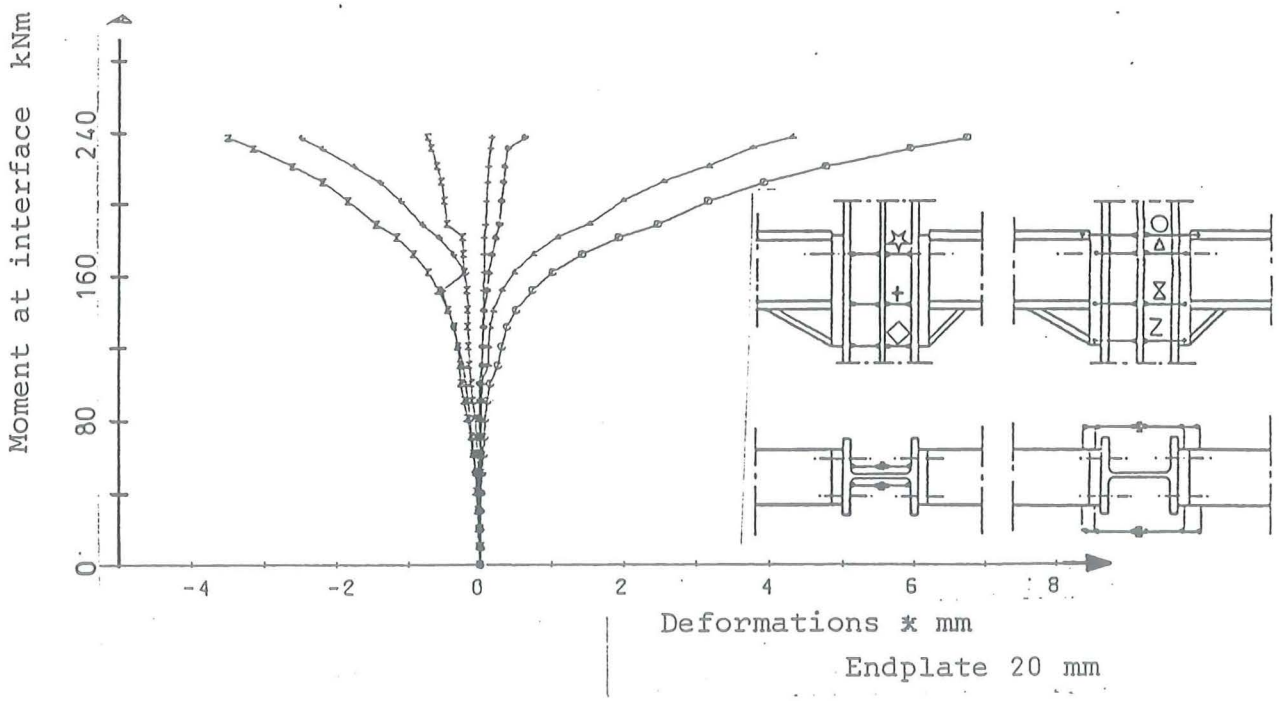

Fig. A.3.5. Moment - deformation curves of test 2

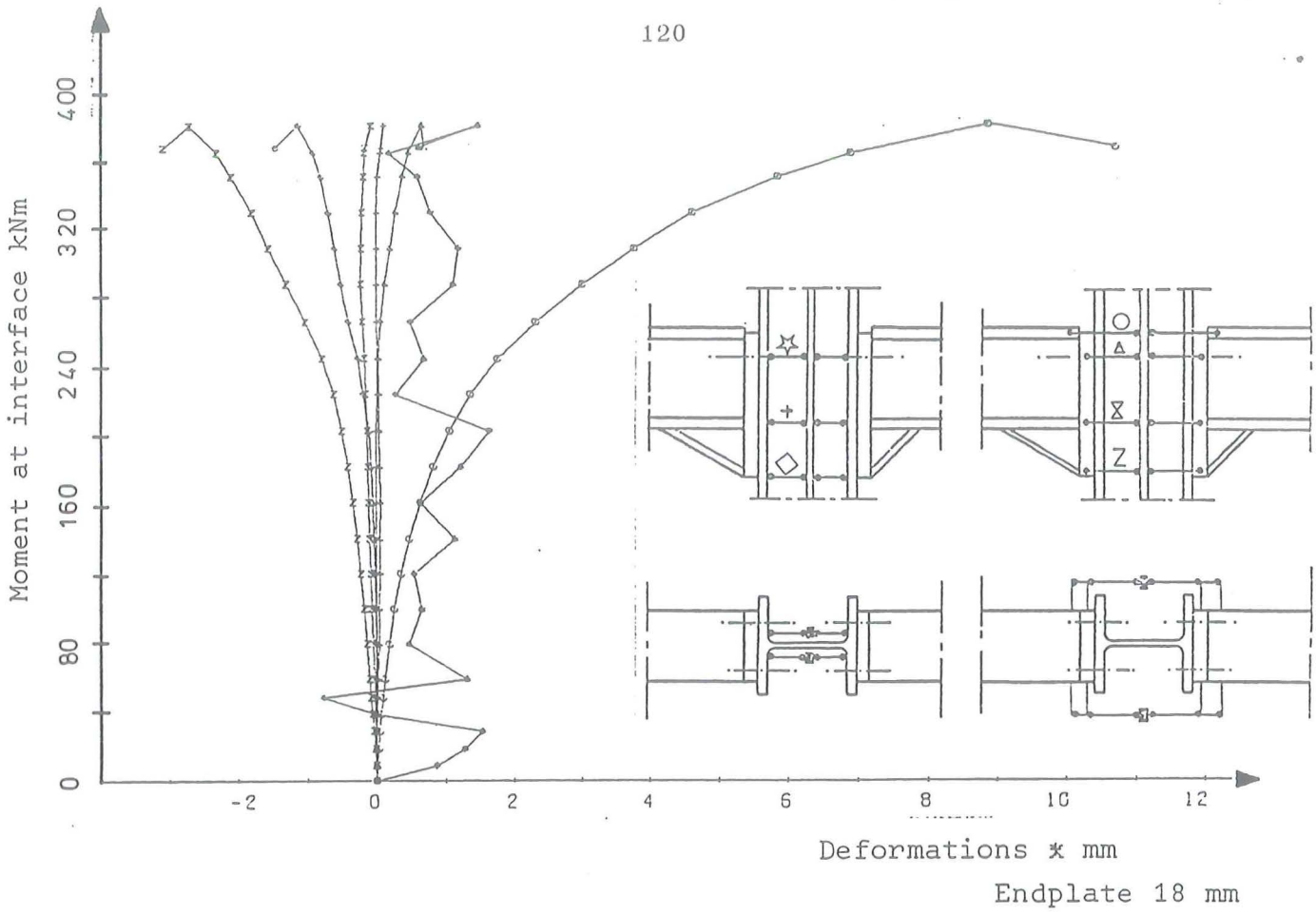

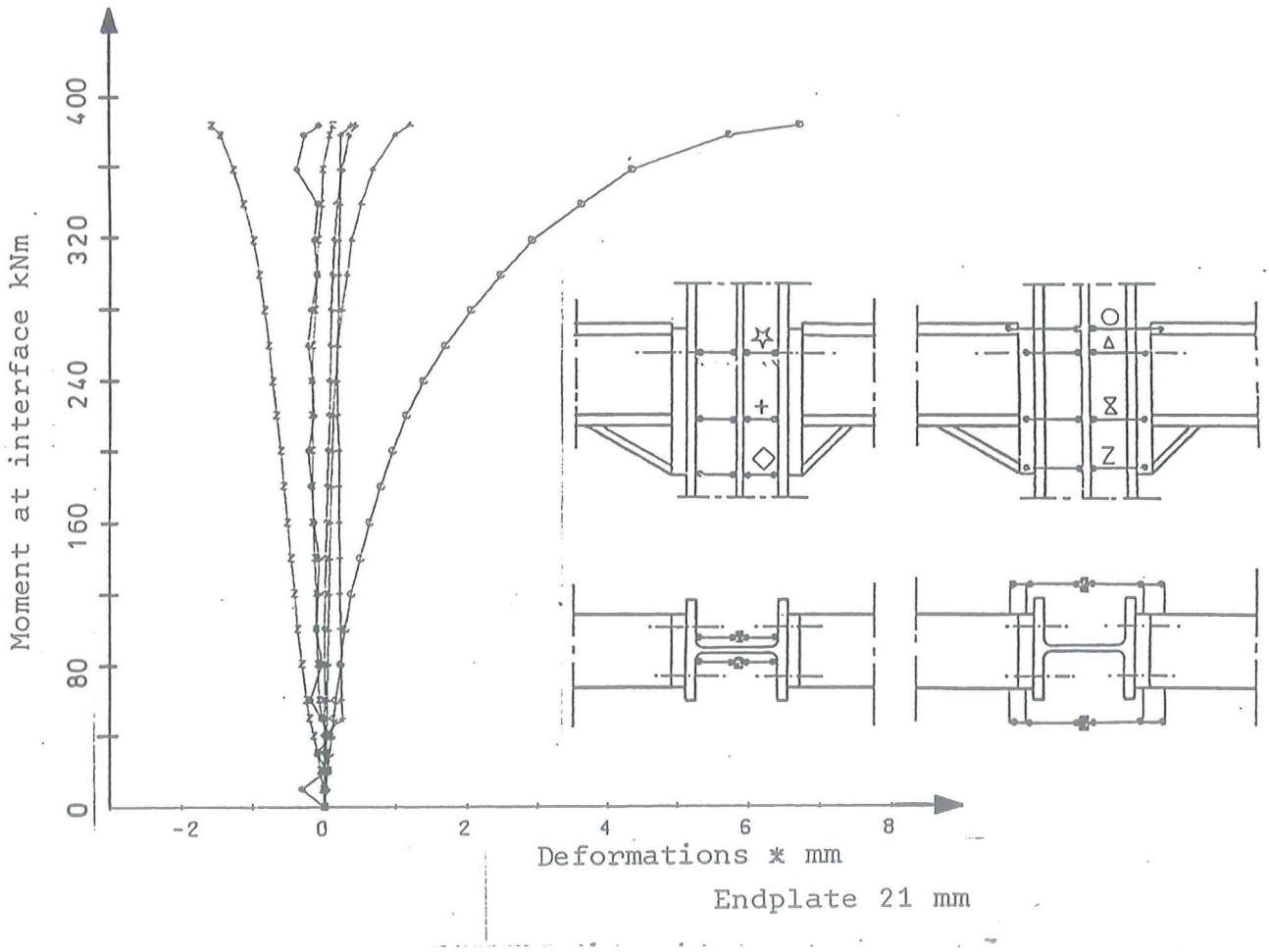

Fig. A.3.6. Moment - deformation curves of test 3

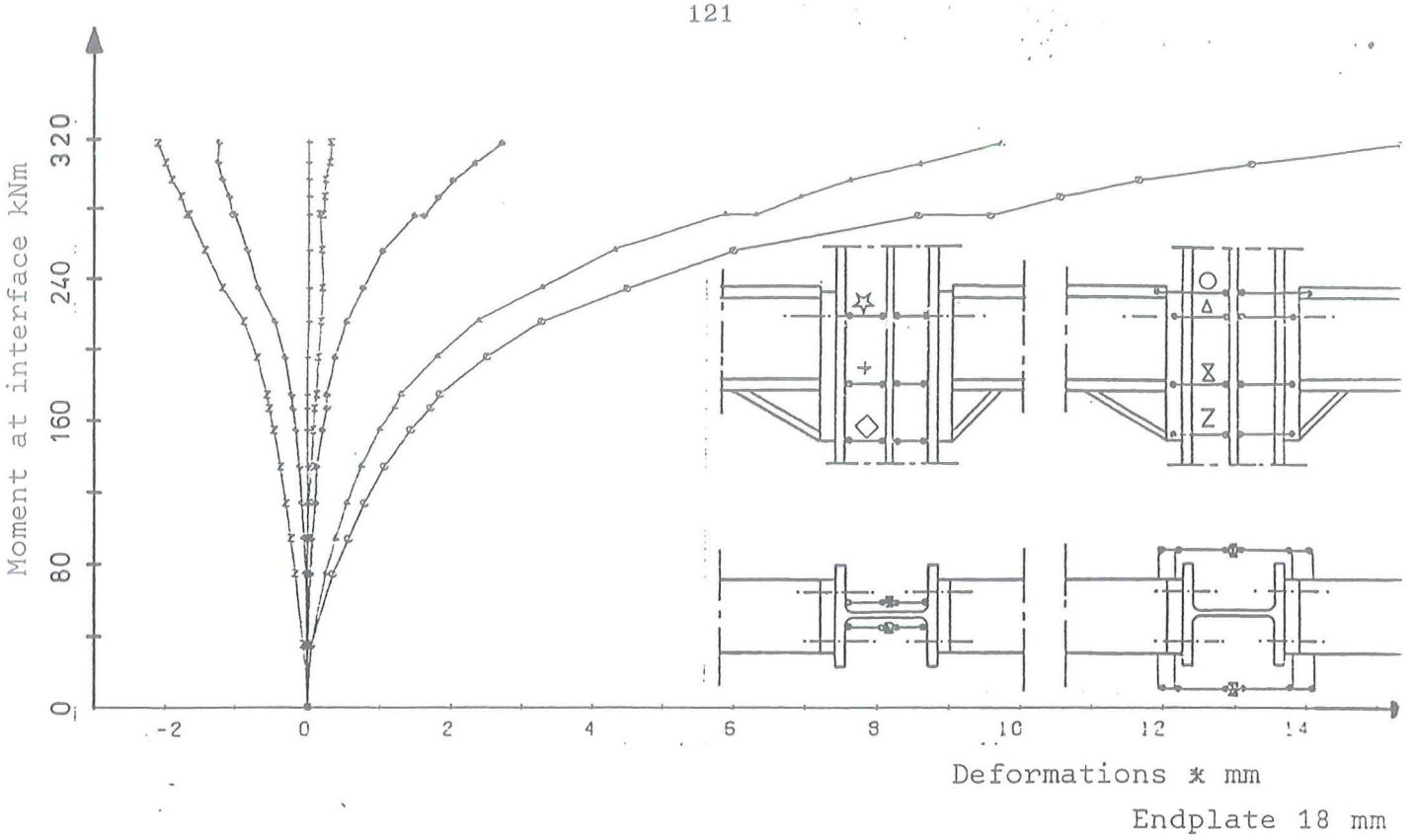

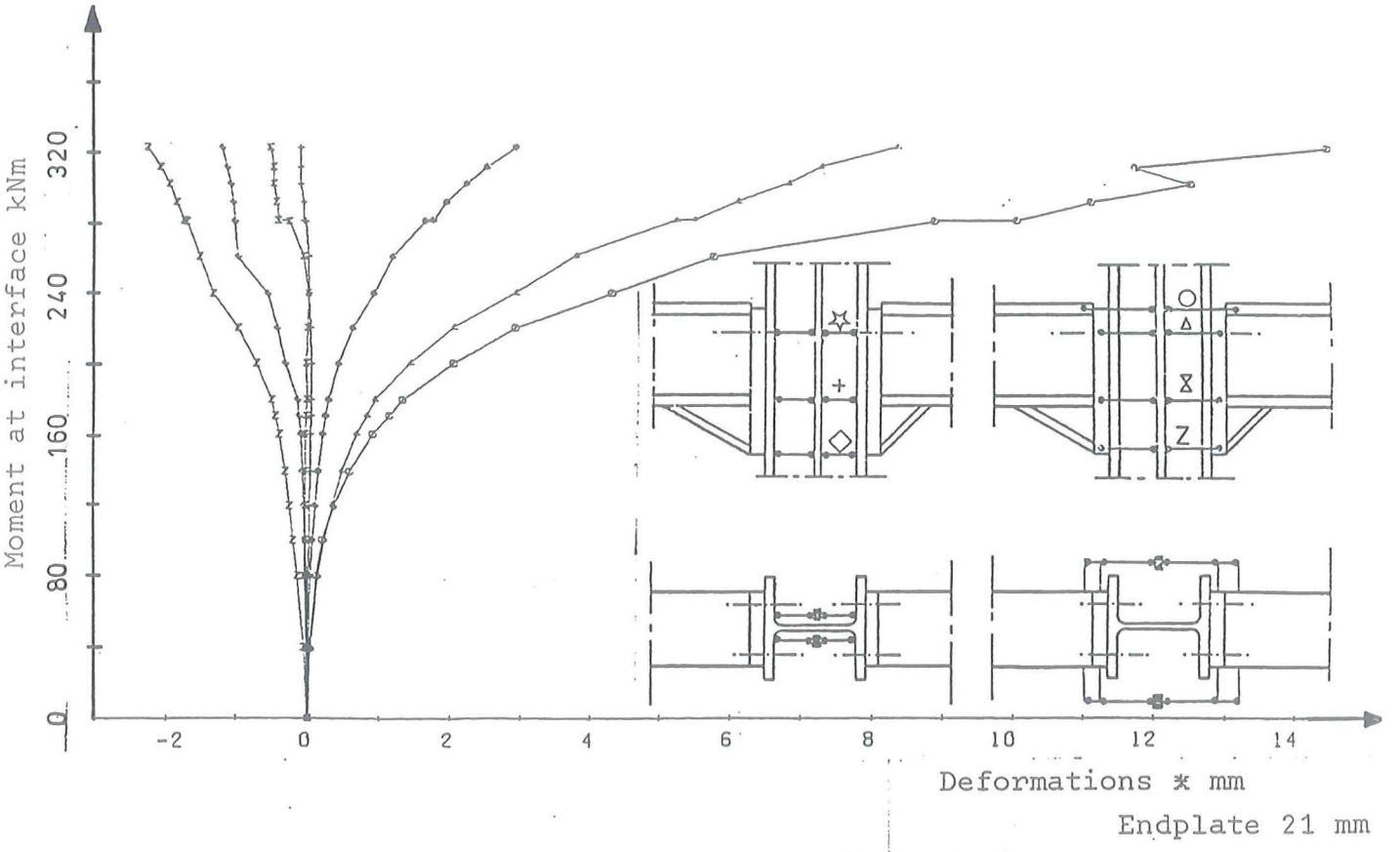

Fig. A.3.7. Moment - deformation curves of test 4

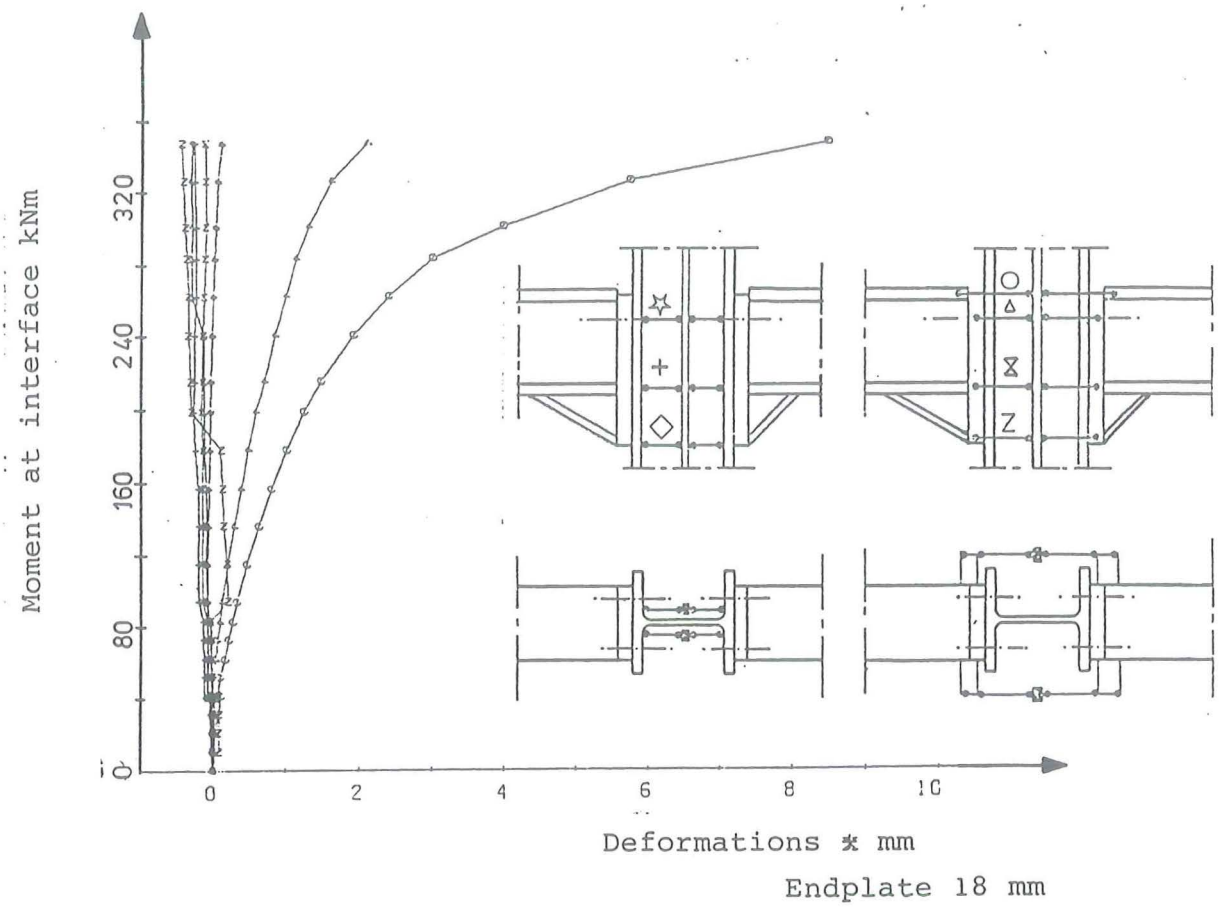

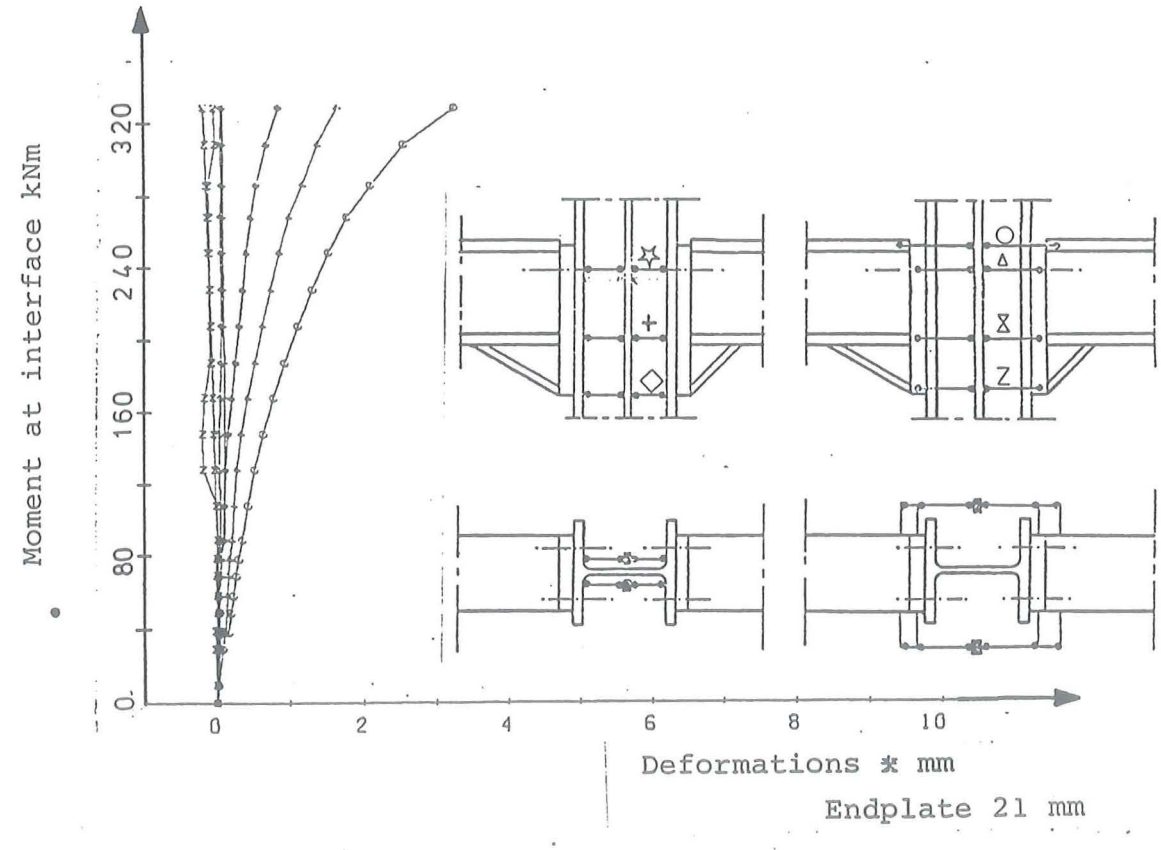

Fig. A.3.8. Moment - deformation curves of test 5

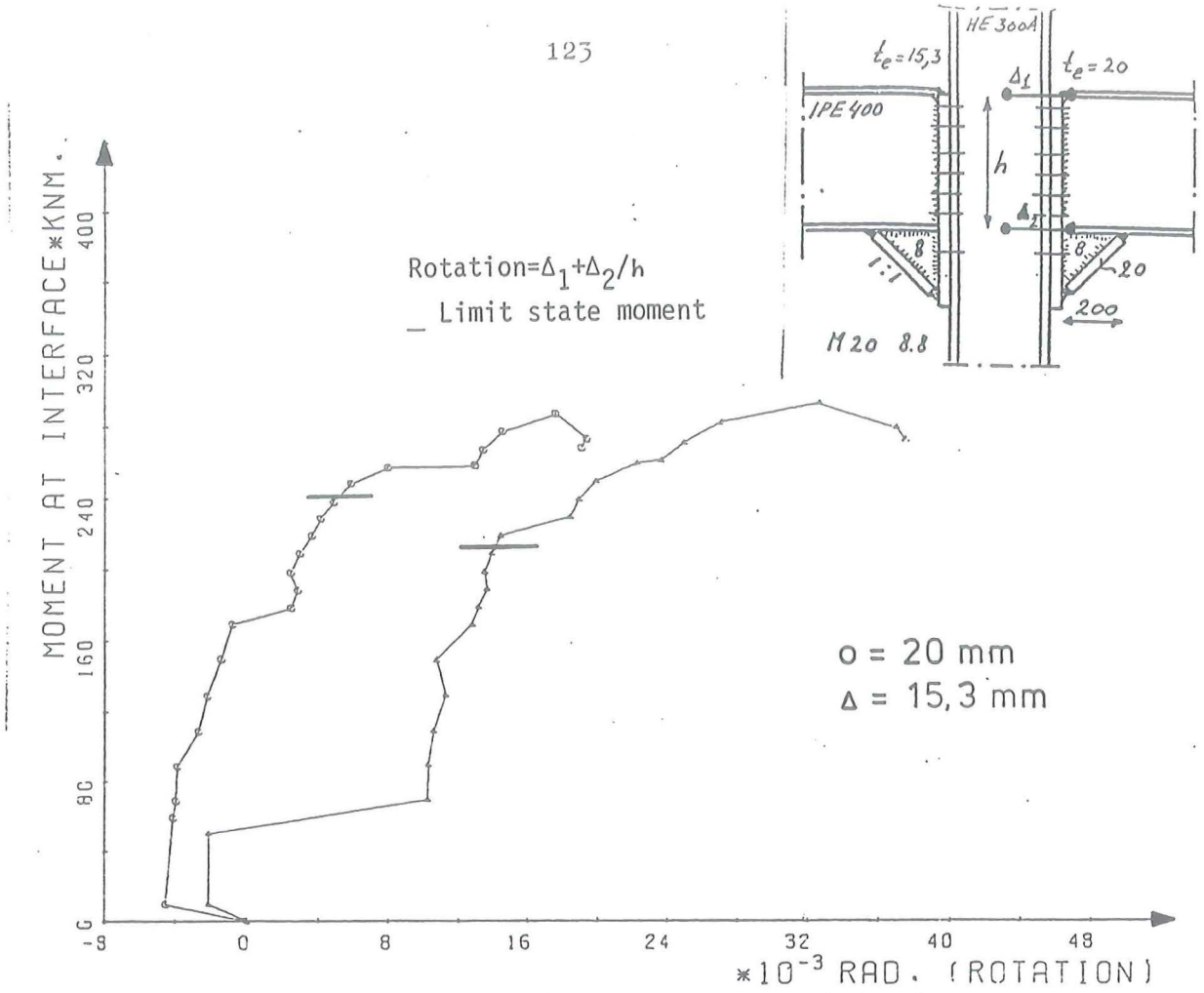

Fig. A. 3.9. Moment-rotation curves of test 1

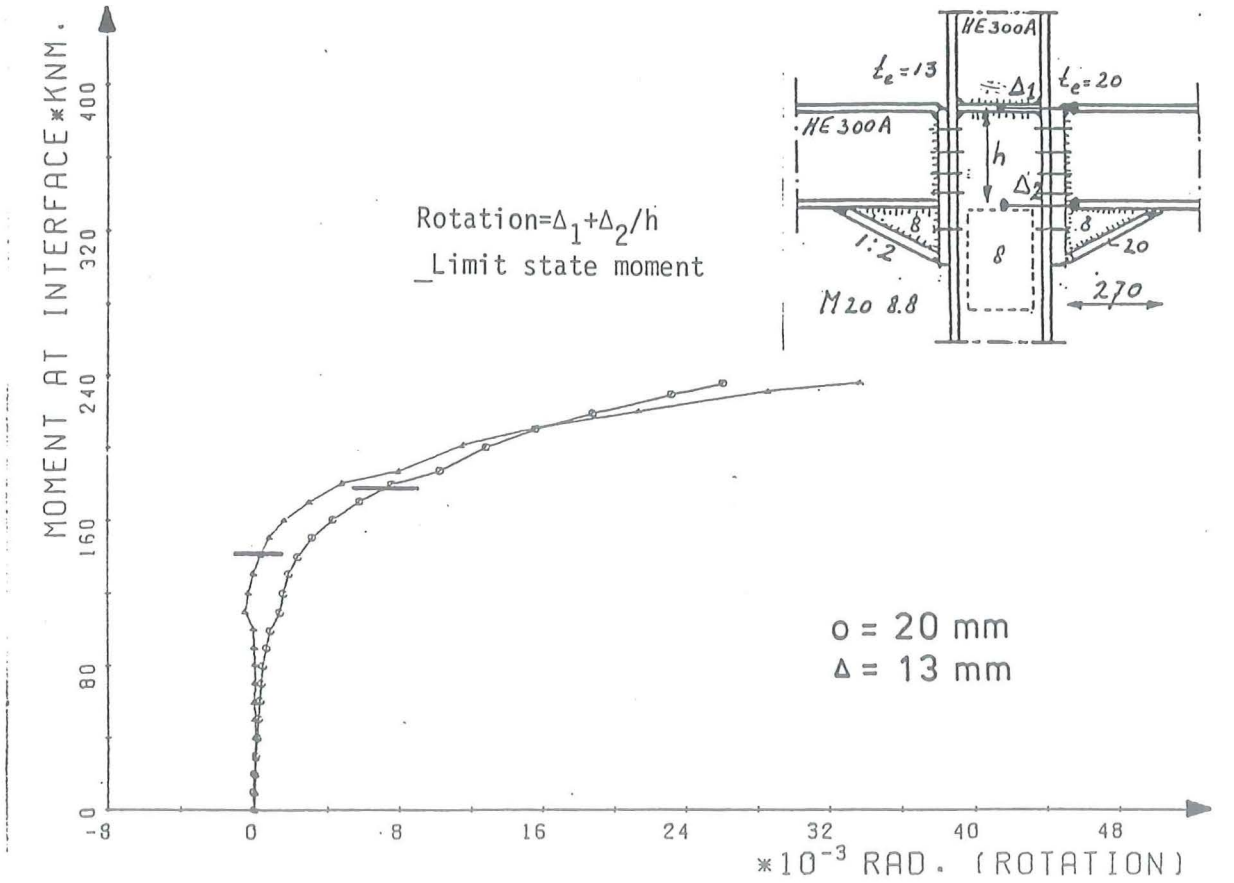

Fig. A. 3.10. Moment-rotation curves of test 2

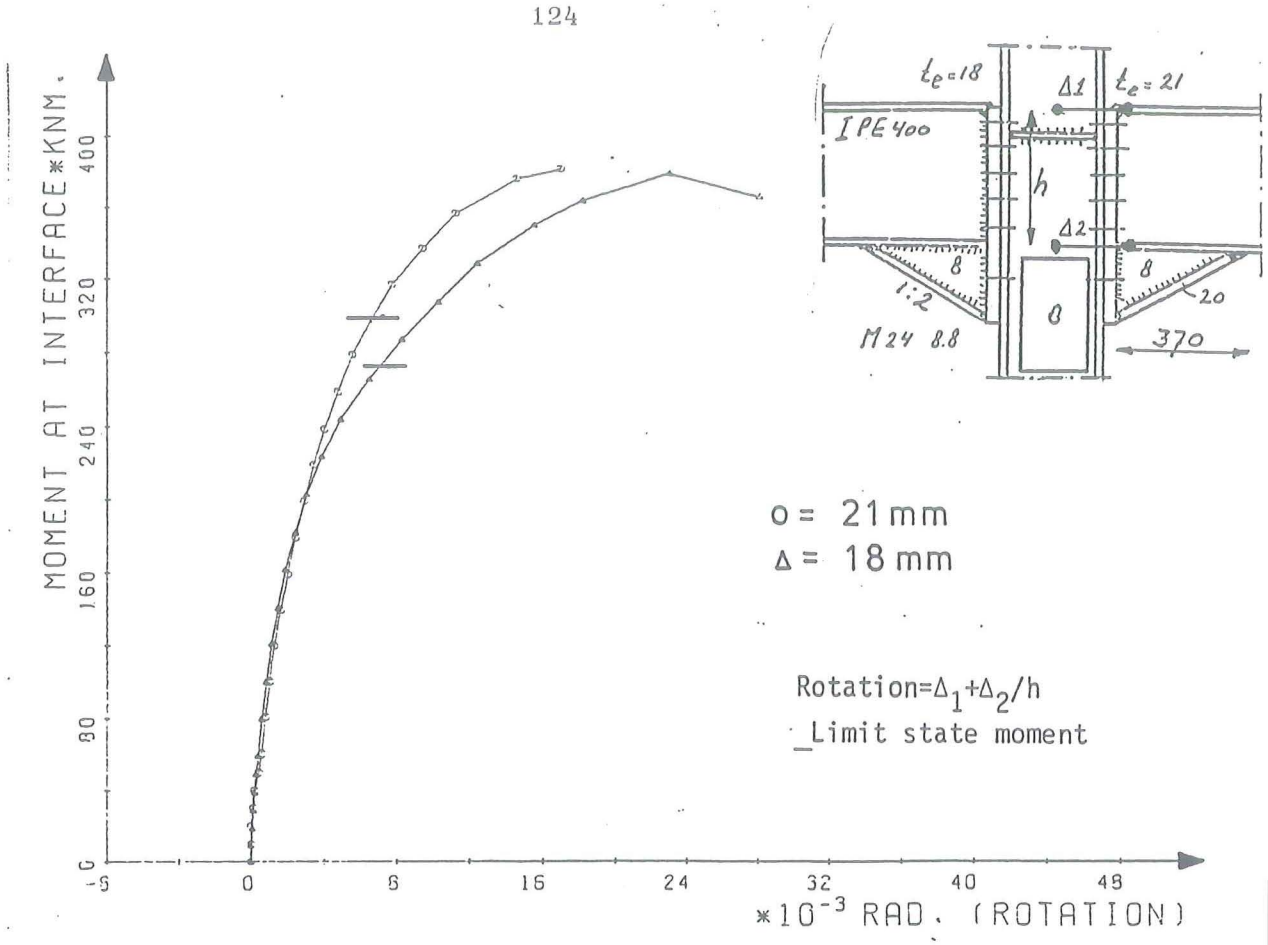

Fig. A. 3.11. Moment - rotation curves of test 3

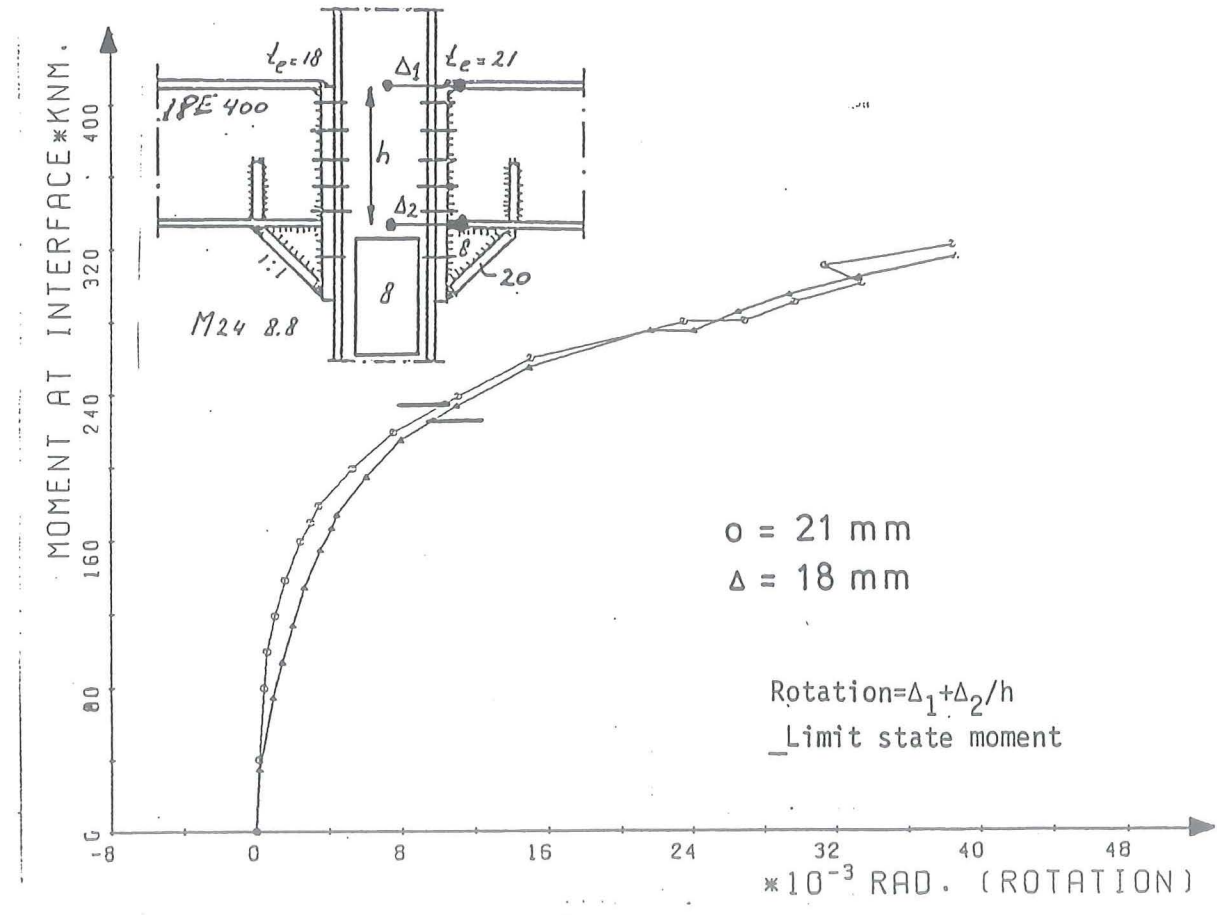

Fig. A. 3.12. Moment - rotation curves of test 4

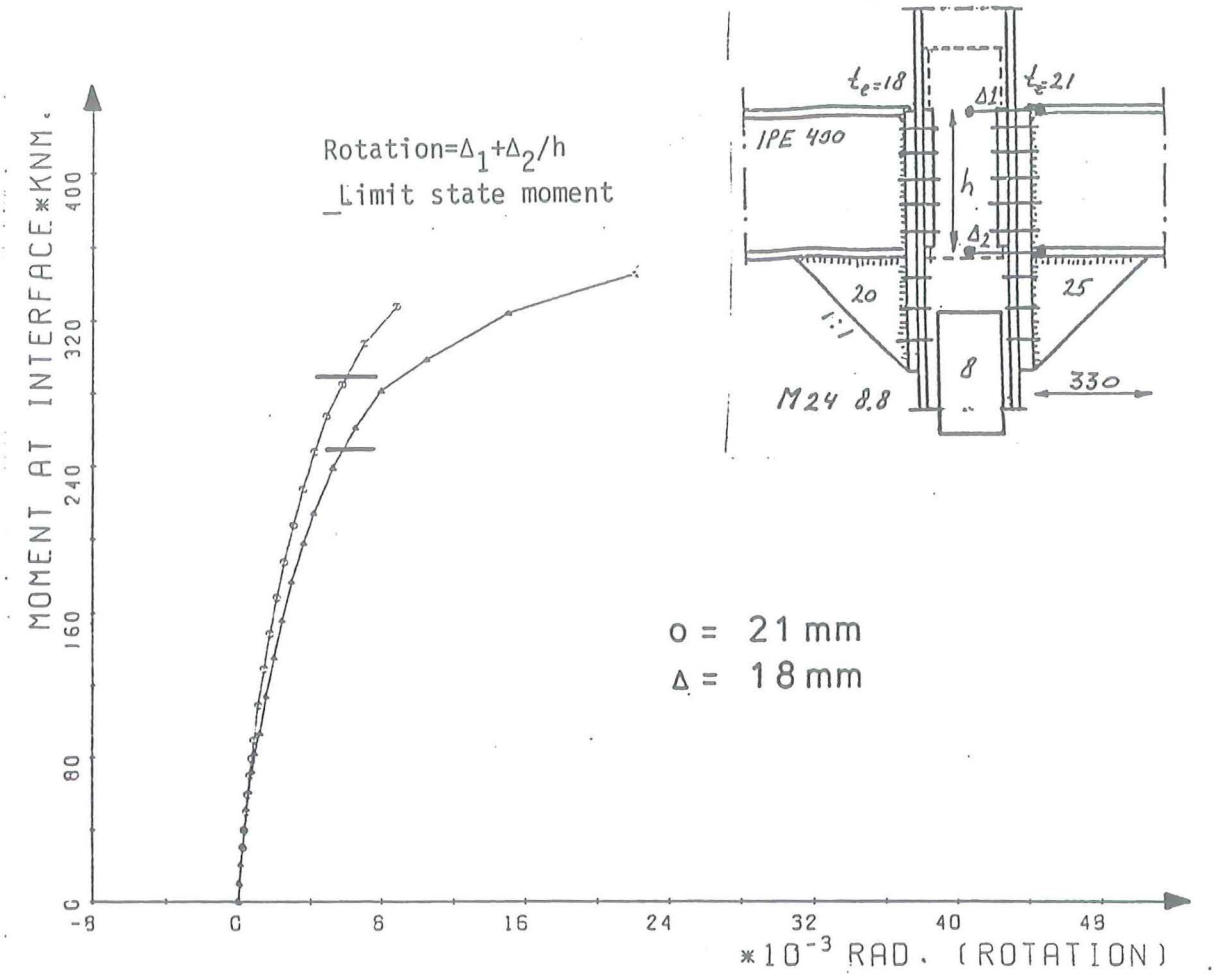

Fig. A.3.13. Moment-rotation curves of test 5

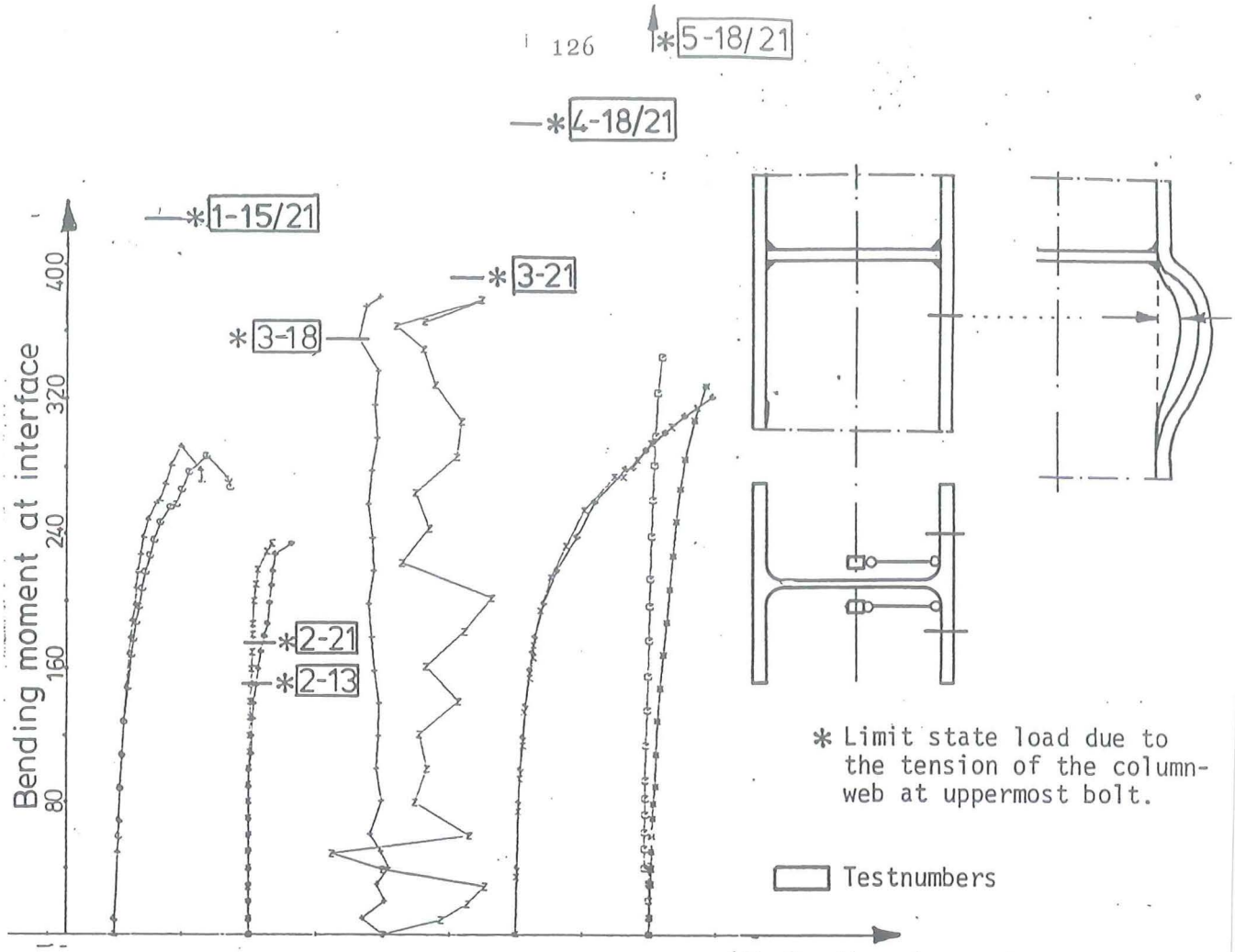

Fig A3 14 Deformation of the column-web on the uppermost boltline.
(all tests)

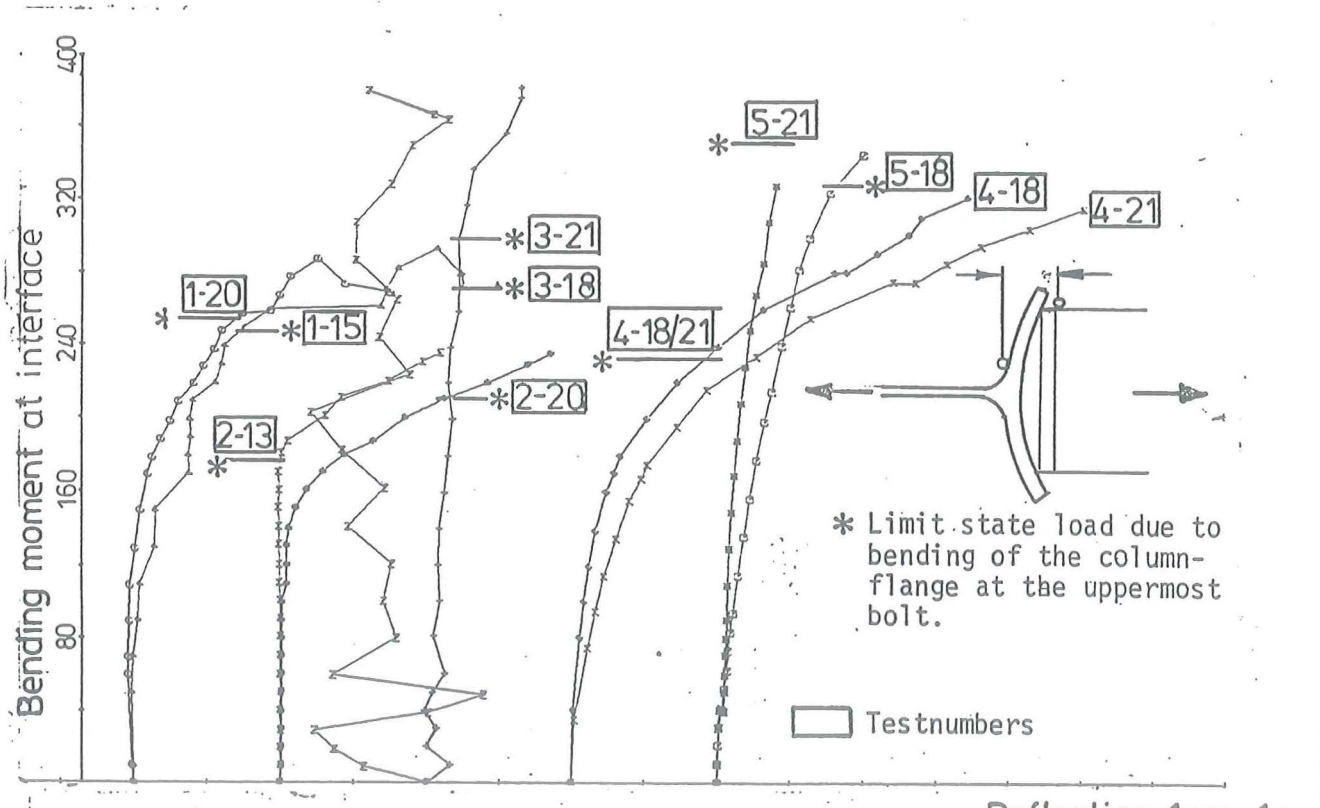

Fig A3 15 Deformation of column-flange at uppermost boltline.
(all tests)

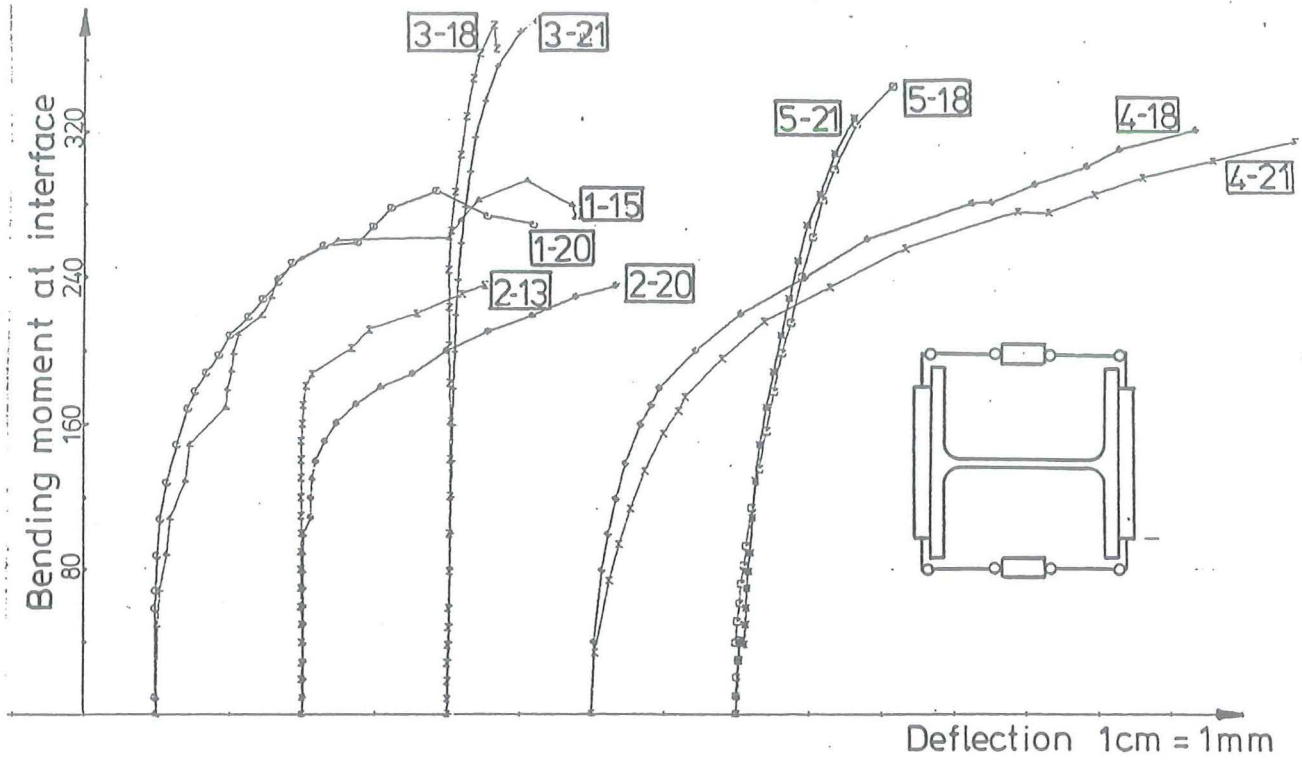

Fig A3 16 Deformation of column-web and flange on the uppermost boltline.
(all tests)

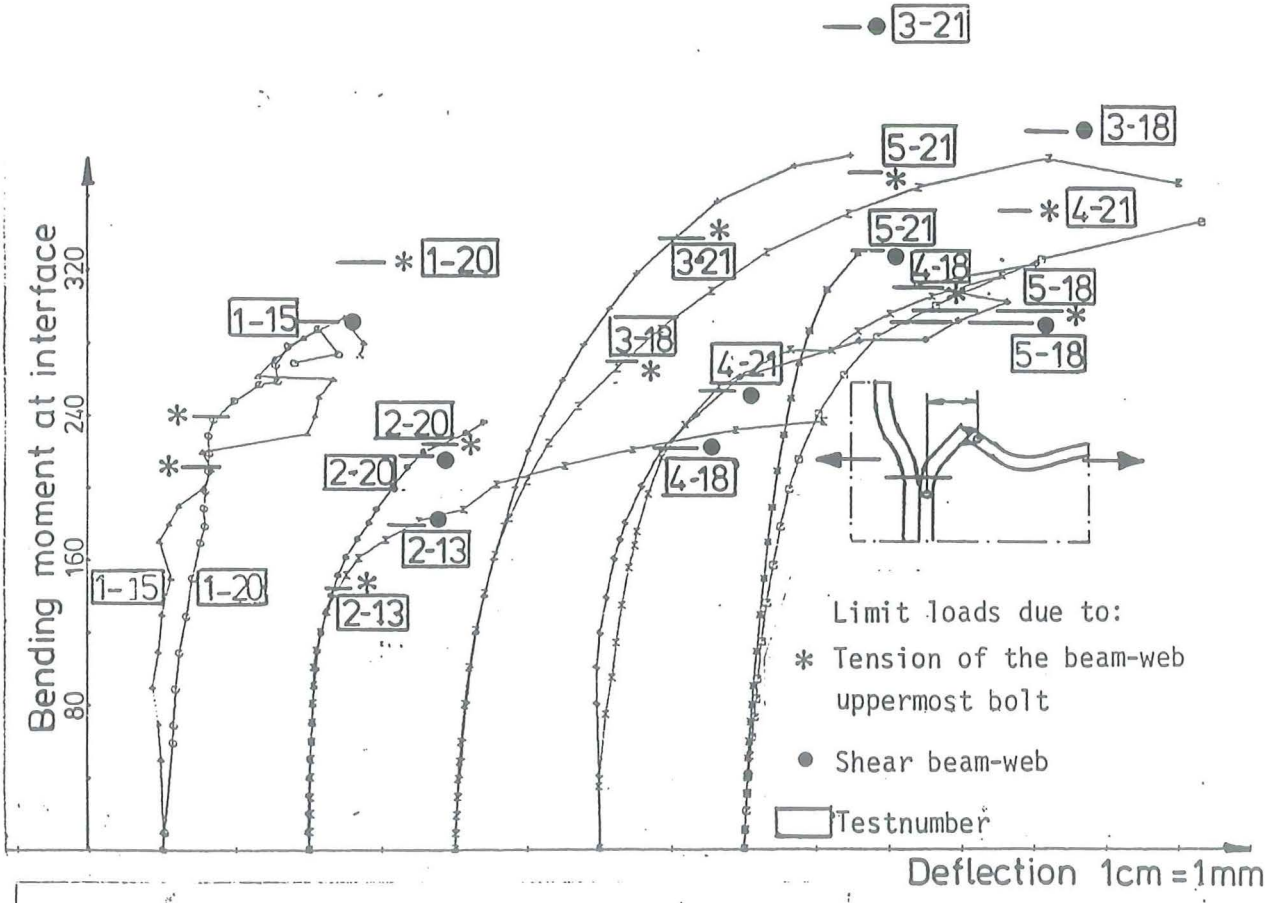

Fig A3.17 Deformation of the end-plate between the uppermost boltline and the beam-flange.
(all tests)

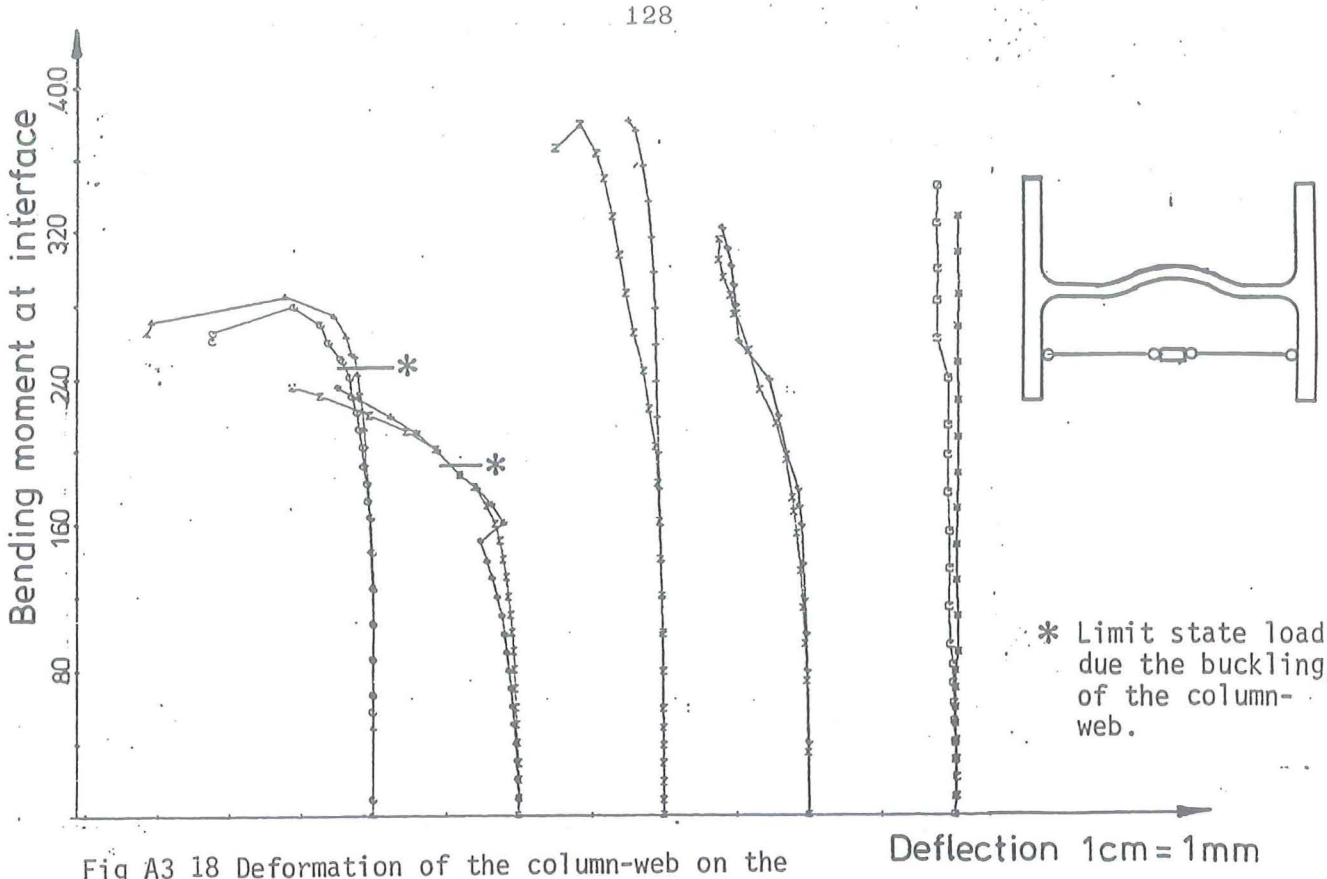

Fig A3 18 Deformation of the column-web on the compression side.
(all tests)

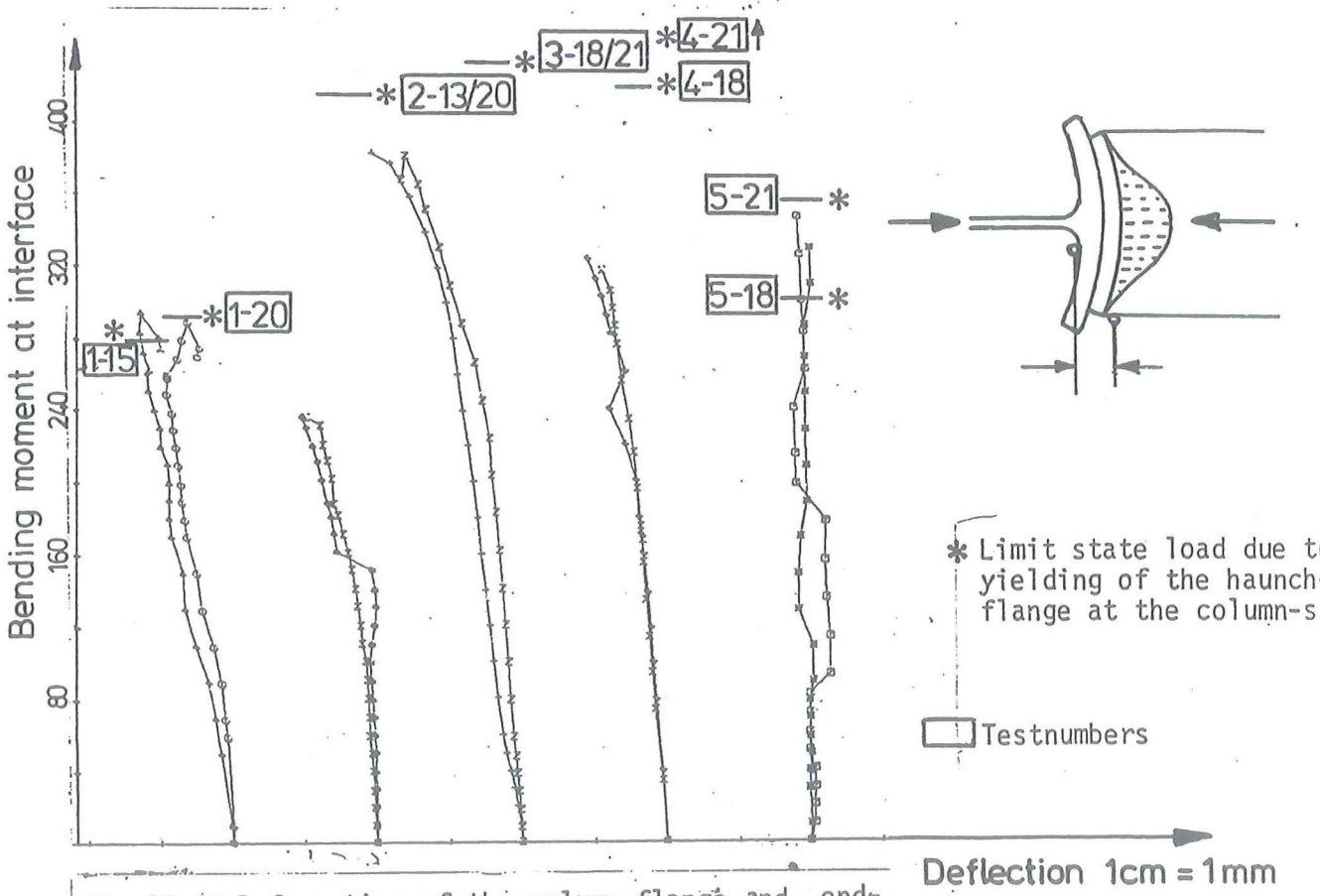

Fig A3 19 Deformation of the column flange and end-plate on the compression side.
(all tests)